UNIVERSITÉ DU QUÉBEC À MONTRÉAL

AUGMENTATION DE LA DÉTECTABILITÉ DES MÉTABOLITES PHOSPHORYLÉS ET THIOLS PAR CHROMATOGRAPHIE LIQUIDE COUPLÉE À LA SPECTROMÉTRIE DE MASSE EN TANDEM

MÉMOIRE

PRÉSENTÉ(E)

COMME EXIGENCE PARTIELLE

À LA MAÎTRISE EN CHIMIE

PAR

KATHRINA KUMARESAN

SEPTEMBRE 2025

UNIVERSITÉ DU QUÉBEC À MONTRÉAL

INCREASING THE DETECTABILITY OF PHOSPHORYLATED AND THIOL-CONTAINING METABOLITES BY LIQUID CHROMATOGRAPHY TANDEM MASS SPECTROMETRY

MASTER'S THESIS

PRESENTED

AS PARTIAL FULFILLMENT

OF THE MASTER'S IN CHEMISTRY

BY

KATHRINA KUMARESAN

SEPTEMBER 2025

REMERCIEMENTS

First and foremost, I am deeply grateful to Prof. Lekha Sleno for the opportunity to join her lab and to learn and be curious. To the members of the Sleno Lab, Nathan Ghafari, Oriana Zambito, Maggy Lépine, Kahina Chabi, Carina Lima, Said Matar, and Leanne Ohlund, thank you for helping me excel and pointing me in the right direction at various points in this journey.

To my family and friends, near and far, you are my heart and my home. Thank you for always believing that I can do anything and everything. I am where I am thanks to you. To my partner, your confidence in me is never faltering, even when my own does.

TABLE DES MATIÈRES

LISTE DES FIGURES

LISTE DES TABLEAUX

LISTE DES ABRÉVIATIONS, DES SIGLES ET DES ACRONYMES

ABC	Ammonium bicarbonate
ACN	Acetonitrile
AICAR	Aminoimidazole carboxamide ribonucleotide
AMP	Adenine monophosphate
CBMT	4-chlorobenzene methanethiol
CE	Collision energy
CID	Collision-induced dissociation
CMP	Cytidine monophosphate
Cys	Cysteine
DC	Direct current
DDA	Data dependant aquisition
DHAP	Dihydroxyacetone phosphate
DIA	Data independent acquisition
DNA	Deoxyribonucleic acid
DP	Declustering potential
DTT	Dithiothreitol
ERT	Enzyme replacement therapy
ESI	Electrospray ionisation
EtOH	Ethanol
FA	Formic acid
FC	Fold change
GAGs	Glycosaminoglycans
GC	Gas chromatography
GMP	Guanosine monophosphate
GSH	Glutathione
GSSG	Glutathione oxidized/glutathione disulfide
HILIC	Hydrophilic interaction chromatography
HLB	Hydrophilic-lipophilic balanced
HMDB	Human Metabolome Database

HPLC	High performance liquid chromatography
HRMS	High resolution mass spectrometry
HRMS/MS	High resolution tandem mass spectrometry
IAM	Iodoacetamide
IDA	Information dependant acquisition
IDS	Iduronate-2-sulfatase enzyme
IMAC	Immobilized metal afiinity chromatography
IPAP	N-(4-hydroxyphenyl)-2-iodoacetamide
IS	Internal standard
LC	Liquid chromatography
LC-HRMS/MS	Liquid chromatography-high resolution tandem mass spectrometry
LC-MS/MS	Liquid chromatography tandem mass spectrometry
LMW	Low molecule weight
MAX	Mixed-mode anion exchange
MeOH	Methanol
MOAC	Metal oxide affinity chromatography
MPA	Mobile phase A
MPB	Mobile phase B
MPS	Mucopolysaccharidosis
MRM	Multiple reaction monitoring
mRNA	Messenger ribonucleic acid
MS	Mass spectrometry
MS/MS	Tandem mass spectrometry
MW	Molecular weight
NAC	N-acetylcysteine
NAD	Nicotinamide adenine dinucleotide
NH_4OH	Ammonium hydroxide
NIST	National Institute of Standards and Technology
NMR	Nuclear magnetic resonance
NP	Normal phase
PCA	Principal component analysis
PEEK	Polyether ether ketone

PFP	Pentaflourophenyl
PPE	Protein precipitate extraction
PPP	Pentose phosphate pathway
Q	Quadrupole mass analyzer
QqQ	Triple quadrupole platform
QqTOF	Quadrupole-time of flight system
RF	Radio frequency
ROS	Reactive oxygen species
RP	Reverse phase
RPIP	Reverse-phase ion pair
RPLC	Reversed-phase liquid chromatography
RT	Retention time
SMDB	Small molecule pathway database
SPE	Solid phase extraction
TFA	Trifluoroacetic acid
TIC	Total ion chromatograms
TiO_2	Titanium dioxide
TOF	Time-of-flight mass analyzer
UHPLC	Ultra high performance liquid chromatography
UMP	Uridine monophosphate
WT	Wild type
XIC	Extracted ion chromatogram
ZrO_2	Zirconium dioxide

LISTE DES SYMBOLES ET DES UNITÉS

%	Percent
^{o}C	Degree Celsius
cc	Cubic centimetres
cm	Centimetre
Da	Dalton
g	Gram
L	Litre
m/z	Mass-to-charge ratio
mg	Milligram
min	Minute
mL	Millilitre
mL/min	Mililitre per minute
mm	Milimetre
mol/g	Grams per mol
ms	Milisecond
pH	Potential of hydrogen
ppm	Parts per million
psi	Pound-force per square inch
rpm	Revolutions per minute
s	Second
V	Voltage
µg	Microgram
µL	Microlitre
µm	Micrometre

RÉSUMÉ

Les métabolites sont de petites biomolécules, incluant les intermédiaires du métabolisme, qui sont impliqués dans des réactions essentielles à la survie d'un organisme. Les métabolites phosphorylés jouent un rôle critique dans plusieurs voies métaboliques telles que la glycolyse, la voie des pentoses phosphates et le métabolisme lipidique. En raison de leur rôles importants, des perturbations dans les concentrations de phosphométabolites peuvent être liées à plusieurs désordres. L'étude de ces composés pourrait permettre une meilleure comprehension des perturbations liées aux maladies. Cependant, dans de nombreux cas, les métabolites phosphorylés sont difficiles à analyser dans des échantillons biologiques complexes. Les métabolites contenant des thiols jouent également un rôle important dans de nombreuses fonctions cellulaires et peuvent souvent être instables en conditions de stress oxydatif, ou même pendant le stockage des échantillons. Les composés thiols libres sont particulièrement difficiles à mesurer avec précision dans des échantillons biologiques complexes, car ils peuvent former des disulfures ou des produits oxydés, ne refletant pas leur concentrations biologiques réelles. Afin d'améliorer la détectabilité de ces composés, des flux de travail utilisant la LC-MS/MS ont été développés. Pour améliorer la détection des phosphométabolites, une plateforme LC-MS/MS à haute résolution a été utilisée suivant différents stratégies de préparation d'échantillons pour l'enrichissement de ces métabolites, avec des mélanges de standards ainsi que des extraits de foie de souris et de *C. elegans* comme matrices biologiques complexes. La comparaison de méthodes pour la détection des phosphométabolites a démontré l'enrichissement de ces molécules avec une résine de dioxyde de titane (TiO_2). L'extraction en phase solide incorporant des interactions d'échanges d'anion et de phase inverse (MAX) est bien adapté aux composés acides, incluant plusieurs métabolites phosphorylés. Pour améliorer la détection des composés contenant des groupements thiols, l'avantage d'utiliser des réactions de dérivatization a été démontré, en incorporant des réactifs marqués légers et lourds pour les rendre plus stable avec une sensibility accrue. Une méthode ciblée utilisant la chromatographie liquide couplée à la spectrométrie de masse en tandem en mode MRM (suivi de réactions multiples) a été développée pour le suivi de trois métabolites spécifiques, dont la cysteine, le glutathion et la cystéine N-acétylée.

Mots clés : Phosphométabolites, thiols, disulfures, métabolites, spectrométrie de masse, chromatographie liquide, métabolomique

ABSTRACT

Metabolites are small biomolecule products and intermediates of metabolism, many of which are involved in reactions essential for the survival of an organism. Phosphorylated metabolites are known to have critical roles in several metabolic pathways such as glycolysis, the pentose phosphate pathway and lipid metabolism. Therefore, perturbations in phosphometabolite concentrations can be linked to several disorders. Studying these specific compounds could provide a better understanding of metabolic perturbations occluding in disease. However, in many cases, phosphorylated metabolites are hard to analyse in complex biological samples. Thiol-containing metabolites also play important roles in many cellular functions and are often unstable under oxidative stress conditions or even during sample storage. Free thiol compounds are therefore difficult to accurately measure in complex biological samples, as they can easily form disulfides or oxidized products. To increase the detectability of these compounds, tailored workflows using LC-MS/MS were developed. For improved detection of phosphometabolites, a semi-targeted method was developed using a high resolution LC-MS/MS platform to detect phosphometabolites that were enriched using various solid-phase extraction methods. The optimized methods were further compared using mouse liver and *C. elegans* biological samples. The comparison of methods for the detection of phosphometabolites demonstrated the enrichment of these molecules with titanium dioxide (TiO_2) resin. Solid-phase extraction incorporating anion exchange and reversed-phase (MAX) interactions is well suited for acidic compounds, including several phosphorylated metabolites. To improve the detection of compounds containing thiol groups, the advantage of using derivatization reactions was demonstrated, incorporating light and heavy labeled reagents to make them more stable with increased sensitivity. A targeted method using liquid chromatography coupled with tandem mass spectrometry in multiple reaction monitoring (MRM) mode was developed for the monitoring of three specific thiol-containing metabolites, namely cysteine, glutathione, and N-acetylated cysteine.

Keywords : Phosphometabolites, thiols, disulfides, metabolites, mass spectrometry, liquid chromatography, metabolomics

CHAPITRE 1

Introduction

Metabolites are small molecules implicated in various biological processes, many of which are essential for the survival of an organism. These molecules are a direct result of biological reactions, and therefore their concentrations can be used as an indication of biochemical activity (Haggarty & Burgess, 2017). In particular, metabolites change more rapidly than genetic material, and even protein synthesis/degradation, making them potentially more representative of an organism's phenotype. As such, by studying the metabolome, the complete set of metabolites present in a biological system metabolites have the potential to contribute to a better understanding of the current state of an organism, such as a metabolic pathway impacted by a particular disease or diet (Cui et al., 2018).

Despite the very promising role metabolomics has for health-related research, it comes with its own set of challenges. The metabolome is made up of highly diverse compound classes, with varying physiochemical properties such as their polarity, charge, size and stabilities. As a result, there is not one *fit-for-all* analytical method that allows for the identification and quantitation of all metabolites in a biological system (Kuehnbaum & Britz-McKibbin, 2013). To circumvent this challenge, various analytical methods have been developed to study particular groups of metabolites, including examples for estrogen conjugates using LC-MS (Nguyen et al., 2010), nucleotide analysis by LC-MS/MS (Yang et al., 2010), and aromatic compounds using GC-MS (Fiehn, 2016). Specific considerations need to be taken when dealing with highly complex biological samples which will be discussed in this Master's thesis.

1.1 Metabolites and Metabolomics

1.1.1 Metabolites

Metabolites are small organic molecules (less than 1500 Da) that are products and intermediates of various metabolic pathways and cellular regulatory processes in a biological system. These compounds undergo modifications during metabolic reactions and are necessary for growth, function and maintenance of living cells (Dwivedi et al., 2010; Haggarty & Burgess, 2017). Comprising of a wide range of chemical and physical structures, they play significant roles in various biological functions (such as energy production and storage, as well as signal transduction). As such, the concentration of these compounds serves as an indication of biochemical activities taking place in an organism, cell, or organ (Cui et al., 2018; Johnson et al., 2016). As

metabolites are a result of enzymatic reactions by proteins, which are in turn a result of gene expression (Figure 1.1A), they are usually representative of a given phenotype and can change very quickly in response to an environmental stressor, pharmacological intervention or disease state (Tan et al., 2016).

1.1.2 Metabolomics

Through omic studies, a better understanding of a biological system can be gained as it gives a more comprehensive understanding of the molecules that make up a cell, tissue or organism, which allows the organism to be studied as a whole. Different omic approaches are aimed at studying important molecules that make up an organism such as genes (genomics), mRNA (transcriptomics), proteins (proteomics), and metabolites (metabolomics). By studying an organism as a whole, it allows for a better understanding of both normal physiological processes and disease processes. Through omic strategies, it allows for biomarker discovery and drug discovery as shown in Figure 1.1B (Horgan & Kenny, 2011).

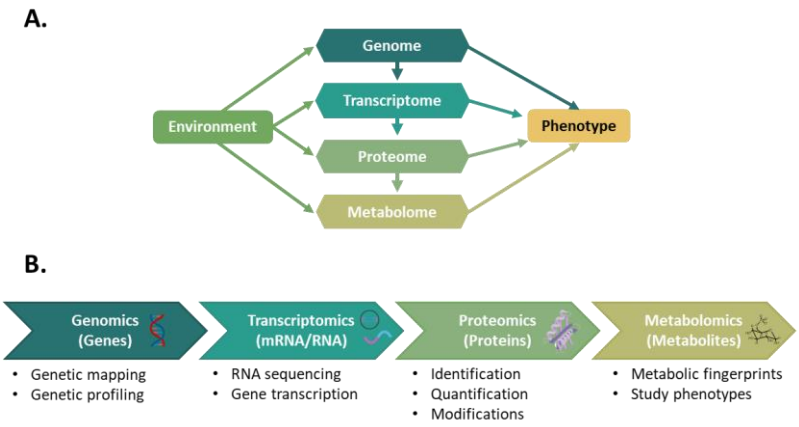

Figure 1.1 A) Interaction of the genome, transcriptome, proteome, and metabolome with the environment in a system, and B) the interaction of the various omic technologies and their applications. Adapted from Tan et al., 2016.

With genomics, the genome of an organism is studied and can reveal genetic abnormalities. Studying these abnormalities help further the understanding of diseases that have a genetic determination. With transcriptomics, one is able to study the genes that are being expressed at any particular moment, while proteomics aims to study the structure and function of proteins within an organism or system (Horgan & Kenny, 2011).

Metabolomics is the study of all the metabolites in a biological system, the metabolome, under a given set of conditions. Metabolites are products and intermediates of biochemical pathways, which are regulated by proteins. These proteins are a product of the translation of mRNA, which in turn is a product of the transcription of DNA. The metabolome often can more adequately describe the phenotype of a given biological system that is being studied, particularly due to the fact that the metabolome changes more rapidly than genetic material (Figure 1.1A). As metabolite concentrations can be linked to different signaling and enzymes activities, metabolomics has the ability to profile important changes occurring in disease and different exposures (Alberts et al., 2002; Haggarty & Burgess, 2017).

There are two main approaches to studying and analyzing metabolites, known as untargeted and targeted methods. When performing an untargeted analysis, a large number of metabolites can be analyzed in an unbiased approach. Also known as a "hypothesis-generating" approach, this type of approach allows for the simultaneous measurement of metabolites within a sample without prior knowledge of its composition. Through an untargeted analysis, novel metabolites can be discovered, which could allow disease mechanisms to be better studied and understood. When using a targeted approach, a specific list of known metabolites is analyzed. This approach is often "hypothesis-driven" for the validation of preliminary results with increased quantitative accuracy usually built into these assays (Becker et al., 2012).

Metabolites have a wide range of diversity in their structures and chemical properties, as well as their function in a biological organism, including several involved in very different metabolic pathways, which makes them quite challenging to study, especially with untargeted workflows. This diversity means that these compounds vary widely in reactivities, structural features, polarity, volatility, and concentrations. Though this diversity allows for the wide functionality of metabolites, it also creates analytical challenges as compounds are often analysed by exploiting specific characteristics of a class of compounds (Zhang et al., 2023). As the metabolome does not consist of a repeated structural element (such as the case is for protein, DNA, and RNA), the exploitation of specific characteristics of a compound is difficult. The differences in concentrations between trace and abundant compounds also make it difficult to measure metabolites. As such, there is no one single analytical technique that allows for the measurement of all metabolites at one time (Collins et al., 2021). Therefore, it is important to use analytical techniques that are versatile and robust enough to study various types of compounds. While sample preparation methods based on compounds of interest help ensure that the analytical method used maintains its robustness and consistency, this is not possible with purely untargeted approaches (Lepoittevin et al., 2023). Based on the

chemical and physical properties of compounds of interest, purification or fractionation techniques can be selected. Once separated, metabolites are then analyzed for structural elucidation and quantitation, with the most common methods involving mass spectrometry (MS) detection, or alternatively, nuclear magnetic resonance (NMR) spectroscopy, each with its own limitations and advantages (Horgan & Kenny, 2011).

In this project, the focus was on the detection of specific classes of metabolites by tailoring semi-targeted approaches to study compounds that have common chemical moieties which can be used for selective purification, derivatization, or that would produce common fragment ions in tandem mass spectrometry (MS/MS) (Wang et al., 2016). To analyze and produce MS/MS spectra, liquid chromatography coupled to high resolution tandem mass spectrometry (LC-HRMS/MS) was employed due to its robustness, sensitivity, and versatility. Samples were prepared using various techniques, including solid phase extraction and derivatization methods to selectively explore phosphorylated and thiol-containing metabolites, respectively.

For untargeted liquid chromatography coupled to tandem mass spectrometry (LC-MS/MS) analyses, the processing workflow (Figure 1.2) was as follows: 1) sample preparation, 2) LC-MS/MS analysis including separation and detection of metabolites, 3) (putative) identification of metabolites by comparing the tandem MS (MS/MS) spectra obtained from the sample to those from various spectral databases, and 4) statistical and pathway analysis to find biologically-relevant changes (such as disease markers). Spectral databases are libraries that contain the MS/MS spectra of pure chemical standards, with the most common spectral databases being the Human Metabolome Database (HMDB) and National Institute of Standards and Technology (NIST). MS/MS spectra is dependent on the instrument used, and so using an in-house spectral database provides increased confidence in the identification of metabolites (Cui et al., 2018; Wishart, 2008).

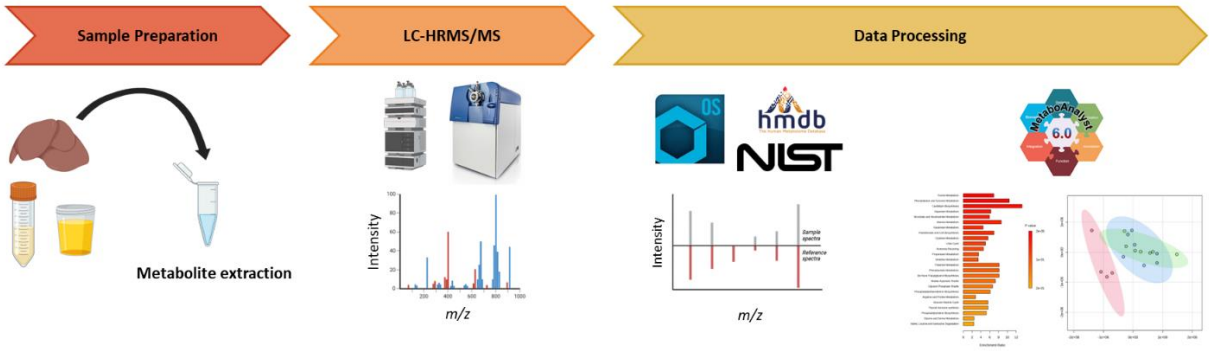

Figure 1.2 LC-HRMS/MS metabolomics workflow from sample preparation to data processing steps

1.2 Liquid Chromatography Coupled to High Resolution Mass Spectrometry (LC-HRMS/MS)

1.2.1 High Performance Liquid Chromatography (HPLC)

Chromatography is a separation technique that is used to separate individual compounds from samples of varying complexities, including complex biological matrices such as plasma, with some of the most common methods using either gas chromatography (GC) or liquid chromatography (LC). Based on the compounds of interest and matrix, chromatography is used prior to introducing the sample into a mass spectrometer to increase the detectablity and to help with the identification of compounds. The separation is based on the principle that compounds in a mixture are distributed based on their physico-chemical properties between the stationary phase in the column and a mobile phase (MP), which is liquid (LC) or gas (GC). It is the interaction between of the compounds in the samples with these two phases that allow for the effective separation of molecules within the mixture. Based on various molecular characteristics such as adsorption, polarity, charge, and the molecular size, compounds will have various levels of affinity to the stationary phase. Therefore, each compound has a characteristic retention time (RT), which is the amount of time taken for a compound to elute. This interaction allows for compounds, such as amino acids, carbohydrates and fatty acids, to be separated within a suitable time interval (Coskun, 2016; Tan et al., 2016).

While GC is used to study volatile and thermally stable compounds, LC can be used for a wide range of thermally unstable and non-volatile samples. High-performance liquid chromatography (HPLC) has become a method of choice to couple with MS detection for highly sensitive methods, including those involving metabolomic applications and biologically active molecules (Coskun, 2016). In the context of this

project, phosphorylated metabolites and thiol-containing metabolites are particularly difficult to detect due to polarity and instability, respectively.

For the separation of various groups of metabolites using LC, different chromatography methods are used, with the most common methods being normal phase (NP), reverse-phase (RP) and hydrophilic interaction chromatography (HILIC). Normal phase chromatography uses a polar stationary phase with a non-polar mobile phase thus leading to polar compounds to be retained for longer on the stationary phase. Unfortunately, the mobile phases that are traditionally used for normal phase are not very compatible with LC-MS applications. When performing reverse-phase chromatography, a solvent gradient of decreasing polarity is used with a hydrophobic non-polar stationary phase in order to retain and separate compounds. As such, polar compounds elute faster than non-polar compounds as the higher the hydrophobicity of the surface of the stationary phase is, the longer the analytes are retained. HILIC chromatography, on the other hand, uses a more hydrophilic stationary phase while using a solvent gradient of increasing polarity, usually involving relatively high salt concentrations (Emwas, 2015; Hanai, 2007). While reversed-phase liquid chromatography (RPLC) has its limitations with its retention times and ability to separate polar compounds, this technique is widely used in metabolomic studies thanks to ease of use, wide-range applicability, and reproducibility compared to HILIC and normal phase (Haggarty & Burgess, 2017).

As the individual compounds interact with the stationary phase, compounds within a mixture can be separated. When performing RPLC, the column is filled with functional groups, such as C18 hydrophobic chains bound to silica particles, making a non-polar column. It is the interaction of the individual compounds and the functional groups of the stationary phase that allow a mixture to be separated. Based on adsorption, partitioning, and ion-exchange mechanisms, the intermolecular interactions between the compounds in a sample and the stationary phase leads to differential migration which then allows compounds to elute at different times (Kuehnbaum & Britz-McKibbin, 2013; Snyder et al., 2011). As the separation of compounds is based on the interaction they have with the stationary phase, it is important that the chemistry of the stationary phase of the column is understood. This is particularly important as the functional group of a column is selective for certain compounds, such as a C18 column that is known for its affinity for non-polar compounds. As such, various columns were explored in the context of this project for their ability to separate the compounds of interest.

1.2.2 Tandem Mass Spectrometry

Mass spectrometry is a qualitative and quantitative analytical technique that ionizes molecules and separates them based on their *m/z* (mass-to-charge ratio) (Garg & Zubair, 2025). Once separated, the compounds are introduced into the mass spectrometer, where they are ionized, accelerated, and detected (Figure 1.3). As the mass analyzer is only able to detect charged compounds, the ionization of compounds is a crucial step for the detection of compounds. This step takes place at the ionization source of the mass spectrometer where the separated molecules are ionized and brought to gaseous phase. Depending on the mode of analysis, this ionization forms ions with either positive or negative charges. These ions then travel through a magnetic or electrical field in the mass analyzer where they are sorted based on their *m/z*. Once they make contact with the detector, the signals are generated and recorded by a computer system. These signals are then displayed graphically as a mass spectrum which shows the relative abundance of the signal according to the *m/z* ratio of the ions (Ho et al., 2003).

Using multiple mass spectrometers in tandem with each other, LC-MS/MS involves multiple steps of mass spectrometry where fragmentation takes place at each stage. By adding multiple stages of mass analyzers, the first analyzer will first isolate the precursor ion. The precursor ion will then fragment through either a dissociation process or a chemical reaction which forms product ions and neutral fragments. These ions and fragments are then passed through to a second mass analyzer (Madeira & Florêncio, 2012; Sleno & Volmer, 2004; Gross, 2004). Thus, *m/z* separation is achieved by the ions being selected in one section of the system, disassociated in the next intermediatory region and the disassociated products are then further analysed in the second mass analyzer. As tandem mass spectrometry uses a combination of analyzers, it exploits the strengths of each analyzer such as the specificity of quadrupoles and the ability of a time-of-flight system to accurately measure mass. When combining two different types of mass analyzers together, a hybrid tandem mass spectrometry system is formed, such as the commonly used quadrupole time-of-flight (QqTOF). Through the use of controlled fragmentation of precursor ions, LC-MS/MS can provide crucial structural information of analytes in the presence of high resolution and mass accuracy (Wang et al., 2023). As such, through LC-MS/MS, identification, quantitation, and structural elucidation of the compounds in a complex sample can be performed. Therefore, the versatility, selectivity,

sensitivity, and quantitative power of LC-MS/MS has made it the most commonly used technique for metabolomic analysis (Emwas, 2015; Wang et al., 2023; Yang et al., 2010).

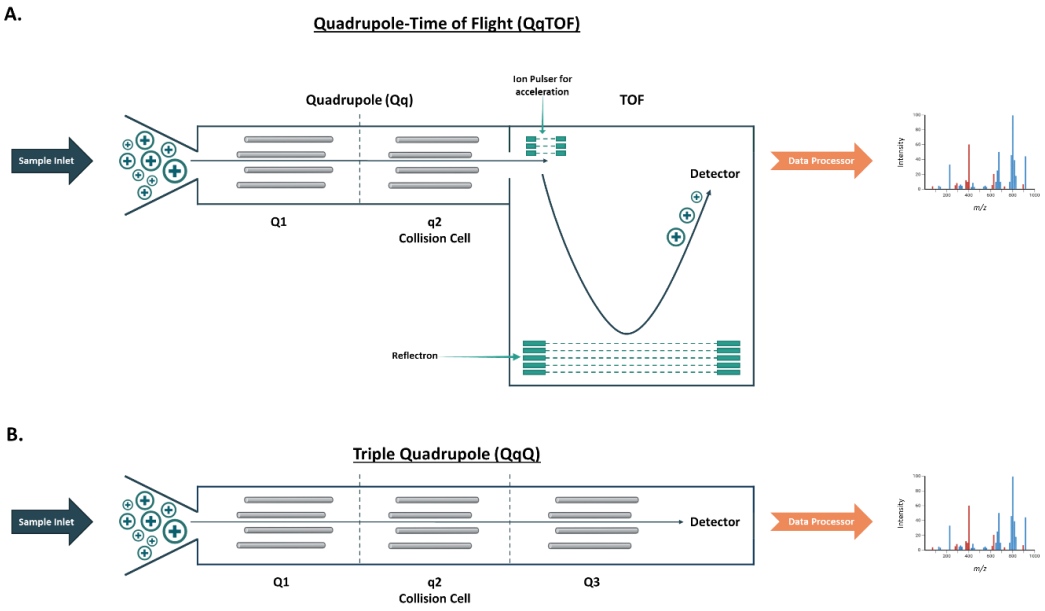

Figure 1.3 Diagram of A) hybrid quadrupole time-of-flight (QqTOF) and B) triple quadrupole (QqQ) tandem mass spectrometry systems. Adapted from Madeira & Florêncio, 2012.

Quadrupole (Q) and time-of-flight (TOF) are two of the most common mass analyzers used to separate ions based on their *m/z*. Different mass analyzers have specifications related to their resolution (or resolving power) and mass accuracy. The resolving power of an analyzer is its ability to separate neighboring ions in a mass spectrum. The mass accuracy is its ability to accurately measure the exact *m/z* of a compound of interest. A system with high resolving power has the potential for high mass accuracy when properly calibrated, and therefore can detect a compound within a low ppm (parts per million) error. To distinguish between different compounds, the error of its measured *m/z* should be as low as possible, to allow confirmation of its chemical formula. Quadrupoles are inherently low resolution analysers and function at unit resolution, whereas modern TOF systems range from 15, 000 to over 50, 000 resolving power, which can be calculated by the measured mass divided by the smallest distance between neighboring ions that can be well separated ($m/\Delta m$).

A Q analyzer is able to separate ions by using quadripolar fields. This analyzer consists of four cylindrical rod electrodes that extend in the z-direction and is mounted in a square configuration. With opposite rods being electrically connected, a radio frequency (RF) potential is applied with a direct current (DC) potential superimposed over each other which cause ions to oscillate as they pass through the quadrupole. By varying the frequency of the RF and potential of the DC, only ions of a specific *m/z* range will have stable trajectories as they do not encounter the charged rods. On the other hand, ions outside of the specified *m/z* range would oscillate into the rods, expelling them from the analyzer. Therefore, it is only the ions with stable trajectories that are detected as ions with unwanted *m/z* are filtered out. One of the major advantages of a Q analyzer is its high transmission capabilities and its ability to isolate ions within a specific *m/z* (Gross, 2004). A TOF analyzer is able to separate ions based on the principle that ions with different *m/z* travel at different speeds as they move through a field-free region. Before entering the flight tube, all the ions have the same kinetic energy. As ion speed is dependent on their *m/z*, ions of smaller *m/z* reach the detector quicker compared to ions with a larger *m/z*. Its high transmission, large *m/z* range and ability to measure exact masses make TOF mass analyzer an ideal choice for studying compounds in an untargeted way in order to differentiate compounds in a complex mixture having similar *m/z* (Haag, 2016; Gross, 2004).

Two distinct LC-MS/MS platforms were used in this research project. A quadrupole-time of flight system (QqTOF) (Sciex TripleTOF 5600+) and a triple quadrupole platform (QqQ) (Sciex QTRAP 5500) were employed for untargeted high-resolution (accurate mass) measurements and targeted multiple reaction monitoring (MRM) assays, respectively, both of which were equipped with electrospray ionization (ESI), as shown in Figure 1.3, both being coupled to HPLC at analytical flow rates (between 0.25 – 0.5 mL/min). ESI is a soft ionization source that minimizes in-source fragmentation and is easily coupled to LC at analytical flow rates, making it ideal for analyzing biologically-relevant metabolites within complex biological samples (Ho et al., 2003).

In a QqTOF system (Figure 1.3A), a Q mass analyzer is followed by a RF-only quadrupole which acts as a collision cell for ion fragmentation, which is then followed by a TOF analyzer allowing for both MS and MS/MS spectra to be acquired at high resolutions. The first quadrupole (Q1) will serve to either pass ions of a certain *m/z* range or isolate specific precursor ions of interest to selectively pass them through the mass spectrometer into the collision cell (Gross, 2017). Collisions between the precursor ion and an inert gas (usually nitrogen (N_2) or argon (Ar)) lead to an increase in internal energy. The increased internal

energy induces the decomposition of the precursor ion to form the fragment ions needed for acquiring a MS/MS spectrum (Haag, 2016; Madeira & Florêncio, 2012; Gross, 2017). QqTOF systems are often employed in untargeted metabolomics analyses. While metabolites have a wide range of structures, there are also a number of metabolites that have very similar elemental formulae. Therefore, in order to differentiate between compounds that are very similar to one another, high resolving power is necessary, in both the MS and MS/MS mode. Coupled with high mass accuracy, high-resolution tandem mass spectrometry (HRMS/MS) can be used to confirm the exact masses of compounds as well as their fragment ions. As the fragmentation pattern is dependent on the structure of the compound, a MS/MS spectrum allows for the confirmation or elucidation of a structure even if their exact masses are very similar to each other, as seen in Figure 1.4. This makes MS/MS crucial for the identification or selective detection of compounds in complex samples. It is through spectral matching with databases of known metabolites that the putative identification of unknown metabolites can help characterize complex biological samples in untargeted metabolomics. The QqTOF instrument was used for the detection of phosphorylated metabolites in standard mixes and complex biological extracts in the context of this project.

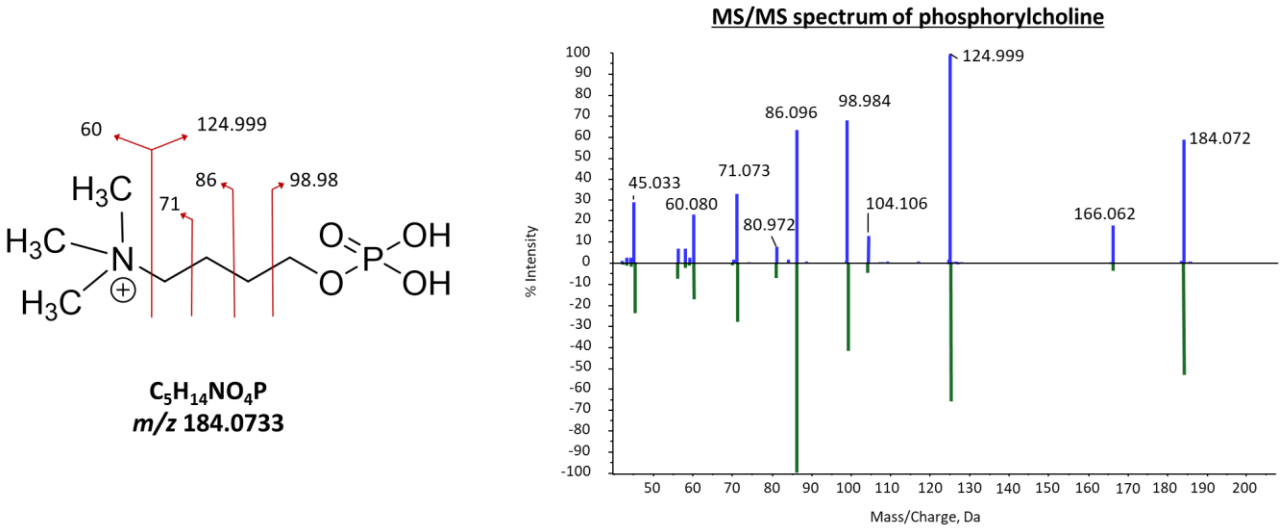

Figure 1.4 Example of MS/MS spectra of a peak putatively identified as phosphorylcholine in a biological sample with proposed fragmentation scheme illustrated on the structure. The mirror plot denotes the MS/MS spectra found in the database showing excellent agreement.

In a QqQ (Figure 1.3B), a third quadrupole (Q3) serves to measure the *m/z* of fragment ions, otherwise the system works in a similar fashion to the QqTOF described above. The most common scan mode used for QqQ platforms is MRM, where the precursor and fragment ions pairs are determined before a targeted

analysis. Therefore, Q1 and Q3 will isolate ions for the detection of a defined ion pair, where the precursor and fragment ion selected is referred to as a transition (Ho et al., 2003). This allows the QqQ to be highly selective and sensitive. LC-MRM performed on the QqQ produces smaller data files with much faster data processing time compared to QqTOF untargeted data files. As such, a targeted MRM method was employed for the study of thiol- and disulfide-containing metabolites.

Two modes of data acquisition can be performed for acquiring MS/MS in an untargeted manner: data-dependant acquisition (DDA) and data-independent acquisition (DIA). As DDA was performed throughout this project, it will be briefly explained. In DDA mode, which is also known as Information Dependant Acquisition mode (IDA), a MS full-scan data acquisition is initially done as a survey scan, which is immediately followed by multiple MS/MS analyses on a list of precursor ions that are selected based on selection criteria (usually the most intense ions in the survey scan). Only precursor ions of a specific intensity within this range are chosen for further fragmentation in the collision cell. With these parameters, the user can specify, for example, that in each cycle, only the ten highest intensity ions will be selected for fragmentation. Depending on the analytes of interest, these parameters can be changed leading to good quality MS/MS spectra as there will be little to no interference from ions outside of the selection window of interest (Figure 1.5).

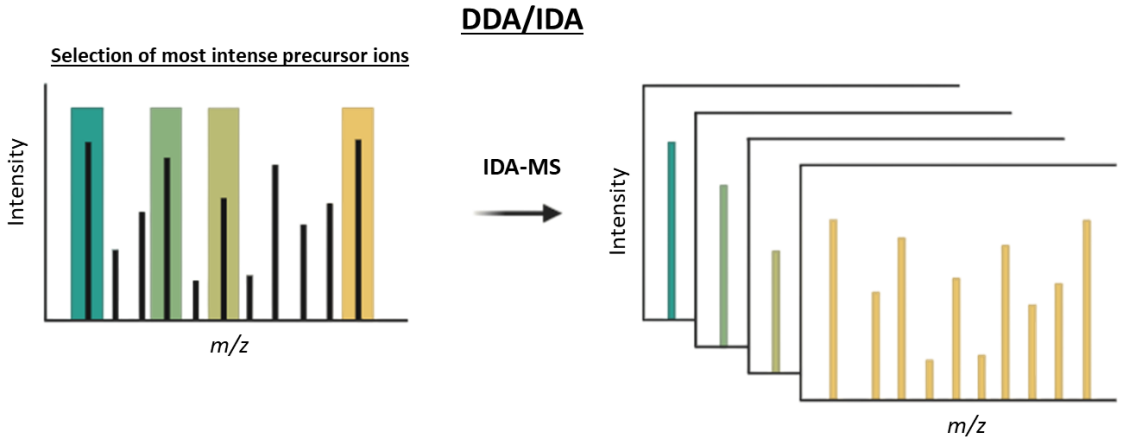

Figure 1.5 Data-dependant aquisition (DDA/IDA) allows high quality MS/MS spectra to be obtained by selecting the most intense precursor ions as shown in this example

Despite the sensitivity of LC-MS/MS for the detection of a wide range of compounds, matrix effects from biological samples can affect results. Matrix effect (ion suppression or ion enhancement) is generally

defined as the difference one sees in the response of a compound in a standard mix compared to the response seen of the same compound in a biological matrix. Matrix effects are caused by the co-elution of endogenous (such as salts, carbohydrates, amines) and exogenous substances (such as mobile phase additives like buffer salts and other contaminants). The presence of matrix effects in ESI makes the detection of certain compounds difficult**.** In particular, if the matrix compounds are present in high concentrations compared to the compound of interest, the matrix compounds can cause ion suppression of the compound of interest, where the ability of a compound to ionize is reduced (Panuwet et al., 2016). To reduce the matrix effect for the detection of compounds, certain classes of metabolites would need tailored workflows in order to improve their detectability (Matuszewski et al., 1998). As such, as phosphorylated metabolites and thiol-containing compounds are two classes of metabolites that have a wide range of polarities and can be present at low concentrations, developing a tailored workflow that would reduce matrix effects is one of the main goals of this Master's thesis.

1.3 Phosphorylated metabolites and possible enrichment methods

By focusing on subclasses of metabolites, a semi-targeted, more tailored method can be developed for their detection and quantitation by LC-MS/MS. One such subclass of interest are phosphorylated metabolites (phosphometabolites), which include several enzyme substrates or products from essential metabolic reactions, signalling molecules, and building blocks of various biomolecules (Figure 1.6) (Wohlgemuth, 2023). These metabolites can be involved in phosphorylation events and are important for various cellular functions such as cell growth, differentiation and energy metabolism (Salovska et al., 2013). As such, perturbations in their concentrations can be linked to energy related disorders. While these metabolites play an important role in various central metabolic pathways such as glycolysis, the Pentose Phosphate Pathway (PPP) and the Krebs Cycle, they come with their own set of analytical challenges, such as low concentrations, a wide range of polarities, and the potential for being affected by deleterious matrix effects (Salim et al., 2012). It is therefore of interest to develop analytical methods that would allow better detectability of these metabolites from complex biological samples.

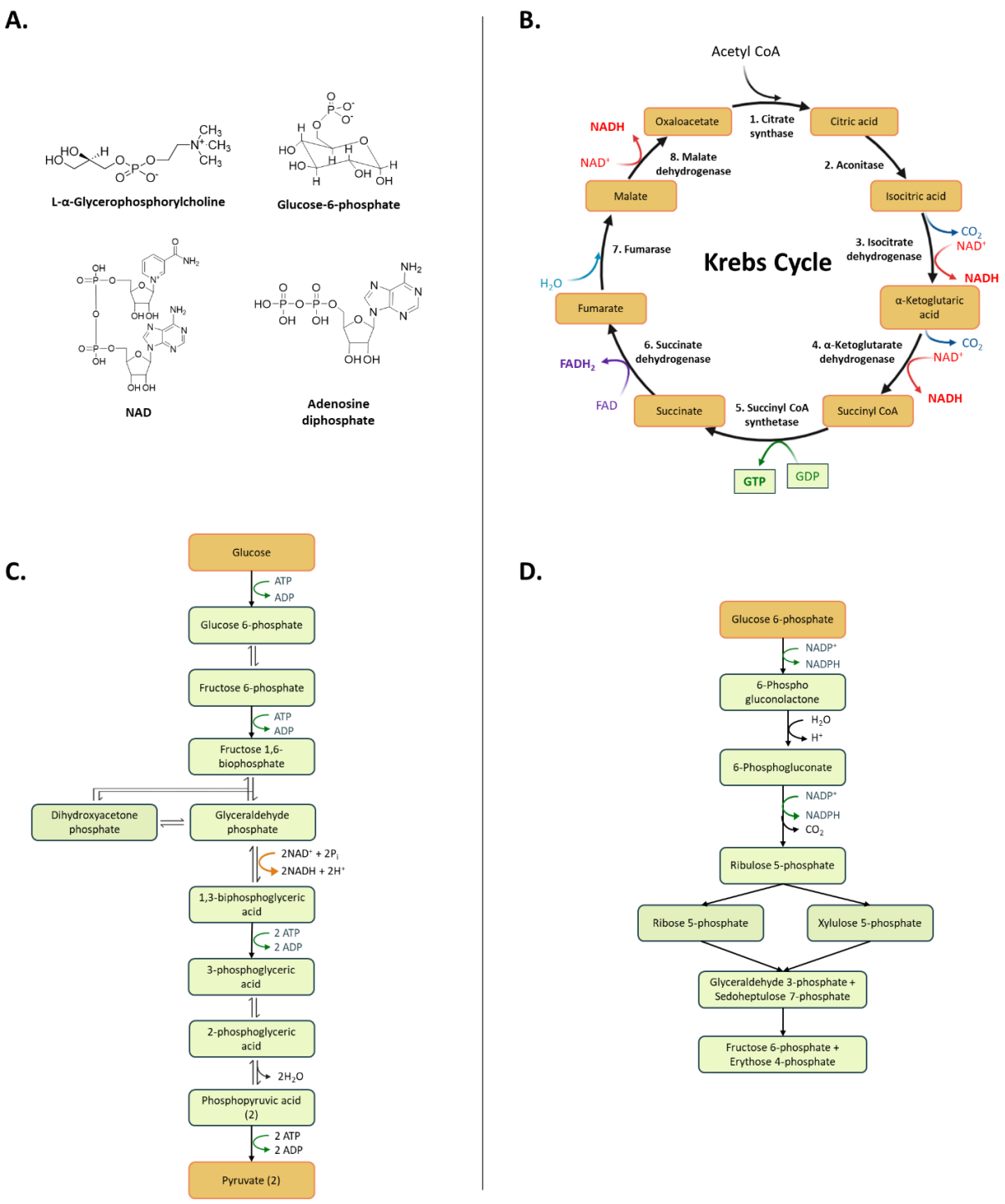

Figure 1.6 A) Four examples of phosphometabolites in an organism. Phosphometabolites play important roles in a number of important metabolic pathways such B) the Krebs cycle, C) glycolysis and D) the PPP. The phosphometabolites involved in these pathways are highlighted in green in this example. Adapted from Salim et al., 2012.

The separation and quantitation of phosphometabolites has been a topic of interest since the early 1960's and 1970's as seen in the work from Bessman, who developed an automated apparatus for phosphorylated intermediate detection (Bessman, 1974), and Kauffman, who studied the PPP in the brain by quantifying phosphometabolites (Kauffman et al., 1969). While numerous other studies, such as the MS detection of *myo*-inositol phosphate compounds (Qiu et al., 2020), have been performed since then, there is still more improvements that are needed to more comprehensively study these metabolites by LC-MS/MS.

In proteomics, phosphorylation sites of specific amino acid residues are important in the context of signaling pathways and have long been a subject of intense research with specific tailored enrichment methods being used over the last couple decades (Salovska et al., 2012). By enriching phosphorylated proteins or peptides prior to LC-MS/MS analysis, increased sensitivity and efficient characterization can be achieved. In phosphoproteomics, the three most widely used techniques include immunoaffinity chromatography using selective antibodies against phosphorylated residues, immobilized metal affinity chromatography (IMAC), and metal oxide affinity chromatography (MOAC), often using titanium dioxide as a solid support for enrichment (Gafken & Lampe, 2006; Thingholm et al., 2009) (Table 1.1).

Table 1.1 Various methods used for the detection of phosphopeptides or proteins from literature

Technique used	Principle	Example	Reference
Immunoaffinity chromatography	Antibodies used to target phosphorylated sites	Anti-phosphotyrosine antibodies enrich tyrosine phosphorylated proteins in cells to study epidermal growth factor receptor signaling pathway	Steen et al., 2002
Immobilized metal affinity chromatography (IMAC)	Positively charged metal ions on a resin chelate to a metal binding ligand	A 10-fold enrichment of phosphorylated peptides achieved compared to non-phosphorylated peptides when using IMAC	TenBroek et al., 2001
Metal oxide affinity chromatography (MOAC)	Metal oxides, titanium dioxide and zirconium dioxide (TiO_2, ZrO_2), used for their affinity to phosphate groups	Phosphorylated peptides were isolated from proteolytic digests using TiO_2 solid phase resin	Pinkse et al., 2004
		Different resins tested for their ability to detect phosphopeptides	Aryal & Ross, 2010; Salovska et al., 2012

When performing immunoaffinity chromatography, using antibodies for phosphoproteins can be costly and the limited selectivity of one antibody would necessitate the use of multiple antibodies for different sites of phosphorylation (Gafken & Lampe, 2006). IMAC is a widely used enrichment method for phosphopeptides, where metal ions (such as iron, aluminium, and zirconium (Fe^{3+}, Al^{3+} and Zr^{4+})) are chelated to a stationary phase such as silica or agarose beads using a metal binding ligand (also known as a metal chelator) like nitriloacetic acid or imidodiacetic acid (Batalha et al., 2012). The metal chelation allows the positive charge on the metal ions to attract the negatively charged phosphate group. However, this method exhibits non-specific binding of non-phosphorylated peptides. As such, there has recently been a rise of using MOAC as an alternative to IMAC. This recently gained popularity comes from the superior specificity and robustness MOAC has over IMAC (Salovska et al., 2013). Using metal oxides, such as titanium dioxide and zirconium dioxide (TiO_2, ZrO_2), that have a strong affinity for phosphate ions, MOAC exploits this property which enables the phosphate ions to bind non-covalently to the metal oxides while washing non-phosphoryalted species away, as demonstrated by Pinkse *et al.* using TiO_2 (Pinkse et al., 2004). This interaction is based on the ion-exchange between the metal oxide and the phosphate group which acts as a Lewis acid-base pair. Between the two metal oxides mentioned, TiO_2 is more commonly used for phosphopeptide enrichment as it is more robust towards experimental reagents, exhibits increased enrichment capabilities and is therefore more commercially available. While these methods have traditionally been used to study phosphopeptides, there has been less exploration of these methods for the detection of phosphometabolites. In this project, some methods designed for phosphoproteomics applications were tested for their usefulness for phosphometabolomics, with a particular focus on MOAC methods.

1.4 Thiol- and disulfide-containing metabolites

The other metabolite subclass studied in this research project are thiol-containing metabolites, which are metabolites that have a free sulfhydryl (-SH) or disulfide moiety. Low molecule weight (LMW) thiols, such as glutathione (GSH), cysteine (Cys), and hydrogen disulfide, are important compounds involved in redox biology (Figure 1.7A). They are involved in various biochemical reactions of cellular metabolism, the detoxification of reactive oxygen and nitrogen species, and the maintenance of cellular redox homeostasis. Thiols are also involved in the structural and functional control of many proteins. However, these compounds can be reactive and unstable and, therefore, have specific detection challenges (L. Wang et al., 2022).

As a well-regulated redox state of an organism is essential for normal physiological function and cellular metabolism, thiols play an important role in the antioxidant defence mechanism of an organism. Through the oxidation of free thiols (LMW thiols), disulfide compounds can form where a covalent bond is formed between two sulfur atoms (R-S-S-R') (Figure 1.7B). As such, through this redox reaction, free thiols have the ability to form and transfer disulfide bonds (Figure 1.7C). Therefore, free thiols are susceptible to direct oxidation or trapping of other reactive metabolites, making them one of the major targets of reactive oxygen species (ROS). High levels of ROS can cause oxidative stress damage in cells and tissues. Therefore, as the redox mechanism of thiols and disulfides maintain the cellular redox environment, pertubations in their concentrations can be linked to oxidative stress (Baba & Bhatnagar, 2018). As oxidative stress is linked to diseases such as cancer and cardiovascular disease, as well as various tissue damage and dysfunction that is associated with aging, thiols can be used as potential biomarkers for these conditions. Therefore, because of the role these thiols play, optimizing a method for their increased stability in biological extracts prior to their quantitation would provide a better understanding of their biological roles in health and disease.

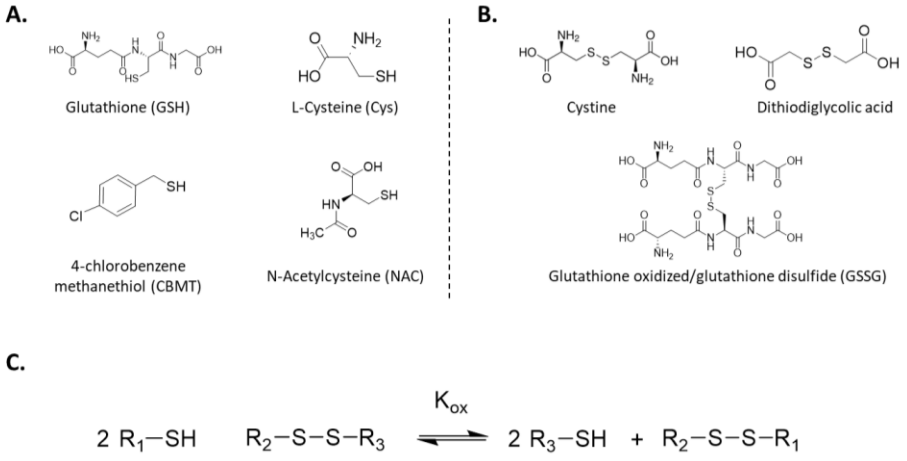

Figure 1.7 A) Examples of thiol- and B) disulfide-containing metabolites. C) Through this redox reaction, thiols and disulfides help maintain the redox state of an organism.

Despite the importance of these compounds, the quantitation of thiol species has remained a challenge largely due to their low concentrations and poor stability. The diversity of thiols also prove to be a major challenge when it comes to the selectivity of a method for thiols within a biological matrix. A method developed by Tominaga and his team has widely been used for the detection of thiols in wine, where

p-hydroxymercuribenzoate sodium is used for a liquid/liquid extraction of 3-mercaptohexanol acetate in wine (Tominaga, 1996). While efficient and specific to volatile thiols, this extraction leads to the inability to detect other non-volatile thiols. The length of the method also increases pre-treatment time and thiol concentration (Berthou et al., 2022). A number of quantitation methods have been developed over the years (Table 1.2). However, some of these methods are time-consuming, expensive, and can involve dangerous solvents and chemicals. While using derivatization agents help improve the detection of thiols, they also increase the sample preparation time. This increased sample preparation time can have a negative impact on the detection on certain types of thiols. Therefore, it is important to consider this when developing a sample preparation method.

Table 1.2 Literature review of quantitation methods for the detection and quantitation of thiol-containing compounds

Method and Principle	Example	Reference
Nanoparticles with affinity for thiols for capture or purification	Various nanomaterials have been used for the detection and quantitation of thiols	Häkkinen, 2012
Pre-treatment of the matrix by acidification, organic solvent addition, or filtration to remove unwanted compounds for improved chromatographic response	Addition of acetic acid for the stabilization and quantitation of GSH in blood	Camera et al., 2001
	Liquid-liquid extraction by p-hydroxymercuribenzoate sodium to isolate volatile thiols	Tominaga, 1996
Derivatization agents to improve the sensitivity and detection of target compound	The use of *n*-propyl chloroformate as derivatizing agent for the detection of homocysteine in human plasma	Sass & Endres, 1997

Nanoparticles (such as gold nanomaterials) have gained popularity thanks to their specificity, reactivity, and stability. However, the use of nanoparticules can be costly as they are non-reusable and their production can be restricted as their specificity to thiols is greatly dependent on their physiochemical properties (Berthou et al., 2022). While pre-treatment methods have been widely used for thiol detection as demonstrated by Camera *et al.* and Tominga, the length of the method must be taken in consideration. This is largely due to the instability of thiols that leads to rapid oxidation which can affect the quantitation of the thiol of interest (Camera et al., 2001; Tominaga, 1996). Using derivatization agents could be used to stabilize the free thiols and prevent their oxidation. By stopping the oxidation reaction, it would allow for a more accurate quantitation of thiols as more stable species whose concentration will not be altered by

oxidation will be present (Sass & Endres, 1997). As such, methods to stabilize these thiol-containing metabolites were explored for the scope of this project. In particular, as thiols are known for the formation of disulfide compounds by oxidation, particular attention was focused on developing a method that would restrict this formation and, by extension, allow for the accurate identification of both thiols and disulfides in a given sample.

1.5 Objectives

Phosphorylated and thiol-containing metabolites are important compounds that are involved in various metabolic pathways and cellular functions. However, these compounds have analytical challenges such as the co-elution with other metabolites in complex samples, exhibiting ion suppression from sample matrices causing difficulty in the detection of these compounds. While there has been various methods developed for the detection of these compounds, there is no one universally accepted method for the detection of all phosphometabolites or thiols. Therefore, the main objective of this project is to work towards tailored workflows that would improve the detectability of these compounds, in the hopes that phosphometabolites and free thiols can be measured quantitatively to follow perturbations in important metabolic pathways in the context of studying oxidative stress, signaling pathways or disease biomarker discovery.

In the semi-targeted analysis of phosphorylated and thiol-containing metabolites, LC-ESI-HRMS/MS was used for the detection and characterization of these compounds. ESI was used as it is a gentle ionization method that is less likely to negatively impact molecules that contain labile groups susceptible to in-source fragmentation or thermal degradation (Koley et al., 2022). As this project focused on improving the detection of specific subclasses of metabolites, various methods that target different metabolite subclasses were explored to increase metabolite coverage for a given sample. Increasing metabolic coverage would give a better understanding of a sample at a metabolic level. For the detection of phosphometabolites, sample preparation methods were studied by adapting methods previously used in phosphoproteomics applications. Results from this work are presented in Chapter 3. For thiol-containing compounds, derivatization methods were explored, as presented in Chapter 4, to stabilize these compounds as well as increasing their retention on the HPLC column, with the goal of improving detectability and quantitation of these compounds from biological matrices.

CHAPITRE 2

Materials and Methods

2.1 Materials

2.1.1 Chemicals

Two commercial metabolite mixes (named “HILIC” and “RPIP” mixes by the vendor) used were obtained from Fluidome Inc (Calgary, AB, Canada). The “HILIC” mix contains a total of 99 compounds (including 7 phosphorylated compounds) with a concentration range of 20 to 1000 µM. The “RPIP” mix contains 14 compounds (including 2 phosphorylated compounds) with a concentration range of 20 to 1000 µM. The metabolites in these mixes belong to three categories: amino acids and derivatives, central carbon metabolites and vitamins, and nucleotides and derivatives. Analytical standards (Tables 2.1 and 2.2) and HPLC grade solvents were obtained from Sigma-Aldrich (Oakville, ON, Canada), including ammonium bicarbonate (ABC), ammonium hydroxide (NH_4OH), iodoacetamide (IAM), acetonitrile (ACN), methanol (MeOH), ethanol (EtOH), and formic acid (FA). Hydrogen peroxide (H_2O_2), glycolic acid and trifluroacetic acid (TFA) were obtained from Fisher (Hampton, NH, USA). Custom derivatization agent N-(4-hydroxyphenyl)-2-iodoacetamide (also named IPAP), as well as its deuterated form (D_4-IPAP) were synthesized in-house as previously described (LeBlanc et al., 2014). Dithiothreitol (DTT) was obtained from Thermo Fisher Scientific Inc. (Waltham, MA, USA). Ultra-pure water (H_2O) was produced using a UV Millipore Synergy system (Billerica, MA, USA).

2.1.2 Sample preparation materials

MAX cartridge (1 cc, 30 mg) was obtained from Waters Ltd (Milford, MA, USA). MassPrep™ Phosphopeptide Enrichment µElution plate and MassPrep™ Enhancer powder was part of the MassPrep™ Phosphopeptide Enrichment Kit that was obtained from Waters Ltd (Milford, MA, USA). Bulk TiO_2 resin was obtained from SiliCycle Inc (Quebec City, QC, Canada) and placed into an empty 1 mL SPE reservoir obtained from Agilent (Santa Clara, CA, USA). Polystyrene thiophenol (PS-Thiophenol) resin (1.37 mol/g, with an average size of 88 µm) was obtained from Artisan Technology Group (Champaign, IL, USA). SiliaMetS Thiol (Si-Thiol) metal scavenger resin (1.15 mol/g with a size range from 40 – 64 µm) was obtained from SiliCycle Inc (Quebec City, QC, Canada).

2.1.3 Biological samples

Mouse liver samples of three different subgroups (control, disease, treated) of a mouse model of Hunter Syndrome, or Mucopolysaccharidosis II (MPS II) were obtained from a collaboration with the Auray-Blais lab (Department of Pediatrics, Université de Sherbrooke, Sherbrooke, QC, Canada). *C. elegans* samples were obtained from the Bénard lab (Department of Biology, UQAM, Montreal, QC, Canada). Healthy wild-type mouse tissue samples (liver, brain and feces) and serum was obtained from the animal facility at UQAM, in collaboration with the Pilon lab (Department of Biology, UQAM).

2.2 Sample preparation methods

2.2.1 Preparation of standards and mixes for method testing

To study phosphometabolites, the two in-house mixes of phosphometabolites prepared contained the analytical standards that are displayed in Table 2.1. The individual analytical standard stocks were prepared in H_2O. To study thiol- and disulfide-containing metabolites, the free thiols and disulfide compounds used are displayed in Table 2.2. The individual analytical standard stock solutions were prepared in H_2O at a concentration of 1 mg/mL.

Table 2.1 Phosphometabolites used for method optimization, including their formula, exact neutral monoisotopic mass and structure

Mix	Compound Name	Formula	Exact monoisotopic mass (neutral)	Structure
MIX 2	6-Phospho-D-gluconate (6PG)	$C_6H_{13}O_{10}P$	277.0319	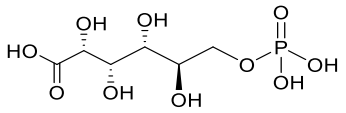
MIX 1	Adenosine diphosphate (ADP)	$C_{10}H_{15}N_5O_{10}P_2$	428.0367	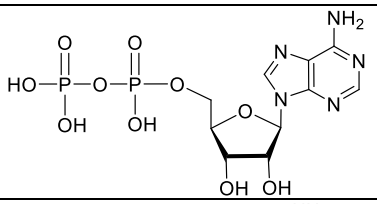
MIX 1	Adenosine monophosphate (AMP)	$C_{10}H_{14}N_5O_7P$	283.0941	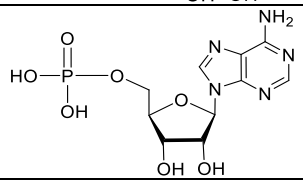
MIX 2	Aminoethylphosphonic acid (AMPA)	$C_2H_8NO_3P$	126.0315	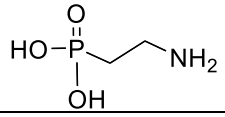
MIX 1	Cyclic adenosine monophosphate (cAMP)	$C_{10}H_{12}N_5O_6P$	330.0598	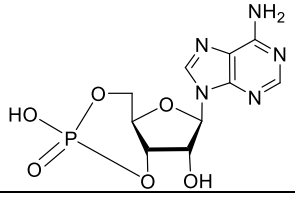
MIX 1	Cytidine monophosphate (CMP)	$C_9H_{14}N_3O_8P$	324.0591	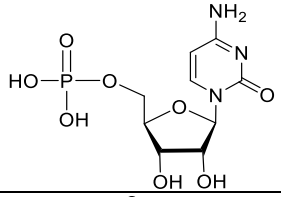
MIX 2	D-Glucose 6-Phosphate (G6P)	$C_6H_{13}O_9P$	261.0370	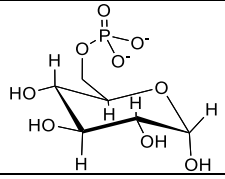
MIX 2	Erythrose 4-phosphate (E4P)	$C_4H_9O_7P$	201.0159	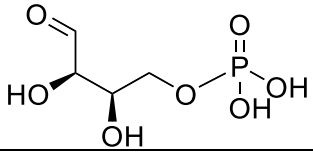

Table 2.1 (continued) Phosphometabolites used for method optimization including their formula, exact neutral monoisotopic mass and structure

Mix	Compound Name	Formula	Exact monoisotopic mass (neutral)	Structure
MIX 1	Fructose-6-phosphate (F6P)	$C_6H_{13}O_9P$	261.0370	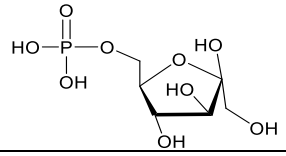
MIX 1	Glyceraldehyde phosphate (GAP)	$C_3H_7O_6P$	171.0053	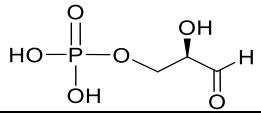
MIX 2	Glycerol 3-phosphate (G3P)	$C_3H_9O_6P$	173.0210	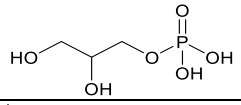
MIX 2	Glycerophosphorylcholine (GPC)	$C_8H_{20}NO_6P$	258.1101	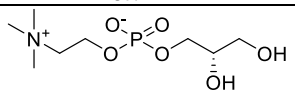
MIX 1	Guanosine monophosphate (GMP)	$C_{10}H_{14}N_5O_8P$	364.0653	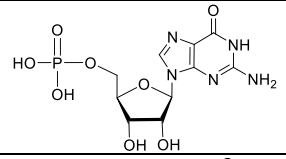
MIX 1	Inosine monophosphate (IMP)	$C_{10}H_{13}N_4O_8P$	349.0544	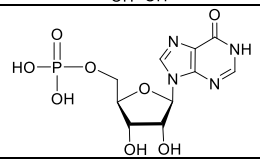
MIX 2	Phosphoserine (SEP)	$C_3H_8NO_6P$	186.0162	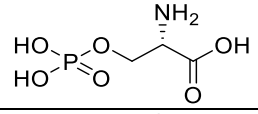
MIX 1	Riboflavin-5-phosphate (R5P)	$C_{17}H_{21}N_4O_9P$	457.1120	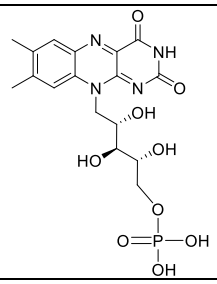
MIX 2	Ribose 5-phosphate (Ri5P)	$C_5H_{11}O_8P$	231.0264	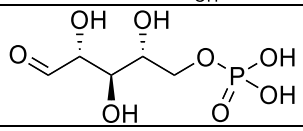
MIX 1	Thymidine monophosphate (TMP)	$C_{10}H_{15}N_2O_8P$	323.0639	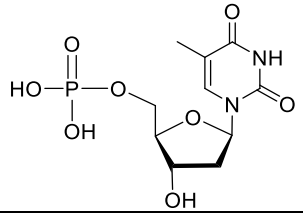

Table 2.2 Thiol- and disulfide-containing compounds used for derivatization tests including their formula, exact neutral monoisotopic mass and structure

Compound Name	Formula	Exact monoisotopic mass (neutral)	Structure
1-Propanethiol	C_3H_8S	76.0347	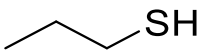
2-methyl-1-propanethiol	$C_4H_{10}S$	90.0503	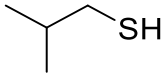
Thioglycolic acid (TGA)	$C_2H_4O_2S$	91.9932	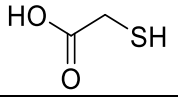
Thiophenol	C_6H_6S	110.0190	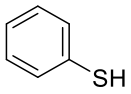
Cysteine (Cys)	$C_3H_7NO_2S$	121.0198	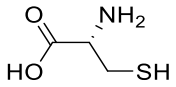
4-Aminothiophenol	C_6H_7NS	125.0299	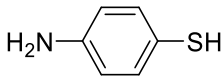
S-Methyl methanethiosulfonate (MMTS)	$C_2H_6O_2S_2$	125.9809	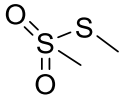
2,6-dimethylbenzenethiol (DMBT)	$C_8H_{10}S$	138.0503	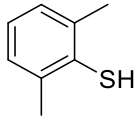
Cystamine	$C_4H_{12}N_2S_2$	152.0442	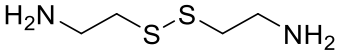
4-chlorobenzene methanethiol (CBMT)	C_7H_7ClS	157.9957	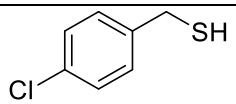
N-Acetylcysteine (NAC)	$C_5H_9NO_3S$	163.0303	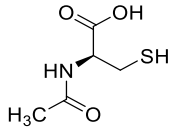
Dithiodiglycolic acid (DTG)	$C_4H_6O_4S_2$	181.9708	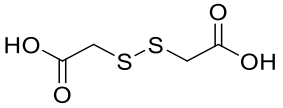

Table 2.2 (continued) Thiol- and disulfide-containing compounds used for derivatization tests including their formula, exact molecular weight and structure

Compound Name	Formula	Exact monoisotopic mass (neutral)	Structure
Cysteine ethyl ester (CEE)	$C_5H_{12}ClNO_2S$	185.0277	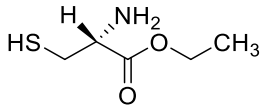
Thioctic acid / Lipoic acid (LA)	$C_8H_{14}O_2S_2$	206.0435	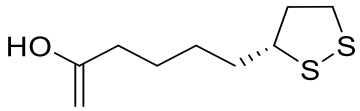
Cystine (Cys-Cys)	$C_6H_{12}N_2O_4S_2$	240.0239	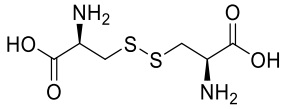
Tetraethylthiuram disulfide (TETD)	$C_{10}H_{20}N_2S_4$	296.0509	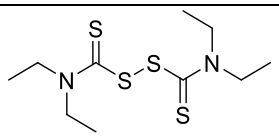
Glutathione (GSH)	$C_{10}H_{17}N_3O_6S$	307.0838	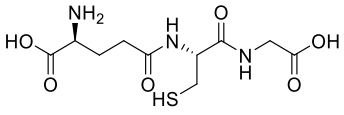
5,5-dithiobis(2-nitrobenzoic acid) (DTNB)	$C_{14}H_8N_2O_8S_2$	395.9722	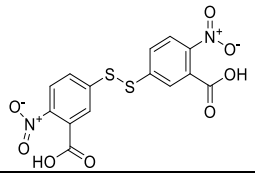
Glutathione oxidized/glutathione disulfide (GSSG)	$C_{20}H_{32}N_6O_{12}S_2$	612.1520	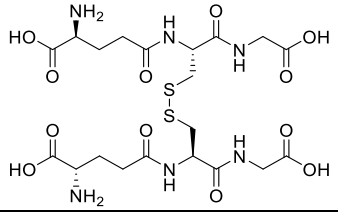

2.2.2 Metabolite extraction from biological samples

2.2.2.1 Mouse liver samples

To prepare the liver samples for extraction, EtOH:H_2O (85:15% v/v) and 0.5 mm glass beads was added to the liver samples in a bead beating tube to homogenize them using a bead beating machine (Bead Ruptor 12) (Omni Inc., Kennesaw, GA, USA). The supernatant was then dried down using a universal vacuum concentrator (SpeedVac) (Fisher Scientific, Mississauga, ON, Canada) and reconstituted with 25% MeOH for analysis (Figure 2.1).

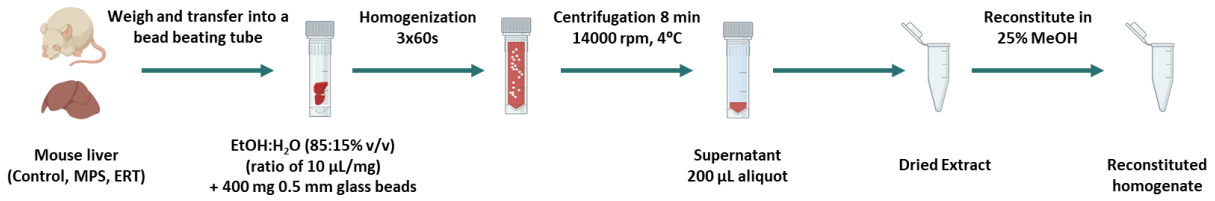

Figure 2.1 Mouse liver sample homogenization method to prepare the liver for analysis

2.2.2.2 *C. elegans* samples

To prepare the *C. elegans* samples for extraction, MeOH and 0.5 mm glass beads was added to the samples in a bead beating tube and homogenized using the Bead Rupter 12. The supernatant was then collected and a simple protein precipitation extraction was performed using MeOH. The supernatant of this extraction was then dried down using the SpeedVac (Figure 2.2) and reconstituted with specific diluant solutions for analysis.

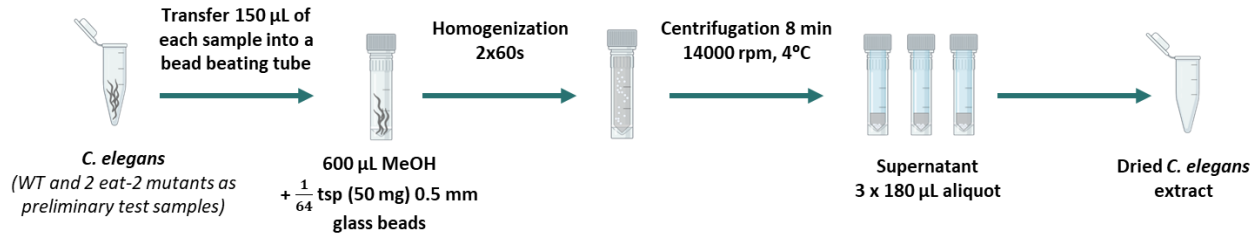

Figure 2.2 Sample homogenization method for the preparation of *C. elegans* samples for untargeted and semi-targeted phosphometabolite analysis

2.2.2.3 Mouse tissue samples

To study thiol-containing metabolites, mouse tissue samples (liver, brain, feces and serum) was extracted. To prepare the feces for analysis, 100 mM ABC buffer pH 8.0 was added to the samples in an Eppendorf tube. The sample was then spun down and the homogenate was then used for further analysis (Figure 2.3A). To prepare the liver and brain samples for extraction, 100 mM ABC buffer pH 8.0 and 0.5 mm glass beads was added into a portion of each tissue type for homogenization using the Bead Ruptor 12. The homogenate was then used for further analysis (Figure 2.3B).

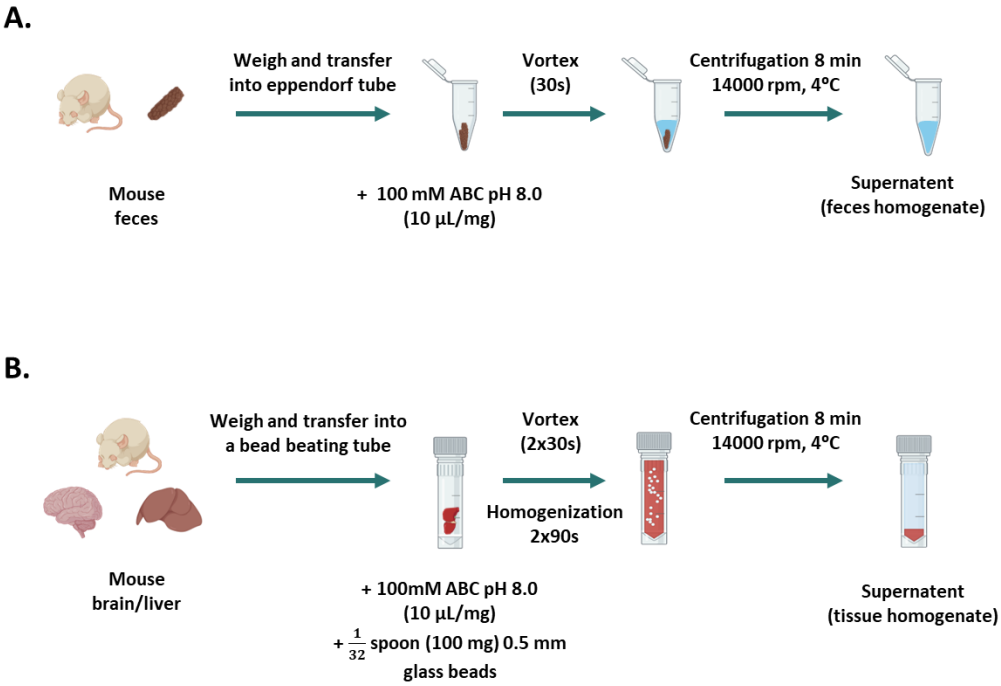

Figure 2.3 Protocol performed for the preparation of A) feces homogenate, B) liver, and brain homogenates for analysis

2.2.3 Phosphometabolite enrichment methods

For the detection of phosphometabolites, three different solid-phase extraction (SPE) methods were tested. A typical SPE cartridge contains a solid chromatographic packing material, also known as the sorbent, that is packed between porous frits. Based on the chemistry of the sorbent that contains surface-modified silica supports, SPE methods are able to separate different compounds of a given sample

through the interaction of the compounds with the sorbent. This interaction allows the compounds to bind to the sorbent which are then released by using an elution solution that is an appropriate organic solvent at a specific pH level. This clean-up method results in a relatively clean and enriched sample with a desirable concentration. As a more concentrated sample is produced, this clean-up method creates enriched samples that would allow for the better detection of low abundant compounds (Figure 2.4). When using a mixed-mode sorbent, a wider range of both hydrophobic and hydrophilic metabolites can be extracted compared to using a sorbent containing only one mode. A mixed-mode SPE exhibits two or more modes of interaction mechanisms as functional groups are attached to the silica surface of the sorbent (Badawy et al., 2022; Poole & Poole, 2012; Wu et al., 2019). As such, compounds can be separated on the basis of both polarity and functional group. The specific properties of the three methods tested are discussed below:

i) **<u>Oasis Mixed-mode Anion-eXchange (MAX) SPE cartridge</u>**

The Oasis MAX SPE cartridge is a quaternary (4^o) amine-based mixed-mode anion-exchange derivative of the Oasis HLB (Hydrophilic-lipophilic Balanced) cartridge that has a polymeric sorbent that is stable from pH 0 – 14. With a mixed-mode sorbent, the MAX SPE has both reversed-phase and ion-exchange functionality. More specifically, it is able to perform anion exchange, which allows the MAX cartridge to have greater selectivity and sensitivity for acidic compounds. With the presence of a 4^o amine (permanently positively charged) group, the sorbent retains negatively charged (anionic) compounds, as the anions bind to the positively charged amine groups. When an acidic elution solution is run through the cartridge, it protonates the anions bound to the sorbent making them neutral. This neutrality unbinds the once negatively charged analyte from the amine group and elutes the compounds (Waters, 2010).

ii) **<u>Metal Oxide Affinity Chromatography (MOAC) using titanium dioxide (TiO_2)</u>**

The principle of MOAC is based on the affinity of certain functional groups to metal oxide surfaces. This method has become an interesting alternative to IMAC due to its specificity and robustness, and was previously demonstrated by Kweon and Håkansson, who further studied MOAC for the detection of phosphopeptides. In the context of this project, TiO_2 was used as a sorbent in a SPE-based enrichment method.

iii) Waters MassPrep™ µElution plate

Waters MassPREP µElution plate is a 96-well micro-scale SPE plate developed by Waters for the selective enrichment of phosphoproteins. Included in the MassPREP™ Phosphopeptide Enrichment Kit, the high affinity sorbent in this plate allows for a high selectivity for phosphopeptides. In contrast to IMAC technology that is commonly used for the detection of phosphopeptides, there is no need for the use of a metal chelator that is normally used because of the affinity phosphate groups have to metal ions. This makes this µElution plate easy to use for phosphopeptide enrichment. This kit also includes a chemical (Enhancer™) which further improves the selectivity of phosphopeptides by displacing non-phosphorylated peptides (Waters, 2007).

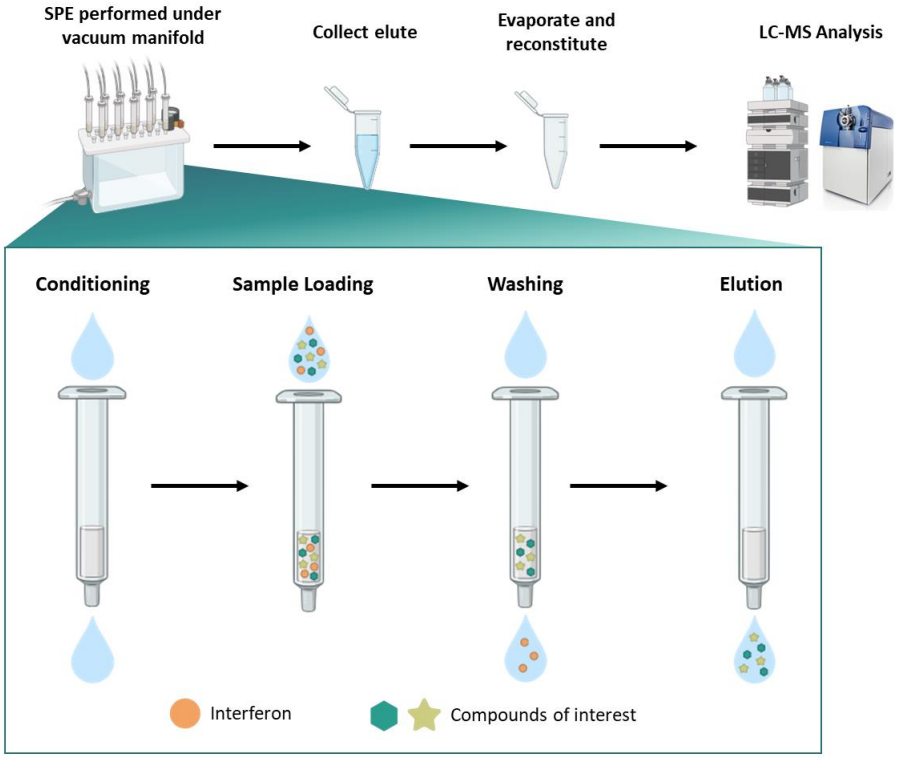

Figure 2.4 General workflow of SPE methods using a vacuum manifold. Before introducing the sample of interest, the SPE cartridge is conditioned to allow analytes of interest to be recovered once the elution solvent is passed through the cartridge.

2.2.4 Thiol derivatization reactions

Through derivatization reactions, derivatization agents are able to chemically alter a compound by targeting a specific site of the compound of interest, such as an alkylating agent that replaces a hydrogen (H) with another group. This modification leads to decreased volatility, modified chromatographic properties, and greater ionization efficiency. Therefore, derivatized compounds are produced that can be better detected using MS/MS (Ghafari & Sleno, 2024). For the optimization of the detection of thiol- and disulfide-containing metabolites, methods that would allow for the stabilization of these compounds were focused on by using the alkylating agents IAM, IPAP, and D_4-IPAP as derivatization agents. To prepare the alkylating agents, a 100 mM IAM solution was prepared in H_2O while the 10 mM and 100 mM IPAP and D_4-IPAP solutions were prepared in ACN. To prepare the reducing agent, 10 mM and 100 mM DTT solutions were prepared in H_2O. Scavenger resins (PS-thiophenol and Si-thiol) was also used in these reactions. The properties and reaction mechanisms of the alkylating agents, reducing agents, and resins are discussed further below:

i) <u>Alkylating agents</u>

a. Iodoacetamide (IAM)

IAM (ICH_2CONH_2) reacts with compounds to form an irreversible carboxamidomethyl derivative ($R\text{-}CH_2CONH_2$) through a nucleophilic substitution reaction (Figure 2.5A and 2.5B).

b. N-(4-hydroxyphenyl)-2-iodoacetamide (IPAP)

IPAP ($C_8H_8INO_2$) reacts with compounds to form an irreversible IPAP derivative ($R\text{-}C_8H_7NO_2$) through a nucleophilic substitution reaction (Figure 2.5A and 2.5C).

c. Deuterated-IPAP (D_4-IPAP)

In order to accurately quantify analytes, internal standards (IS) are used where it should have similar properties to the analyte of interest and, most importantly, not be present in the samples of interest. As such, isotopically labeled IS's such as deuterated (D, ^2H) and ^{13}C-labeled analogues have become the golden standard for quantitation as they would share the same chemical characteristics as the analyte of interest. By using a labeled IS, the analyte of interest and the IS would have similar extraction efficiency and chromatographic retention times, where the mass shift

between the two compounds would allow for their differentiation by mass spectrometry (Ghafari & Sleno, 2024). By using a deuterium-labeled IPAP (D_4-IPAP, $C_8H_4D_4INO_2$), it would react with compounds in a similar fashion to IPAP through a nucleophilic substitution reaction, forming an irreversible heavy labeled D_4-IPAP derivative (R-$C_8H_4D_4NO_2$) (Figure 2.5A and 2.5D).

ii) <u>Reducing agent</u>

a. Dithiothreitol (DTT)

DTT is a dithiol that is commonly used to reduce disulfides. In this reaction, the DTT itself is converted into a cyclic disulfide and the disulfide is reduced into the free thiols (Figure 2.6A and Figure 2.6B).

iii) <u>Scavenger resins</u>

Scavenger polymer resins are resins that are used to quench a completed reaction and selectively react with any excess reactants and/or reaction byproducts. This reaction would produce reactants that are bonded to the scavenger resin and can then be removed by filteration. Based on its functional group, different scavenger resins will be selective for certain chemical groups.

a. Polystyrene-Thiophenol (PS-Thiophenol)

PS-Thiophenol is a lightly cross-linked polystyrene thiophenol resin that is based on an aminomethyle resin with a tethered thiophenol functionality. Functioning as an electrophile scavenger, this resin has the ability to bind to alkylating agents such as alkyl halides and to quench the reaction and remove any excess present in a given sample (*Resins and Reagents*, n.d.) (Figure 2.7A).

b. Si-Thiol

Made up of irregular silica gel, Silia*MetS®* Thiol (Si-Thiol) is a metal scavenger with the ability to scavenge for a wide range of metals such as silver, mercury, and copper (Figure 2.7B) (*SiliaMetS Specification Sheet*, n.d.).

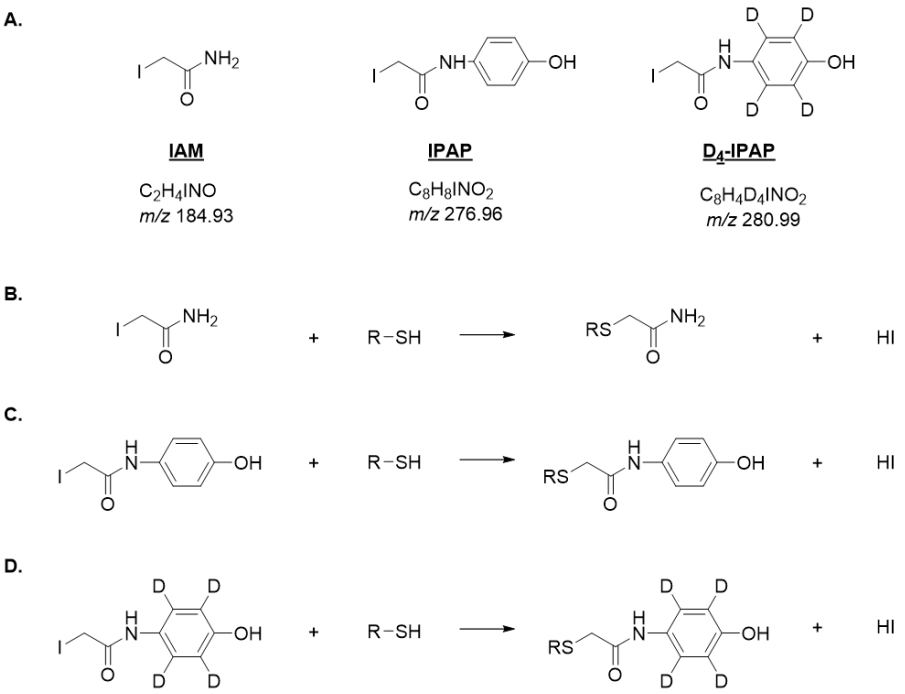

Figure 2.5 Alkylation agents used as derivatization agents, where A) depicts the molecular compounds of IAM, IPAP, and D_4-IPAP. The reaction of free thiols with (B) IAM, (C) IPAP, and (D) D_4-IPAP show the derivative compounds that would form when each agent is used.

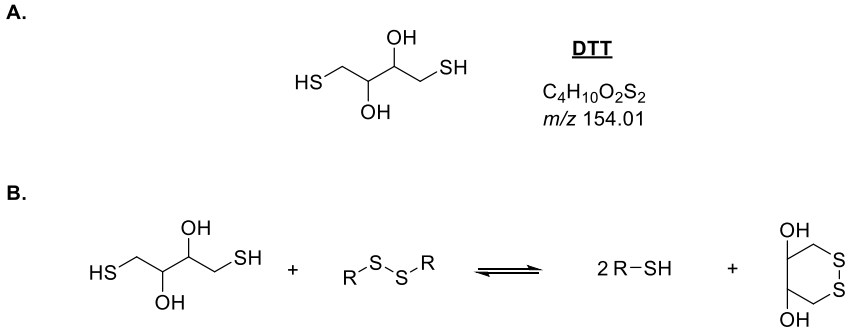

Figure 2.6 A) Molecular structure of the reducing agent (DTT). Figure B depicts the reduction mechanism of disulfides using DTT.

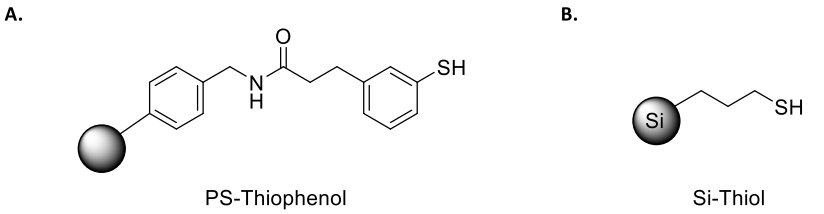

Figure 2.7 A) PS-Thiophenol and B) Si-Thiol scavenger resins used in derivatization reactions for the detection of thiol- and disulfide-containing metabolites

2.3 LC-MS/MS analyses

The columns used for the project were obtained from Imtakt USA (Portland, OR, USA) (Scherzo™ SM-C18 and Scherzo™ SM-C18 Metal Free), Phenomenex (Torrance, CA, USA) (Luna RP PFP™ (2) 100Å and Luna C18(2)), Thermo Fisher Scientific (Waltham, MA, USA) (Acclaim™ Organic Acid), and Agilent Technologies (Santa Clara, CA, USA) (ZORBAX Eclipse Plus C18) (Table 2.3 and Figure 2.8).

Table 2.3 Properties of the LC columns used for the detection of phosphometabolites and thiol- and disulfide-containing metabolites

Column	Dimensions	Chemistry	Retention mechanism	Selectivity
Scherzo™ SM-C18 (Scherzo column)	150 x 3 mm, 3 µM	Weak anion and cation ligands combined with C18 reverse phase chemistry	Reversed phase, Cation and anion exchange	Basic and acidic compounds; selective for highly polar compounds
Scherzo SM-C18 Metal-Free (Scherzo MF column)	150 x 2 mm, 3 µM	Weak anion and cation ligands; metal-free PEEK column body	Reverse phase, Cation and anion exchange, Normal phase	Basic and acidic compounds; selective for highly polar compounds
Luna RP-PFP™ (PFP column)	100 x 2.1 mm, 3 µM	Pentafluorophenyl propyl (PFP) group bound to silica; porous core	H-bonding, Dipole-dipole, π-π interactions, Hydrophobicity	Acidic, polar, and aromatic compounds
Luna C18(2) (Mercury column)	20 x 2.0 mm, 3.0 µm	C18 column; octadecyl silane bound to silica surface in porous particles	Hydrophobicity	Halogenated, aromatic, and conjugated compounds
Thermo Acclaim™ Organic Acid (Organic Acid column)	100 x 2.1 mm, 2.6 µM	Porous C18 phase; metal-free PEEK column body	Reverse phase	Small organic acids, e.g, nucleic acids and aromatic acids
ZORBAX Eclipse Plus C18 (ZORBAX column)	50 x 4.6 mm, 1.8 µm	C18 column; dimethyl-n-octadecylsilane bonded to a porous silica support	Reverse phase	Acidic, basic, and highly polar compounds

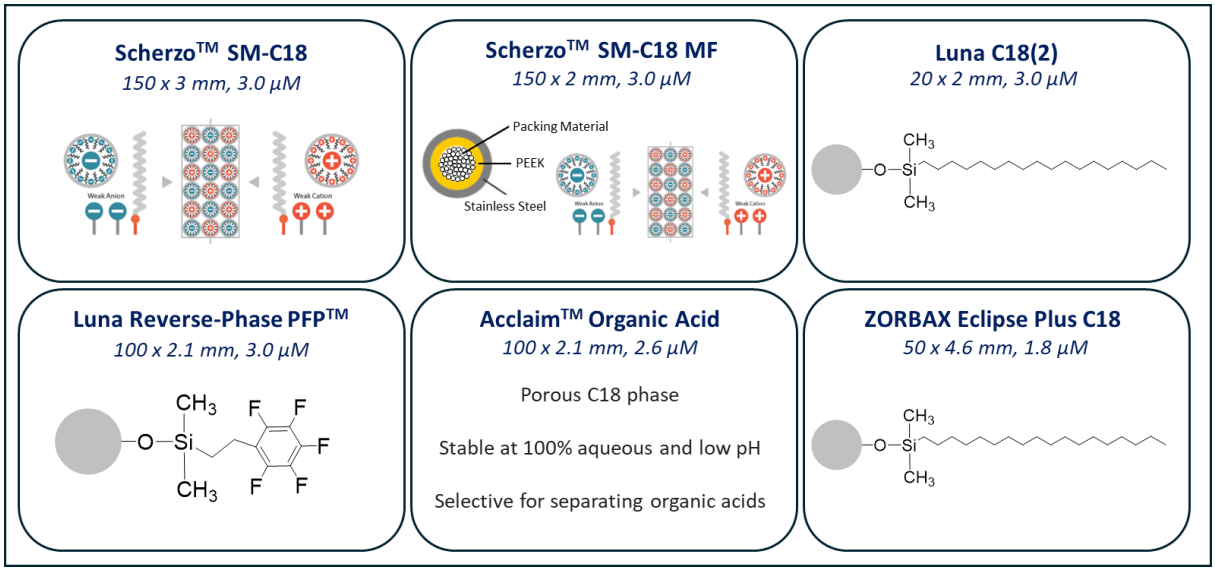

Figure 2.8 Differences in the chemistries of the six columns used throughout the project, along with their dimensions. From (*Acclaim Columns Overview*, n.d.; *Agilent ZORBAX Eclipse Plus C18*, n.d.; *Imtakt Scherzo Metal Free Column*, n.d.; *Phenomenex LC Product Guide*, n.d.; *Scherzo C18 Family*, n.d.)

2.3.1 LC-HRMS/MS (instrumentation, sources conditions, MS/MS parameters, LC conditions)

LC-HRMS/MS analysis was performed by injecting samples onto a LC column using a Nexera UHPLC (Shimadzu, Columbia, MD, USA) coupled to a TripleTOF 5600+ (QqTOF) mass spectrometer (SCIEX, Concord, ON, Canada) equipped with a DuoSpray source in both positive and negative electrospray mode.

The ion source parameters were set at 450^{o}C for source temperature, 5000 (or -4500) V for ion-spray voltage and 80 V for declustering potential (DP), 35 psi for curtain gas, 50 psi for nebulizer gas (nitrogen) and drying gases. The collision energy (CE) voltage was set at 10 V for MS acquisition and 30 V for MS/MS acquisition. An in-house standard mix (from *m/z* 120 – 922) was injected every four samples for auto-calibration of the system in MS and MS/MS mode to ensure the systems accuracy. While the same set of samples were analyzed, each of the columns used for LC-HRMS/MS analysis were of different compositions and sizes. Therefore, the acquisition parameters (LC separation, MS, and MS/MS) must be adjusted and optimized to achieve optimal results for each column. The LC separation parameters and the MS and MS/MS parameters for the columns used are described in Table 2.4.

Table 2.4 LC-HRMS/MS parameters used for LC-HRMS/MS analysis based on the column used

Parameters	Columns					
	PFP	**Scherzo**	**Scherzo MF**	**Organic Acid**	**Mercury**	**ZORBAX**
Mobile Phase A (MPA)	H_2O + 0.1% FA	H_2O + 0.1% FA				
Mobile Phase B (MPB)	100% MeOH	ACN + 0.1% FA				
Flow rate (mL/min)	0.25	0.30	0.30	0.30	0.50	0.50
Column Temperature (^oC)	NA	NA	NA	NA	40	40
Aquisition mode	IDA (8 most intense ions)				Full scan	IDA (5 most intense ions)
Gradient elution (% of MPB)	**18 min:** 3% for 2 min, 65% at 15 min, 95% at 15.5 min and held for 2.5 min				**3 min:** 10% for 0.5 min, 50% at 1.8 min, 95% at 1.9 min and held for 0.6 min	**8 min:** 5% for 0.5 min, 20% at 3 min, 85% at 5 min and held for 0.5 min
TOF MS range (*m/z*)	80 – 980 (200 ms accumulation time)				75 – 975 (900 ms accumulation time)	120 – 925 (300 ms accumulation time)
MS/MS range (*m/z*)	40 – 800 (100 ms accumulation time)				NA	50 – 625 (150 ms accumulation time)
Cycle time (sec)	1.1				1.0	1.1

2.3.2 LC-MRM (instrumentation, sources conditions, MS/MS parameters, LC conditions)

LC-MRM analysis was performed by injecting samples onto the ZORBAX column using a Nexera UHPLC (Shimadzu, Columbia, MD, USA) coupled to a QTRAP 5500 (QqQ) mass spectrometer (SCIEX, Concord, ON, Canada) equipped with Turbo IonSpray ion source in positive electrospray mode. MRM acquisition mode was used, with the transitions used detailed in Table 2.5. For each dwell transition, the minimum dwell

time was 50 ms and a total cycle time of 1.1 sec. Chromatographic separation of metabolites of interest was performed using the ZORBAX column with a flow rate of 0.5 mL/min, column temperature of 40^{o}C, and gradient elution with H_2O (MPA) and ACN (MPB), both containing 0.1% FA. This column used the same gradient elution for both the QqTOF and QqQ (Table 2.4).

Table 2.5 MRM method for the detection of GSH, Cys, and NAC IPAP and D_4-IPAP derivatives using the specific transitions for each derivative

Compound	Q1 Mass (Da)	Q3 Mass (Da)	Dwell Time (ms)	CE (V)
Cys IPAP	271	140	50	31
		182	50	19
Cys D_4-IPAP	275	144	50	31
		186	50	19
GSH IPAP	457	140	50	41
		208	50	41
		182	50	31
		328	50	19
		382	50	25
GSH D_4-IPAP	461	144	50	41
		212	50	41
		186	50	31
		332	50	19
		386	50	25
NAC IPAP	313	140	50	41
		166	50	41
		208	50	41
NAC D_4-IPAP	317	144	50	41
		170	50	41
		212	50	41

2.4 Data processing

Data was acquired using Sciex Analyst TF (v1.7.1) software and data visualization used PeakView (v2.2) with MasterView 1.1 from Sciex. For untargeted data processing, MarkerView (v1.2.1, Sciex) software was used for peak picking to find unique features using *m/z* and RT. The putative identification of metabolites was performed on Sciex OS-Q by importing the features list produced through MarkerView. The identification of the metabolites was done by performing spectral matching using several databases (SCIEX all-in-one HR-MS metabolite library, NIST database, and an in-house library of standard metabolites). The putative metabolites were determined using a mass error cutoff of ± 10 ppm and a library score of 80 for MS/MS spectral matching. This library score is based on the MS/MS spectra generated from the experiment and is compared to the MS/MS spectra in the libraries, where a high library score indicates a higher similarity to the library. Therefore, with the mass error cutoff and a high library score, the confidence in the identification can be increased. To ensure adequate signal/noise and proper integration of each putative metabolite, peak verification was performed using MultiQuant software (Sciex).

For the comparison of some of the biological samples, the results were first processed using the MultiQuant software and were then imported into MarkerView for most likely ratio normalization prior to statistical analysis using a Welch corrected t-test and Principal Component Analysis (PCA). Heat maps were constructed using NG-CHM Builder from MD Anderson Cancer Centre (Houston, TX, USA), where a csv file was used to upload the data of the defined peak area of each compound identified in a given sample (Ryan et al., 2020)**.** For each compound, the peak areas were normalized relative to the highest peak area for a given compound. For the heat map, hierarchical clustering was applied to row ordering options specifying Euclidean distance metric and Ward agglomeration with the original order was specified for column ordering options and no covariates were assigned. To further analyze the metabolites, enrichment analysis and group identification was performed using MetaboAnalyst 5.0 (Montreal, QC, Canada) (Pang et al., 2021). The HMDB numbers of the metabolites were used for analysis with Small Molecule Pathway Database (SMDB) based pathways selected and using metabolite sets containing at least 2 entries.

CHAPITRE 3

Enrichments methods to improve the detection of phosphorylated metabolites

Phosphometabolites are known to be challenging to analyze by LC-MS/MS given their low abundance and limited ionization efficiency. Therefore, developing an optimized method for the detection and quantitation of phosphometabolites will allow for the development and discovery of biomarkers by following perturbations in impacted metabolic pathways. For the development of this optimized workflow, various chromatographic methods and pre-column purification methods were explored and optimized using LC-HRMS/MS.

3.1 Method Optimization

3.1.1 HPLC Chromatography Optimization

While the separation of compounds through LC is driven by the distribution equilibrium of a solute between a mobile phase and the stationary phase, the selectivity of specific compounds comes from the interaction of the compounds within a mixture to the compounds that make up the stationary phase of the column. Therefore, it is important to take into consideration the chemical structure of the stationary phase when choosing the column for LC-MS/MS (Hanai, 2007; Kuehnbaum & Britz-McKibbin, 2013). When performing RPLC, such as is the case in this project, the surface of the silica particles on the solid phase is coated with an organic layer. This layer is mostly made up of siloxanes with alkyl ($-C_nH_{2n+1}$) or aryl ($-C_5H_5$, an aromatic ring with one H atom removed) end groups. The end group determines how the analytes of interest interact with the stationary phase. Based on the number of carbon atoms bound to the silica particles of the column, the column is able to retain various degrees of polar and non-polar compounds, with the hydrophobicity increasing with the increasing alkyl chain length. Long alkyl chains such as a C18 column will retain less polar compounds for a longer period of time leading to the more polar compounds eluting first, while a C8 column will elute less polar compounds earlier as these compounds would be retained for a shorter period of time (Gross, 2017). The mobile phases used for RPLC is composed of water and organic solvents, such as ACN or MeOH, and it passes through the stationary phase through isocratic elution or gradient elution. Isocratic elution is performed by retaining the same composition of mobile phase solvent throughout the separation, while the percentage of the mobile phase solvents change over time when using a gradient elution. By using a gradient elution, as is the case for this project, it would allow very hydrophobic molecules to elute from the column (Snyder et al., 2011). As such, as

phosphometabolites have a wide range of polarities, columns with different chemistries were tested using a gradient elution to study their ability to separate and therefore, improve the detection of phosphometabolites.

When performing untargeted metabolomics analysis in the Sleno lab, the Scherzo and the PFP columns are commonly used. In particular, the Scherzo column is known for its ability to separate highly polar and ionizable compounds and the PFP column is known for its ability to separate small polar compounds. By using the two columns for the same sample, complementarity is gained as a diversity of compounds can be separated and, ultimately, detected. While a good amount of diversity is gained when using the two columns, the main goal of testing different columns was to see if there was a major improvement in the chromatographic response when using different columns. In particular, the Scherzo MF and the Organic Acid columns were tested due to the chemistry of their stationary phases. Similar to the Scherzo column for retention mechanisms, the Scherzo MF column is considered metal free as the internal tubing surface of this column is made with polyether ether ketone (PEEK) material which is surrounded by its stainless-steel casing. The presence of the PEEK tubing makes it inert to chelating compounds, which are compounds that form complexes with metal ions by binding to multiple points. In the presence of metal, these chelating compounds will interact with the metal surface of the LC column causing chromatographic tailing and an increased RT. As the Scherzo MF column uses PEEK for its internal tubing, chelating compounds will have a lowered interaction with metal producing less peak tailing, sharper chromatographic peaks and an earlier RT. As the phosphate group in phosphometabolites allows them to form strong bonds with metal ions, the lack of metal in this column makes it an interesting alternative for better detection. This reduced interaction would also allow for compounds that would elute later on the Scherzo to be eluted earlier on the MF column (Product Guide MagReSyn Zr-IMAC HP, 2022). As such, if there are compounds that elute too late on the Scherzo column, the MF column has the potential to be able to separate and detect them. The Organic Acid column is made up of a porous C18 phase and is stable when using 100% aqueous and low pH conditions. This stability makes it suitable for separating organic acids, such as nucleic acids. This column is also packed with a metal-free PEEK column body, reducing the potential for peak tailing similar to the Scherzo MF column. As some phosphometabolites are small in size, this column was an interesting alternative for the detection of small phosphometabolites.

To compare the four columns (Scherzo, PFP, Scherzo MF, and Organic Acid columns), a mix containing phosphometabolites of known concentrations was created (Table 2.1). This mix was created by diluting

the individual standards in 25% MeOH to create a solution of µM concentrations. The phosphometabolite Mix 1 (Table 2.1) was then analyzed by injecting 10 µL in both positive and negative mode on the QqTOF in IDA mode for the 8 most intense ions, using the parameters described in Table 2.4. By using the same mix for all the columns, it would allow for the direct comparison of the columns ability to separate and detect the phosphometabolites.

3.1.1.1 HPLC Chromatography results

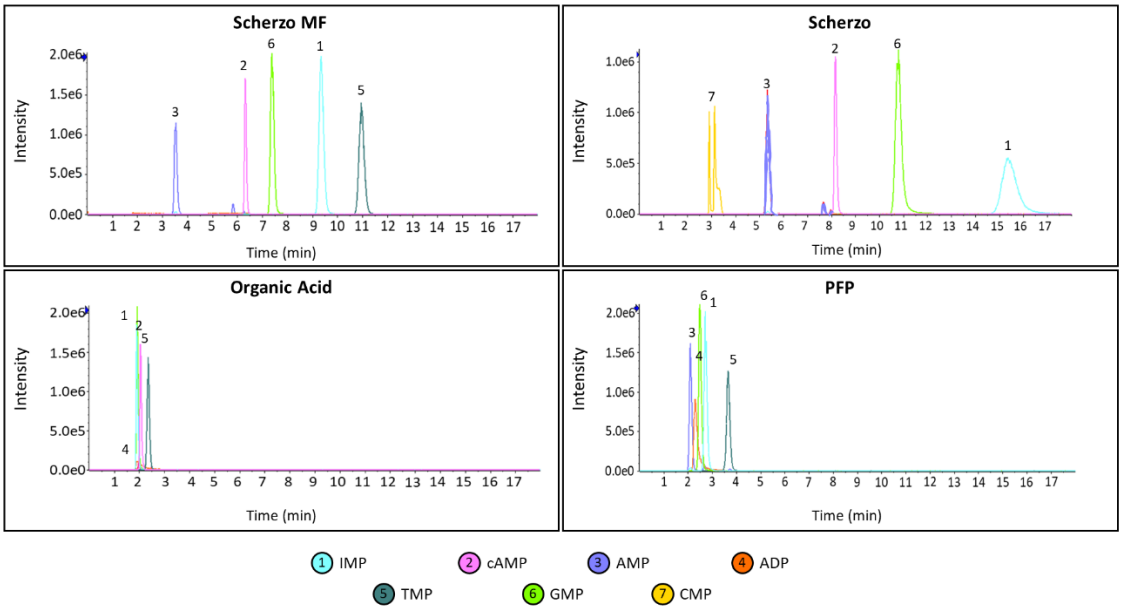

Figure 3.1 Extracted ion chromatogram (XIC) of phosphometabolite Mix 1 in negative mode when injected on Scherzo MF, Scherzo, Organic Acid, and PFP columns

From the extracted ion chromatograms (XIC) of the four columns (Figure 3.1), the four columns were able to identify seven out of ten compounds that were present in the mix. The XIC of a compound is the chromatrogram of a peak of a specific *m/z* value recorded as a function of the retention time. Similar to the Scherzo column, the MF column was able to separate the phosphometabolites well and produced sharp peaks. As the MF column contains less metal, the phosphometabolites eluted earlier compared to when they eluted when using the Scherzo column. For example, cAMP eluted at around 8 min on the Scherzo while it eluted at around 6 min on the MF column. While this shift in retention would allow compounds that elute later on the Scherzo column to be detected when using the MF column (RT of IMP is 16 min on the Scherzo column vs the RT of IMP is around 9 min on the MF column), there is the potential

that if a compound is too polar, it would not be detected when using the MF column. This scenario is seen in the XIC results of CMP on the Scherzo and MF column, where the RT of CMP on the Scherzo column is around 3 min, while CMP is not detected when using the MF column. From XIC of the Organic Acid column, the compounds eluted around 2 min with barely any separation. As such, this showed that the Organic Acid column would not be able to separate the compounds of interest. From the XIC of the PFP column, most of the compounds elute before 5 min. While the separation is not as clear as that seen on the Scherzo column, there a number of compounds detected using the PFP column (TMP and ADP) that were not seen when using the Scherzo column.

Therefore, from the results of the four columns, the Organic Acid column was removed from further testing due to its inability to separate the compounds. While the MF column was able to separate the compounds of interest well, there was no advantage of using the MF column over the Scherzo column. As such, from the results, there was no significant advantage of using different columns to the Scherzo and PFP columns already used in the lab. By using both the Scherzo and PFP columns, polar compounds that are not well retained on the Scherzo column are more likely to be retained when using the PFP column, thereby increasing the number of compounds detected when using the two columns in conjunction with each other. In addition, as untargeted analysis is performed using the two columns, the Scherzo and PFP columns, the optimized methods for phosphometabolites developed can be compared to any untargeted analysis performed. As there was no significant advantage in using a different column, pre-column enrichment methods for increased phosphometabolite detection were then explored.

3.1.2 Enrichment methods optimization

Based on the compounds of interest, it is important that the appropriate sample preparation method is chosen prior to LC-MS/MS analysis. As such, similar to the selection of the LC column, the type of sample preparation method used for the purification and enrichment of the sample of interest must take into the consideration. In brief, sample preparation methods are used to remove interfering molecules and compounds in the matrix of interest. Therefore, it is important to consider the interaction between the compound of interest and the chemistry of the preparation method as the sample containing the compound of interest must be in its most concentrated form possible for detection and measurement when injected in the LC-MS/MS system. One major drawback of LC-ESI-MS is the occurrence of ion-suppression or enhancement that is caused by the matrix or other interferons in the sample as it can lead to poor and unreliable data and can heavily affect the reproducibility, linearity, and accuracy of a method.

As such, sample preparation methods are used to try to reduce the introduction of matrix components into an analytical system. Through these methods, it not only increases the number of detected metabolites of interest, it also prevents build-up on the LC column and reduces the matrix effect in a given sample (Hanai, 2007; Lepoittevin et al., 2023; Trufelli et al., 2011). As this matrix effect continues to be one of the major challenges in the detection of phosphometabolites, various enrichment methods were explored to reduce this effect which would, in turn, enrich the low abundant phosphometabolites.

The most widely used sample preparation method is a protein precipitation extraction (PPE) where a miscible organic solvent (such as MeOH or ACN) is used, largely due to its large metabolic coverage and low cost. While a large metabolic coverage from a method is normally desirable, the wide range of specificity from solvent-based precipitation methods hinders the detection of low abundant metabolites, such as phosphometabolites. Therefore, to gain more specificity, a more selective method such as combining a solvent extraction with a SPE can be used. While performing a SPE would reduce the overall metabolic coverage of an extraction, it can also reduce the matrix effect of a complex sample and enrich the sample before being analyzed by LC-MS/MS (Lepoittevin et al., 2023; Wu et al., 2019). This makes this sample preparation method an ideal choice for the detection of low abundant phosphometabolites. The three SPE methods explored were MAX SPE cartridge, TiO_2 SPE cartridge and the MassPREP™ µElution plate (as described in Chapter 2, Section 2.2.3) by adapting and optimizing methods that were used for the detection of phosphopeptides such as those based on affinity, metal ion, and ion exchange interactions (Batalha et al., 2012).

The MAX SPE cartridge was tested as, while not specific for phosphorylated compounds, it is known to be selective for acidic compounds and a number of phosphometabolites are also acidic. The use of TiO_2 was explored as metal oxide surfaces (such as TiO_2 and ZrO_2) are known to have a particular affinity to phosphate-group containing compounds (Kweon & Håkansson, 2006). This affinity is due to the bidentate nature of the negatively charged phosphate group ($-PO_4^{3-}$) where two electron pairs are donated to the positively charged metal ion and the ability for the metal oxide to act as Lewis acids. TiO_2 and ZrO_2 have been used for SPE-based enrichment methods for phosphopeptides and phosphoproteins, with TiO_2 being more commonly used compared to ZrO_2 (Si-Hung et al., 2019). While much of this work has been focused on the detection of phosphopeptides, the same cannot be said for using the principle of MOAC for the enrichment of phosphometabolites, making TiO_2 an interesting approach for the selectivity of phosphometabolites. To use TiO_2 as a sorbent in a SPE method, approximately 50 mg of bulk TiO_2 resin

was placed into an empty 1 mL capacity reservoir (with one frit). The Waters MassPREP™ µElution plate was tested as it was developed for the detection of phosphopeptides. As the detection for phosphopeptides comes from the interaction of the phosphate groups with the affinity sorbent, this plate was tested to see if this same affinity would allow for the enrichment of phosphometabolites. The Enhancer™ from the MassPREP™ kit was also tested to study its ability to displace non-phosphorylated compounds which, by extension, would be able to enrich phosphorylated compounds. For the development of an optimized protocol using the three extraction methods, a literature review was performed and the protocols were adapted and tested to study their ability to detect phosphometabolites (Aryal & Ross, 2010; Salovska et al., 2013; Yu et al., 2007).

In order to test these methods for the detection of phosphometabolites, a metabolite mix of 104 metabolites and 8 phosphometabolites (Mix 2, Table 2.1) was extracted using the methods shown in Figure 3.2. For this mix (Mix 2), a combination of the two commercial mixes and additional phosphometabolites (aminoethylphosphonic acid, glycerophosphorylcholine, erythrose 4-phosphate) were combined together and diluted in 25% MeOH to create a solution of µM concentrations. A total of 10 different extraction methods were tested, with 6 methods being tested with the MAX SPE cartridge (Figure 3.2) and 4 methods for both the TiO_2 SPE cartridge and the MassPREP™ µElution plate each (Table 3.1). By using a mix with both phosphometabolites and non-phosphorylated metabolites, the strength of the methods for the detection of phosphometabolites can be better studied. To study the efficiency of the sample preparation methods, recovery samples were prepared which represents a sample with a 100% yield as this sample was simply prepared as a mix and injected and was not subjected to any extraction methods. The recovery samples were prepared by combining 100 µL of Mix 2 and 100 µL of 50% MeOH for the MAX methods, and 100 µL of Mix 2 with 100 µL of 0.5% FA in 25% MeOH for the TiO_2 and MassPREP™ µElution plate enrichment methods. For this analysis, 10 µL of the final sample for each method and their recovery samples was injected on the Scherzo and PFP columns and analyzed on the QqTOF in both ESI modes.

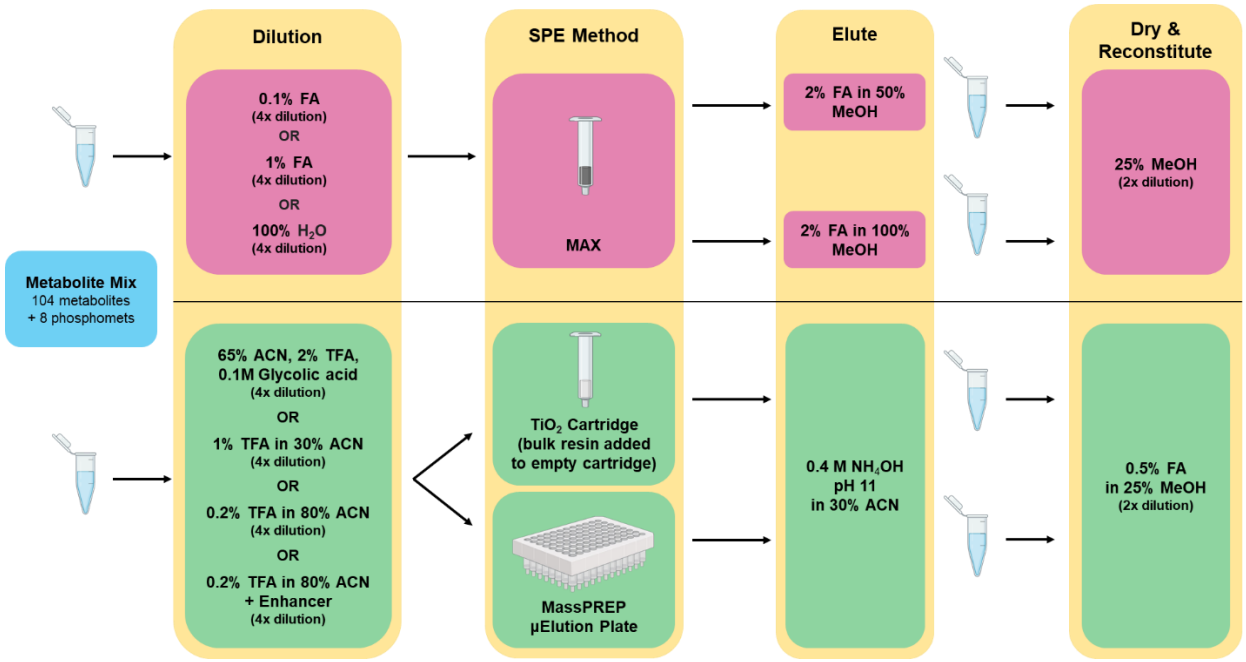

Figure 3.2 Protocol used to test enrichment methods using MAX SPE catridge, TiO_2 SPE cartridge, and the MassPREP™ µElution plate

For the MAX SPE methods, three different loading buffers with varying levels of acidification using FA (0% FA (100% H_2O), 0.1% FA in H_2O, and 1% FA in H_2O) was tested. As the MAX SPE cartridge is selective for anionic compounds, acids are generally used for pH control which in turn can affect the retention selectivity of the cartridge. However, if the sample is too acidic, it could cause protonation of the compounds leading to more anionic compounds. This could potentially lead to more compounds being formed that are not true anions themselves, where they are rather adducts formed from other compounds present in the mixture. The formation of these adducts could then lead to the misidentification of unknown compounds. Therefore, by changing the amount of FA, the effect acidification levels has on the ability of a compound to be retained on the sorbent can be studied. As the ionization state of a compound changes the way it interacts with the SPE sorbent, it is important to use an elution solution that allows for the greatest number of compounds to be eluted. When using the appropriate elution solution, the interaction between the analyte of interest and the functional group of the sorbent in weakened, allowing the compounds to be eluted. By using a polar solvent, which is considered a weak elution solution, compounds would be retained on the sorbent for a longer amount of time which, in turn, would improve the fractionation and retention of compounds. Therefore, two elution solutions (2% FA in 50% MeOH and

2% FA in 100% MeOH) for the MAX SPE methods were tested, where the presence of H_2O in the 2% FA in 50% MeOH would increase the polarity of the solution. By testing the two elution solutions, it would help determine which elution solution would allow for the retention of a wider range of compounds.

To test the TiO_2 cartridge and the MassPREP™ µElution plate, four methods were adapted and tested. When used for the detection of phosphopeptides, previous studies have demonstrated that ACN would prevent hydrophobic interactions between peptides and the sorbents used for their enrichment. By creating a more acidic environment, TFA would minimize the binding of non-phosphorylated peptides. The addition of glycolic acid was shown to be an effective non-phosphorylated peptides-excluding agent (Salovska et al., 2013). When using MassPREP™ µElution plate, a loading buffer solution of 0.2% to 0.5% TFA in 80% ACN was recommended to be used (Waters, 2007). From the MassPREP™ kit, the MassPREP™ Enhancer powder is solubilized in the same loading buffer solution recommended. The MassPREP™ Enhancer power is used to improve the selectivity of phosphopeptides by displacing the non-phosphorylated peptides from the sorbent of the MassPREP™ µElution plate. As these additions have been shown to improve the detection of phosphopeptides, the same additions were tested to study their effectiveness on the detection of phosphometabolites. As such, to study the effect of ACN and TFA, various concentrations were tested. Glycolic acid was added into the loading buffer to study its ability to exclude non-phosphorylated metabolites. To test the Enhancer power, the Waters method was tested by preparing the loading buffer with and without the Enhancer powder.

For the MAX methods, 100 µL of Mix 2 was diluted in 400 µL of the loading buffer for a total of 500 µL of the sample. The MAX cartridge was conditioned using 1 mL of MeOH, followed by 1 mL of H_2O before loading the sample onto the conditioned cartridge. The cartridge was then washed with 200 µL of 2% NH_4OH followed by 200 µL of MeOH. To elute the compounds of interest, 500 µL of elution solution was then used which was then dried down using the SpeedVac. The dried sample was then reconstituted in 200 µL of 25% MeOH. To test the effect of acid in the loading buffer, MAX methods 1 and 4 used 0.1% FA, MAX methods 2 and 5 used 1% FA, and MAX method 3 and 6 used 100% H_2O. To test the elution solution, MAX methods 1 to 3 used 2% FA in 100% MeOH and MAX methods 4 to 6 used 2% FA in 50% MeOH.

For the TiO_2 cartridge and MassPREP™ µElution plate methods, 100 µL of Mix 2 was diluted in 300 µL of the loading buffer for a total of 400 µL of sample. For clarity, the loading buffers, conditioning and wash

solutions used in these two methods are described in Table 3.1. Following these steps, 400 µL of 0.4M NH_4OH pH 11 in 30% ACN was used to elute the compounds of interest which was then dried down using the SpeedVac. The dried sample was then reconstituted in 200 µL of 0.5% FA in 25% MeOH. To test the MassPREP™ Enhancer power, a 50 mg/mL Enhancer solution was prepared using 0.1 g of the powder dissolved in 2 mL of 0.2% TFA in 80% ACN, as previously described (Waters, 2007).

Table 3.1 The conditioning solutions, loading buffers, and washing solutions used for the optimization of TiO_2 cartridge and MassPrep™ µElution plate methods 1 to 4

	Method 1	**Method 2**	**Method 3**	**Method 4**
Conditioning	NA	200 µL of 1% TFA in 30% ACN	200 µL H_2O 200 µL of MeOH	200 µL H_2O 200 µL of MeOH
Loading Buffer (300 µL)	65% ACN	1% TFA in 80% ACN	0.2% TFA in 80% ACN	50 mg/mL Enhancer powder in 80% ACN and 0.2% TFA
Wash 1 (200 µL)	0.1M Glutamic acid in 65% ACN and 2% TFA	NA	NA	NA
Wash 2 (200 µL)	0.5% TFA in 65% ACN	1% TFA in 50% ACN	0.2% TFA in 80% ACN	0.2% TFA in 80% ACN
Wash 3 (200 µL)	30% ACN	30% ACN	0.2% TFA in 80% ACN	0.2% TFA in 80% ACN

3.1.2.1 Enrichment method results

The recovery of each phosphometabolite was calculated by comparing the area under the chromatogram of the phosphometabolite of interest in the recovery sample to the area under the chromatogram of the phosphomet when extracted using a specific enrichment method (Equation 3.1). With this percentage, one is able to study the efficiency of an analytical extraction process by using a known amount of an analyte (Kumar et al., 2022). Therefore, by comparing the recoveries of the phosphometabolites from each method, it would determine which method would best enrich the phosphometabolites of interest.

Eq 3.1

$$Recovery\ \% = \left(\frac{Area\ of\ compound\ when\ extracted}{Area\ of\ compound\ in\ recovery\ samples}\right) * 100$$

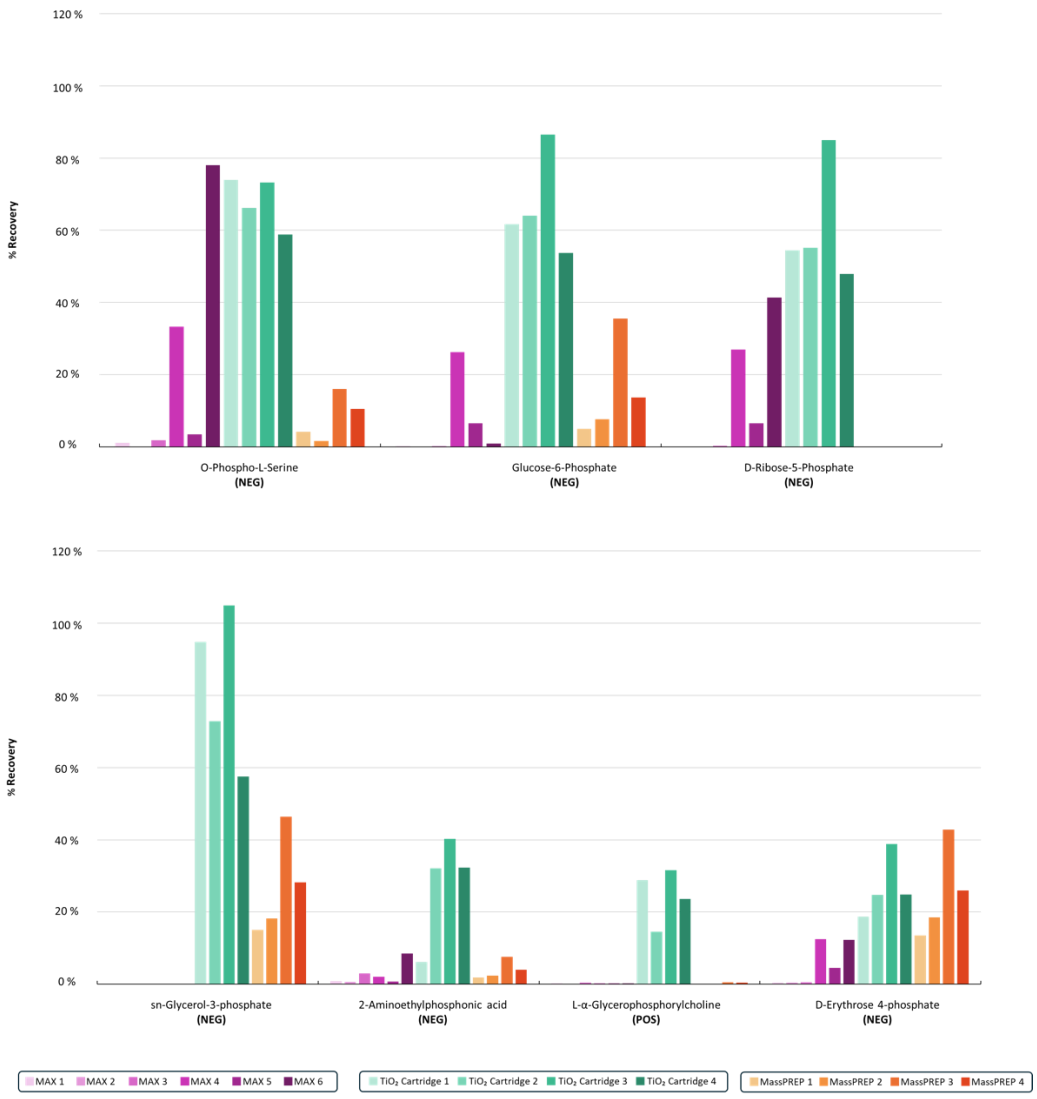

Figure 3.3 Recovery percentages of the phosphometabolites of interest injected on the Scherzo column when extracted using the MAX SPE cartridge, the TiO_2 SPE cartridge, and the MassPREP™ µElution plate. Most phosphometabolites were better detected in negative mode, while glycerophosphorylcholine was only detected in positive mode.

Based on the results on Figure 3.3, the MAX and TiO_2 enrichment methods gave the best recoveries of the phosphometabolites, while the MassPREP™ µElution plate gave low recoveries of phosphometabolites, with a maximum recovery of 46%. This could be due to the sorbent of the µElution plate being part of a kit specifically designed for the enrichment of phosphoproteins, where the composition of the sorbent is known to have an affinity for phosphopeptides. This affinity could, in turn, mean the sorbent has a low affinity for phosphometabolites. This low affinity could be due to the difference in size between phosphopeptides and phosphometabolites, where phosphopeptides are larger than phosphometabolites. As the µElution plate is designed for the enrichment of phosphopeptides, the size of the sorbent could allow for an increased interaction between the phosphopeptides and the sorbent, thereby potentially making the sorbent size too large for phosphometabolites. An increased sorbent size could mean that the phosphometabolites would not be able to bind to the sorbent, thus allowing the phosphometabolites to pass through the µElution plate instead of being retained and enriched.

As such, between the MassPREP™ µElution plate and the TiO_2 cartridge, the optimization using the TiO_2 cartridge was further explored instead of the µElution plate. When looking at the recoveries of the phosphometabolites, they were well recovered across the four TiO_2 enrichment methods. Among the four methods, TiO_2 Cartridge 3 (using 0.2% TFA in 80% ACN and a conditioning step) gave the best overall recovery (average recovery of 66%). From the MAX enrichment methods, phosphoserine had a high recovery percentage of 78% using MAX 6 (using 100% H_2O as the loading buffer and 2% FA in 50% MeOH as the elution solution). However, the other phosphometabolites were poorly recovered, with the MAX methods 1 to 3 using 2% FA in 100% MeOH being unable to recover any of the phosphometabolites of interest.

In a follow-up experiment, the selectivity for phosphometabolites of the MAX and TiO_2 enrichment methods were studied, focusing on the two methods with the best recoveries of phosphometabolites for both MAX and TiO_2. In order to study this selectivity, the recovery of non-phosphorylated metabolites was calculated (Figure 3.4). From the results, MAX 6 showed high recovery percentages of non-phosphorylated metabolite groups, where the recovery percentages of acetyl amino acids are 81% and the recovery percentage of nucleotides/co-factors and vitamins was 83%. MAX 4 (wash solution: 0.1% FA in H_2O and elution: 2% FA in 50% MeOH) had lower recovery percentages of the three groups (14% vs 18%, 58% vs 81%, 63% vs 83%). This confirms the ability for the MAX enrichment methods to recover not only phosphometabolites, but more generally, compounds with acidic moieties. When looking at the TiO_2

enrichment methods, the recovery percentages were much lower compared to that of the MAX enrichment methods, with the highest recovery percentage being 14% when using TiO_2 Cartridge 3. This shows that the TiO_2 enrichment methods are more selective for phosphometabolites, as expected.

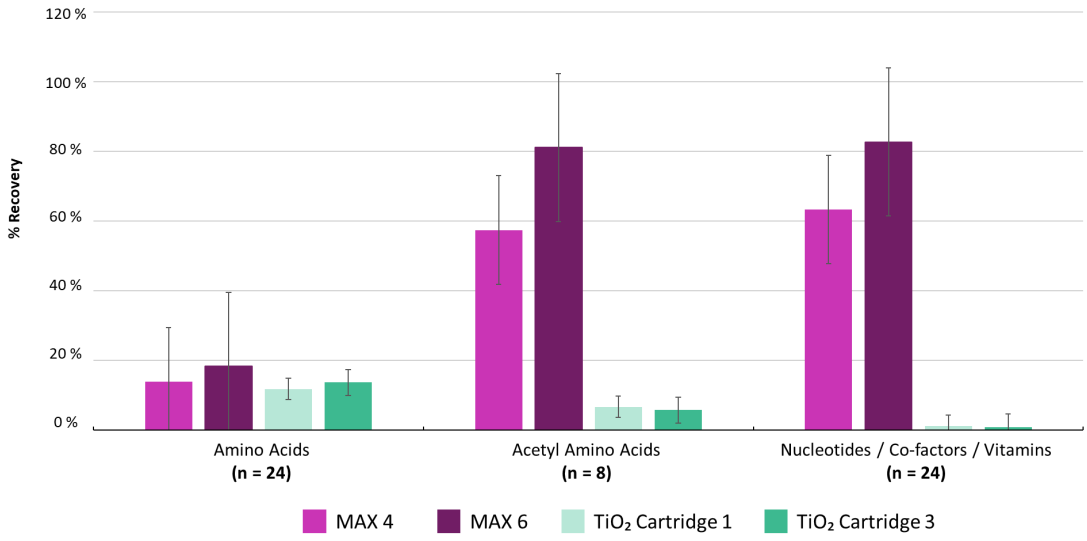

Figure 3.4 Comparison of the percentage recovery of non-phosphorylated metabolite groups for the selectivity of phosphometabolites when using the two methods recovering the most phosphorylated compounds in the standard tested with MAX and TiO_2 SPE cartridge. The error bars for each method are based on measuring several compounds in each class.

Based on the recovery results of the different methods tested, the TiO_2 Cartridge 3 and MAX 6 methods were used for further testing. The TiO_2 Cartridge 3 method includes a conditioning step and uses 0.2% TFA in 80% ACN as the loading buffer and 0.4M NH_4OH pH 11 in 30% ACN as the elution solution for the enrichment of phosphometabolites. MAX 6 uses 100% H_2O as the loading buffer and 2% FA in 50% MeOH as the elution solution for the enrichment of more acidic compounds. These optimized methods were then used to extract biological samples to further study the validity of the methods.

3.2 Metabolite extraction from biological samples

While the phosphometabolites of interest were well detected when using a standard mix, it is important to study the effectiveness of an optimized method using real biological samples. Based on the results from the optimization of enrichment methods, the two best MAX and TiO_2 methods (MAX 6 and TiO_2 Cartridge 3) were used for metabolite extraction from mouse liver and *C. elegans* samples. To compare the strength of

the more selective methods, the samples were also extracted using a generic EtOH and MeOH extraction method respectively that would serve as the untargeted analysis.

3.2.1 Metabolomics study from a MPS II disease mouse model

A set of liver samples available from a study on MPS II in a mouse model was used as a biological model sample set to further investigate the improvement of detecting phosphometabolites in complex biological samples. These same samples were previously investigated using a more generic untargeted metabolomics workflow in the Sleno lab, serving for a direct comparison of results for metabolite coverage and, more specifically, phosphometabolite quantitation. Briefly, Mucopolysaccharidosis Type II (MPS II), also known as Hunter Syndrome, is a rare X-linked lysosomal storage disorder that is mainly seen in boys. This disorder is caused by a deficiency of the iduronate-2-sulfatase enzyme (IDS), which causes an accumulation of mucopolysaccharides, also known as glycosaminoglycans (GAGs), in lysosomal cells. When there is insufficient IDS, GAGs cannot be broken down, which in turn causes various systemic impairments and physical symptoms such as liver enlargement, heart disease, and skeletal deformities. While there is currently no cure for MPS II, several treatments are available to help with the various physical ailments it causes. To target the deficiency of IDS directly, the current course of treatment involves enzyme replacement therapy (ERT) where the patient receives recombinant IDS to compensate for the lack of the enzyme. With a global occurrence of about 1:100, 000 to 1:170, 000 male births, the rarity of MPS II makes it difficult to study (Stapleton et al., 2017).

Three groups of mice were included in this study: the control group (healthy wild type (WT) mice), the IDS-knockout mice (as a model of MPS II), and the latter following treatment with ERTwhich is used as a clinical therapy for most MPS II patients, as previously described (Menkovic et al., 2019). From this previous study, it was shown that the liver tissue had high levels of GAG accumulation, making it interesting to further study, particularly as MPS II is known to cause liver enlargement. As such, liver samples from these three groups were accessed through a collaboration with the Auray-Blais lab (at University of Sherbrooke's hospital research center) for a metabolomics study by LC-MS/MS.

Samples were first homogenized as previously described in Chapter 2, section 2.2.2.1**.** The reconstituted liver homogenates (50 μL) were diluted 10-fold in 100% H_2O for the MAX enrichment method and in 0.2% TFA in 80% ACN for the TiO_2 enrichment method (as shown in Figure 3.5). Once the samples were loaded onto the conditioned cartridge, 500 μL of each washing solution was used.. At the addition of the elution

solution, 600 µL of each elution solution was used for the respective methods. The resulting extracts were dried in the SpeedVac and reconstituted with 200 µL of 25% MeOH (Figure 3.5). For untargeted analyses, the liver homogenates were dried directly and reconstituted in 25% MeOH. For the analysis, 10 µL of each sample was injected on the Scherzo and PFP columns (as described in Chapter 2, Section 2.3) and analyzed on the QqTOF in positive and negative ion modes.

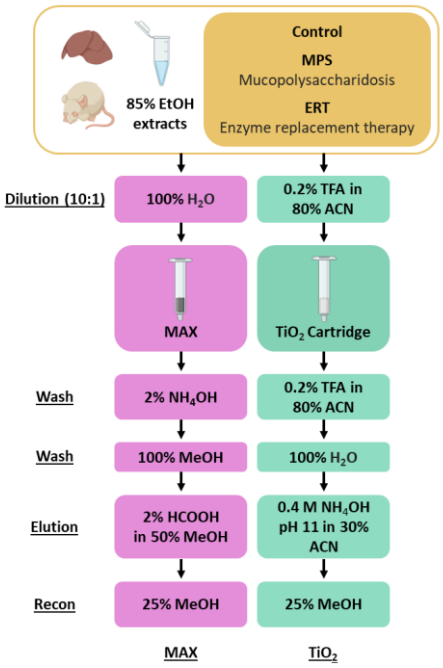

Figure 3.5 MAX and TiO_2 SPE enrichment methods used to study mouse liver samples

3.2.1.1 Results

To study the results of the MPS II liver extracts and the ability of the optimized methods to detect phosphometabolites, the results from the EtOH extraction, and the MAX and TiO_2 enrichment methods were compared. The enrichment ability of the MAX and TiO_2 enrichment methods were first studied by comparing the total ion chromatogram (TIC) of the three extraction methods, where the TIC is the sum of the intensities of all the mass spectral peaks produced from one scan. From the results of the TIC (Figure 3.6), the intensity of the TIC of the EtOH method was higher than that of both the MAX and TiO_2 enrichment methods. Between the MAX and TiO_2 enrichment methods, the intensity of the TIC of the TiO_2 enrichment method is lower that of the MAX enrichment method. As the optimized methods are meant

to enrich and reduce the complexity of a given sample, the reduced complexity would lead to a TIC of lowered intensity which is reflected in the results. As the TiO_2 enrichment method is more specific than the MAX enrichment method, the difference in the intensities of their TIC demonstrated that the TiO_2 enrichment method is able to reduce the complexity of a sample more than the MAX enrichment method. Therefore, the two enrichment methods would allow for the detection and determination of compounds that would otherwise be masked when using the EtOH extraction.

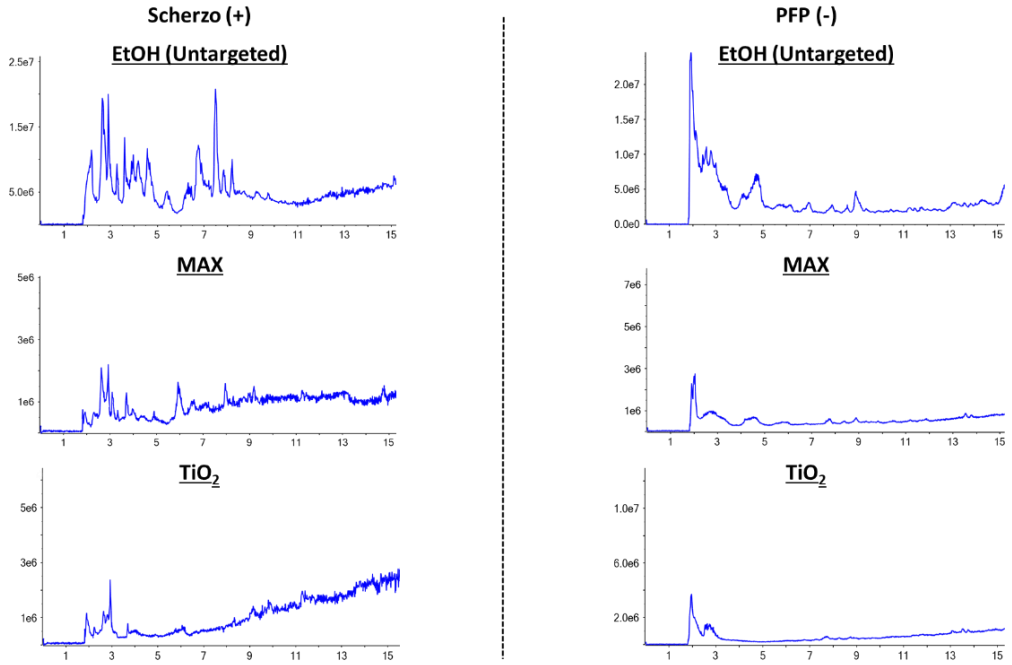

Figure 3.6 Selected total ion chromatogram (TIC) results shown from the three extracts of the MPS II liver samples, injected on the Scherzo column (in positive mode) and PFP column (in negative mode), showing the large decrease in overall signal as the sample preparation method selectivity increases

Identified features (putative metabolites) were then studied to determine how many metabolites can be detected and identified when using a particular method, where a feature is defined as a peak that corresponds to a specific *m/z* that elutes at a specific retention time. A feature is then identied as a specific compound using a mass cutoff of ± 10 ppm and a spectral matching library score of ≥ 80. The total number of metabolites identified from the Scherzo and PFP columns for each method in both positive and negative mode are displayed in Figure 3.7.

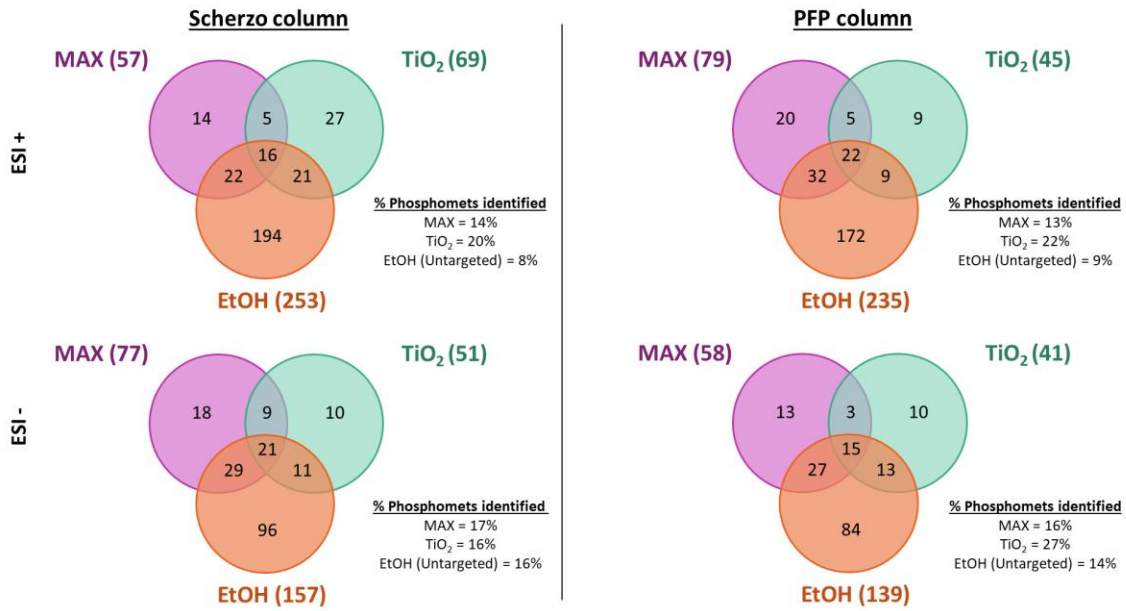

Figure 3.7 Venn diagram of putative metabolites identified from the EtOH, MAX, and TiO_2 methods and analysed on Scherzo and PFP columns in both ESI modes. From the total number of identified features, the percentage of phosphometabolites identified was also calculated.

From the results in Figure 3.7, the EtOH extraction yielded the largest number of identified features compared to the other methods and the MAX enrichment method yielded a larger number of identified features compared to the TiO_2 enrichment method. However, a higher percentage of phosphometabolites were identified when using the MAX enrichment method compared to the EtOH method and an even higher percentage of phosphometabolites were identified using the TiO_2 enrichment method compared to the MAX enrichment method. While there were some unique compounds identified using the different methods, there was also an overlap of compounds being identified. This shows that there is a certain degree of complimentarity among the three methods, where certain compounds are only seen when one method is used, meaning that more information can be gained when performing more specific methods.

In the context of the MPS II disease, putative biomarkers were identified by performing a t-test between the control samples and the disease MPS II samples (Table 3.2). When there is a significant change in an identified feature between two sample groups, it is considered as a putative biomarker. Significantly changing features were determined by performing a t-test to obtain the p-values (≤ 0.05) and fold change (FC) values (± 1.5). When looking at these results, similar results to identified features was seen, where the EtOH extraction yielded a greater number of putative biomarkers compared to the two other

enrichment methods. When comparing the putative biomarkers, it was seen that the MAX method was able to identify a number of unique phosphometabolites compared to the EtOH extraction. While a lower number of putative biomarkers were identified, a number of phosphometabolites were identified using the TiO_2 enrichment method that are not seen when performing the other two methods. These results demonstrate the complementarity of data that can be obtained from the two enrichment methods, which would, in turn, allow for greater insight of the metabolic changes in a disease model.

Table 3.2 List of putative phosphometabolites found as significantly changing in MPS mouse model liver using three extraction methods (using EtOH extraction, MAX SPE, and TiO_2 cartridge)

Metabolite name (putative ID)	Formula	*m/z*	RT (min)	Column (polarity)	Sample extraction	FC (EtOH)	p-value (EtOH)	FC (MAX)	p-value (MAX)	FC (TiO_2)	p-value (TiO_2)
Adenosine monophosphate	$C_{10}H_{14}N_5O_7P$	346.1	2.4	PFP -	EtOH	1.69	2.1E-03	1.88	2.6E-02		
Adenosine monophosphate	$C_{10}H_{14}N_5O_7P$	346.1	4.5	PFP -	EtOH	-1.69	5.6E-03	-1.60	4.5E-02		
Arabinofuranosyluracil monophosphate	$C_9H_{13}N_2O_9P$	323.0	2.5	PFP -	EtOH	3.54	2.1E-02				
Cytidine monophosphate	$C_9H_{14}N_3O_8P$	322.0	2.0	PFP -	EtOH	1.88	2.1E-04	1.69	4.1E-03		
Fructose 1,6-bisphosphate	$C_6H_{14}O_{12}P_2$	339.0	2.4	PFP -	EtOH	1.52	1.9E-02				
Glycerol 3-phosphate	$C_3H_9O_6P$	171.0	2.2	PFP -	EtOH	-1.61	7.2E-03			-1.80	2.9E-02
Guanosine monophosphate	$C_{10}H_{14}N_5O_8P$	362.1	3.1	PFP -	EtOH	3.17	7.4E-04	3.84	2.5E-03		
Inosinic acid	$C_{10}H_{13}N_4O_8P$	347.0	2.9	PFP -	EtOH	4.02	1.1E-02			3.63	1.0E-02
Adenosine monophosphate	$C_{10}H_{14}N_5O_7P$	348.1	2.4	PFP +	EtOH	2.11	1.5E-04				
Citicoline	$C_{14}H_{26}N_4O_{11}P_2$	489.1	3.0	PFP +	EtOH	1.92	3.5E-04	1.78	1.1E-03	1.77	3.4E-03
Glucose-1-phosphate	$C_6H_{13}O_9P$	261.0	2.0	PFP +	EtOH	1.77	1.5E-02				
Glycerol 3-phosphate	$C_3H_9O_6P$	173.0	2.2	PFP +	MAX			-1.62	4.3E-02	-1.82	2.5E-02
Glycerophosphocholine	$C_8H_{20}NO_6P$	258.1	2.7	PFP +	EtOH	-1.96	7.1E-04			-1.67	2.4E-02
Guanosine monophosphate	$C_{10}H_{14}N_5O_8P$	364.1	2.7	PFP +	EtOH	4.63	6.2E-04	3.68	9.1E-04		
Inosinic acid	$C_{10}H_{13}N_4O_8P$	349.1	2.9	PFP +	EtOH	4.45	4.8E-03			3.44	8.2E-03
Uridine monophosphate	$C_9H_{13}N_2O_9P$	325.0	2.5	PFP +	EtOH	7.04	1.5E-03				
Adenosine monophosphate	$C_{10}H_{14}N_5O_7P$	346.1	6.5	Scherzo -	EtOH	1.75	6.8E-03	1.66	4.4E-03		
Adenosine monophosphate	$C_{10}H_{14}N_5O_7P$	346.1	8.2	Scherzo -	MAX			-1.53	4.0E-02		
Cytidine diphosphate ethanolamine	$C_{11}H_{20}N_4O_{11}P_2$	445.1	2.9	Scherzo -	EtOH	1.55	3.8E-02				
Cytidine monophosphate	$C_9H_{14}N_3O_8P$	322.0	2.9	Scherzo -	EtOH	2.69	7.8E-05	1.73	4.2E-04		
Glycerol 3-phosphate	$C_3H_9O_6P$	171.0	10.7	Scherzo -	TiO_2					-1.94	2.1E-03
Guanosine monophosphate	$C_{10}H_{14}N_5O_8P$	362.1	14.8	Scherzo -	EtOH	4.09	3.9E-03	4.16	1.5E-03	3.21	4.5E-04
Inosinic acid	$C_{10}H_{13}N_4O_8P$	347.0	16.4	Scherzo -	TiO_2					3.65	3.5E-03
myo-inositol diphosphate	$C_6H_{14}O_{12}P_2$	339.0	11.5	Scherzo -	EtOH	1.64	3.6E-02				
Adenosine monophosphate	$C_{10}H_{14}N_5O_7P$	348.1	6.5	Scherzo +	EtOH	1.37	5.0E-04				
Adenosine monophosphate	$C_{10}H_{14}N_5O_7P$	348.1	8.2	Scherzo +	TiO_2					-1.51	2.6E-02
Citicoline	$C_{14}H_{26}N_4O_{11}P_2$	489.1	2.9	Scherzo +	MAX			1.77	1.6E-04	1.79	3.0E-03
Cytidine monophosphate	$C_9H_{14}N_3O_8P$	324.1	3.6	Scherzo +	EtOH	1.57	4.9E-06				
Glucosamine-6-phosphate	$C_6H_{14}NO_8P$	260.1	2.5	Scherzo +	MAX			1.92	3.2E-02	1.80	4.8E-02
Glycerol 3-phosphate	$C_3H_9O_6P$	173.0	10.6	Scherzo +	TiO_2					-1.66	3.3E-02
Glycerophosphocholine	$C_8H_{20}NO_6P$	258.1	2.9	Scherzo +	EtOH	-1.74	8.0E-04			-1.85	1.8E-02
Guanosine monophosphate	$C_{10}H_{14}N_5O_8P$	364.1	15.0	Scherzo +	EtOH	1.89	1.5E-03			3.41	6.3E-04
Uridine monophosphate	$C_9H_{13}N_2O_9P$	325.0	13.1	Scherzo +	TiO_2					1.70	3.1E-02

FC: Fold change of peak areas between MPS vs. WT groups of mouse liver samples

p-value: from Student's t-test of normalized peak areas from each high-resolution extracted chromatogram

Principal Component Analysis (PCA) was performed on the three groups (Control, ERT, and MPS II) to study the clustering of the putative metabolites identified (Figure 3.8A and 3.8B). From the supervised PCA plots, a clear separation of the control and MPS II samples was seen. However, between the MPS II group and the ERT group, there was no clear distinction, particularly when using the MAX and TiO_2 enrichment methods. The EtOH extraction showed a better distinction between these two groups. This lack of distinction seen when using the enrichment methods seems to suggest that while the methods detect putative biomarkers, the biomarkers are not involved in the pathways that are specifically impacted by the disease.

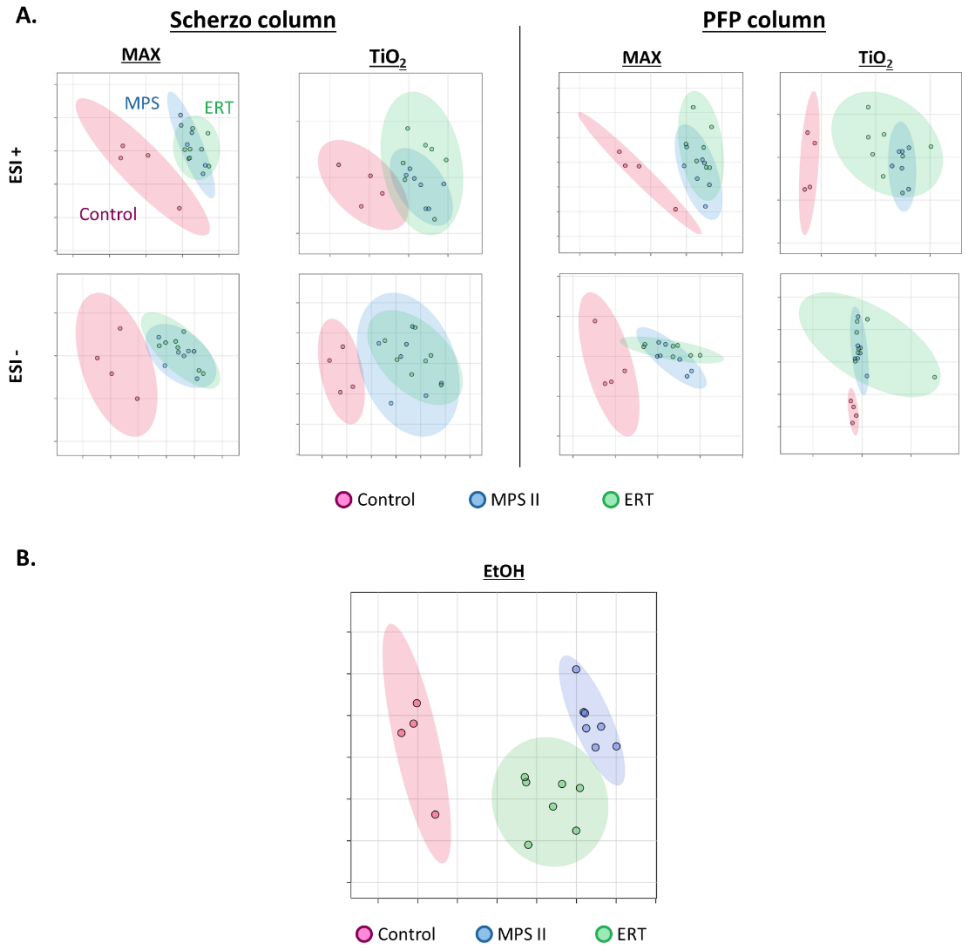

Figure 3.8 A) Supervised PCA plots for the MAX and TiO_2 enrichment methods using Scherzo and PFP columns in both positive and negative mode. B) Supervised PCA plot for EtOH extractions using the combined data from both Scherzo and PFP column in both positive and negative mode.

A pathway enrichment analysis was then performed on the putative biomarkers from each method to show which pathways the metabolites originate from (Figure 3.9). Through this analysis, the impact of a disease can be better understood as if a group of metabolites identified from a disease sample originate from one specific pathway, it would indicate the impact the disease has on a metabolic level. From this analysis, there were a number of similar pathways being impacted by all three methods. However, there were certain pathways that are only impacted when only one of the methods was performed, such as butyrate metabolism pathway that seems to be unique to the TiO_2 enrichment method and pyrimidine metabolism pathway that seems to be unique to the MeOH extraction. There also seemed to be pathways identified only when the enrichment methods are used (for example, De Novo Triacylglycerol pathway seen when both MAX and TiO_2 extractions were performed) and are not seen when performing the less selective EtOH extraction. This shows that there is a level of complimentarity when using enrichment methods alongside a less selective method like the EtOH extraction. While performing a pathway analysis on its own is limited without studying specific compounds, it can be used as a preliminary tool to look at the complementarity of various methods. For example, in this analysis, as some of the same pathways are impacted with different enrichment levels, combining two datasets, such as the TiO_2 and the untargeted dataset could reveal an increased number of metabolites changing and help prioritize certain impacted pathways for further studies.

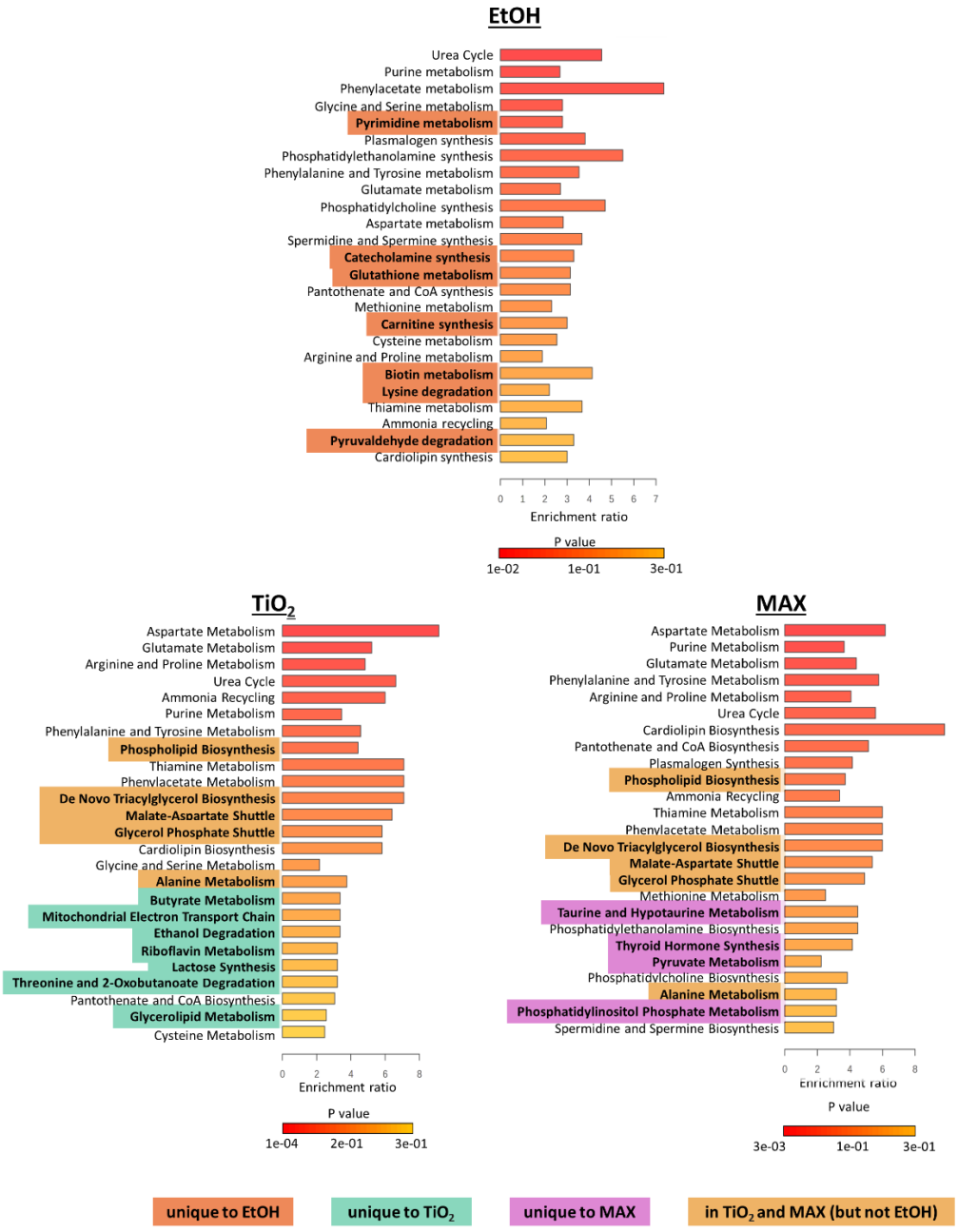

Figure 3.9 Pathway enrichment analysis of EtOH extraction, and MAX and TiO_2 enrichment methods

3.2.2 *C. elegans* samples subjected to phosphometabolite enrichment methods

Caenorhabditis elegans (*C. elegans*) is a well characterized model organism that is widely used in biology, and is increasingly useful to study mechanisms of disease. This 1 mm long, free-living soil nematode (microscopic worm) has a short life cycle of approximately 30 days and its transparent body allows for easy

observation and labelling, making it an ideal biological model (Li et al., 2023). As such, this model organism was also used to study the metabolomics coverage obtained using the two methods that were developed through this work on phosphometabolites. It was chosen since, through previous untargeted experiments performed in the Sleno lab, it was noted that a large number of phosphometabolites were identified. For comparison of the samples in this study, approximately 30, 000 mixed stage dried *C. elegans* extracts (from a generic MeOH extraction procedure with bead beating, as described in Chapter 2, Section 2.2.2.2) were reconstituted with 100 µL of 0.5% FA in 10% ACN and subjected to untargeted metabolomics workflows. For the MAX and TiO_2 enrichment methods, the dried extracts were reconstituted with 450 µL of their respective reconstitution solutions and subjected to the same two enrichment method as for the liver samples. The resulting extracts were then dried down under nitrogen and reconstituted in 100 µL of 0.5% FA in 10% ACN (Figure 3.10).

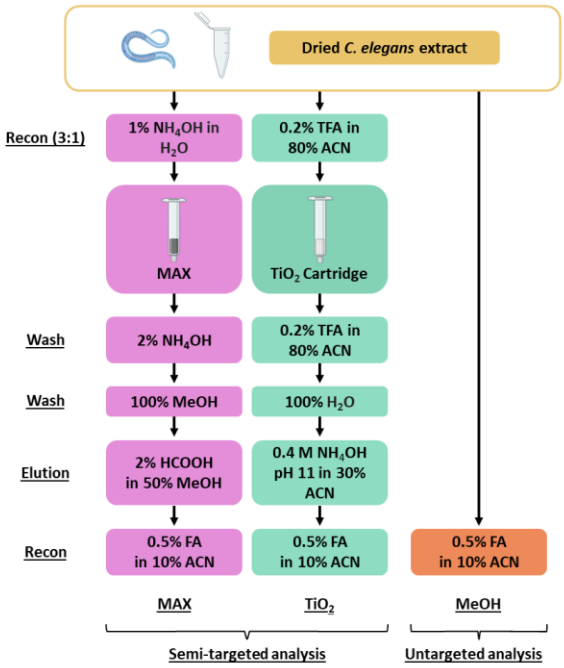

Figure 3.10 Sample extraction methods for semi-targeted analysis (using MAX and TiO_2 enrichment methods) and untargeted analysis (using MeOH extraction)

Similar to the mouse liver samples, the results from MeOH extraction, and MAX and TiO_2 enrichment methods were compared. More specifically, the phosphometabolites identified using the three methods were studied and compared in Figure 3.11. From this heatmap, while there are a number of

phosphometabolites seen from each method, there was also considerable overlap of the phosphometabolites identified. However, there was still a wider range of phosphometabolites seen when using the TiO_2 enrichment method compared to the MAX enrichment method and the MeOH extraction method. In many cases, some phosphometabolites that were identified in multiple worflows yielded greater peak areas with the TiO_2 procedure, as shown in a few examples highlighted in Tables 3.3 and 3.4. As mutant *C. elegans* samples were tested, this preliminary data helped highlight the metabolic differences between the WT species and mutant species, which would help point towards future further studies of these differences.

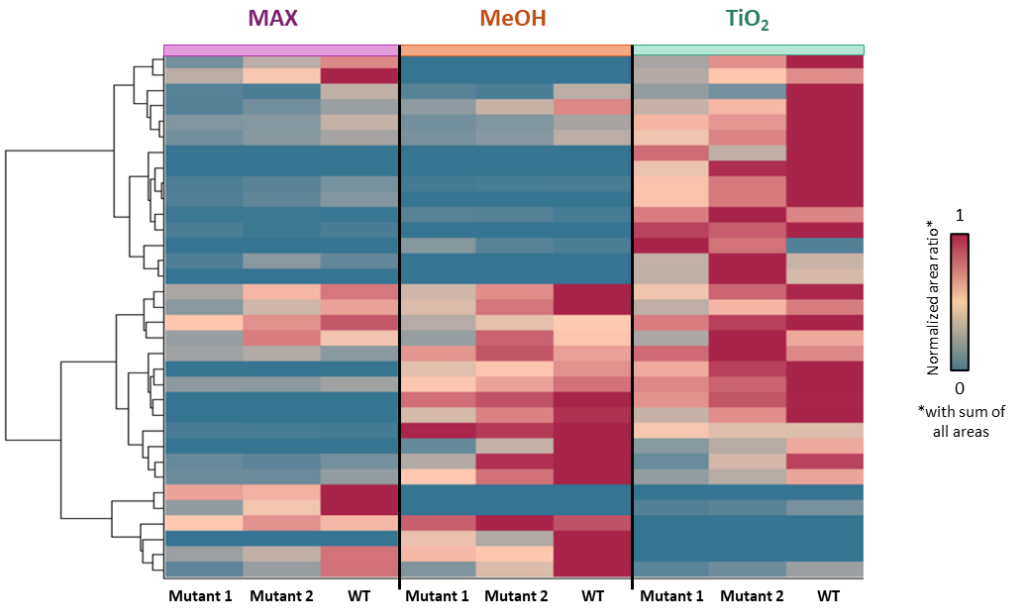

Figure 3.11 Heatmap of putative phosphometabolites identified from Scherzo and PFP columns in both ESI modes using MeOH, MAX, and TiO_2 extraction methods

Table 3.3 List of putative metabolites from *C. elegans* identified with different sample extraction methods (from negative ion mode data)

Metabolite Name (putative ID)	Formula	*m/z*	RT (min)	Column (polarity)	Peak Area (MeOH)	Peak Area (MAX)	Peak Area (TiO_2)
ADP	$C_{10}H_{15}N_5O_{10}P_2$	426.0	2.3	PFP -			2.19E+05
AMP	$C_{10}H_{14}N_5O_7P$	346.1	2.3	PFP -	2.27E+07		4.89E+07
CMP	$C_9H_{14}N_3O_8P$	322.0	2.0	PFP -	8.89E+05	1.40E+06	
Flavin mononucleotide	$C_{17}H_{21}N_4O_9P$	455.1	12.1	PFP -	1.27E+06		1.91E+06
Glucose phosphate	$C_6H_{13}O_9P$	259.0	2.3	PFP -	1.03E+07	2.98E+06	1.72E+07
Glycerol 3-phosphate	$C_3H_9O_6P$	171.0	2.2	PFP -	1.03E+07	5.05E+06	2.18E+07
GMP	$C_{10}H_{14}N_5O_8P$	362.1	2.8	PFP -	4.22E+07		7.17E+06
Inosinic acid	$C_{10}H_{13}N_4O_8P$	347.0	3.5	PFP -		6.87E+06	
Phosphoglyceric acid	$C_3H_7O_7P$	185.0	2.7	PFP -		4.41E+05	1.45E+06
Phosphoserine	$C_3H_8NO_6P$	184.0	2.1	PFP -		2.03E+05	
Ribose phosphate	$C_5H_{11}O_8P$	229.0	2.1	PFP -	1.74E+06	2.54E+05	1.35E+06
Uridine diphosphate	$C_9H_{14}N_2O_{12}P_2$	403.0	2.3	PFP -			3.38E+05
UDP-glucose	$C_{15}H_{24}N_2O_{17}P_2$	565.0	2.1	PFP -	8.73E+03		1.10E+04
UMP	$C_9H_{13}N_2O_9P$	323.0	2.5	PFP -		1.70E+07	1.56E+07
AMP	$C_{10}H_{14}N_5O_7P$	346.1	5.3	Scherzo -	6.88E+07	6.66E+07	8.51E+07
AMP	$C_{10}H_{14}N_5O_7P$	346.1	7.8	Scherzo -	6.57E+05	7.35E+05	7.86E+05
AICAR	$C_9H_{15}N_4O_8P$	337.1	7.2	Scherzo -	7.40E+04	6.72E+04	1.15E+05
cAMP	$C_{10}H_{12}N_5O_6P$	328.0	8.8	Scherzo -		4.17E+04	
CMP	$C_9H_{14}N_3O_8P$	322.0	3.0	Scherzo -	3.23E+06	3.63E+06	1.27E+07
dCMP	$C_9H_{14}N_3O_7P$	306.0	3.3	Scherzo -	2.70E+05	2.29E+05	1.52E+06
Deoxy-glucose phosphate	$C_6H_{13}O_8P$	243.0	10.0	Scherzo -	1.69E+06	6.01E+05	2.41E+06
dAMP	$C_{10}H_{14}N_5O_6P$	330.1	6.8	Scherzo -	3.21E+05	3.14E+05	4.17E+05
dGMP	$C_{10}H_{14}N_5O_7P$	346.1	11.7	Scherzo -		7.92E+05	1.63E+06
DHAP	$C_3H_7O_6P$	169.0	10.6	Scherzo -	2.60E+06	4.07E+05	2.36E+06
Glucosamine phosphate	$C_6H_{14}NO_8P$	258.0	2.5	Scherzo -		3.93E+05	2.69E+05
Glucose phosphate	$C_6H_{13}O_9P$	259.0	8.5	Scherzo -	2.87E+07	1.28E+07	
Glycerol 3-phosphate	$C_3H_9O_6P$	171.0	6.5	Scherzo -	8.13E+04	5.91E+04	1.16E+05
Glycerol 3-phosphate	$C_3H_9O_6P$	171.0	10.0	Scherzo -	4.22E+07	1.81E+07	6.06E+07
GMP	$C_{10}H_{14}N_5O_8P$	362.0	11.0	Scherzo -	7.97E+07	5.12E+07	9.97E+07
NAD	$C_{21}H_{27}N_7O_{14}P_2$	662.1	5.9	Scherzo -	4.10E+05	1.45E+05	
Phosphorylethanolamine	$C_2H_8NO_4P$	140.0	2.6	Scherzo -	5.96E+05	1.64E+05	1.04E+06
Phosphoserine	$C_3H_8NO_6P$	184.0	7.0	Scherzo -	2.62E+05	2.71E+05	5.73E+05
Pyridoxal phosphate	$C_8H_{10}NO_6P$	246.0	7.0	Scherzo -			2.46E+05
Ribose phosphate	$C_5H_{11}O_8P$	229.0	9.6	Scherzo -	7.29E+06	1.83E+06	4.17E+06
UMP	$C_9H_{13}N_2O_9P$	323.0	12.4	Scherzo -			1.64E+08

Table 3.4 List of putative metabolites from *C. elegans* identified with different sample extraction methods (from positive ion mode data)

Metabolite Name (putative ID)	Formula	*m/z*	RT (min)	Column (polarity)	Peak Area (MeOH)	Peak Area (MAX)	Peak Area (TiO_2)
AMP	$C_{10}H_{14}N_5O_7P$	348.1	2.3	PFP +	2.58E+07	2.83E+07	3.03E+07
Citicoline	$C_{14}H_{26}N_4O_{11}P_2$	489.1	3.3	PFP +	1.04E+06		3.50E+05
CMP	$C_9H_{14}N_3O_8P$	324.1	2.0	PFP +	7.75E+05	1.31E+06	1.71E+06
dAMP	$C_{10}H_{14}N_5O_6P$	332.1	2.4	PFP +		3.25E+04	7.67E+04
Flavin mononucleotide	$C_{17}H_{21}N_4O_9P$	457.1	12.2	PFP +	6.13E+05		8.20E+05
Glucose phosphate	$C_6H_{13}O_9P$	261.0	2.3	PFP +			6.44E+05
Glycerol 3-phosphate	$C_3H_9O_6P$	173.0	2.2	PFP +	4.43E+05	8.94E+04	1.29E+06
Glycerophosphocholine	$C_8H_{20}NO_6P$	258.1	2.8	PFP +	1.12E+07		
GMP	$C_{10}H_{14}N_5O_8P$	364.1	2.8	PFP +	1.81E+07	1.17E+07	1.66E+06
NAD	$C_{21}H_{27}N_7O_{14}P_2$	664.1	2.6	PFP +	7.85E+04	1.21E+05	
Phosphorylcholine	$C_5H_{14}NO_4P$	184.1	2.7	PFP +		2.36E+05	7.75E+06
Phosphorylethanolamine	$C_2H_8NO_4P$	142.0	1.9	PFP +			2.80E+05
Thiamine Monophosphate	$C_{12}H_{17}N_4O_4PS$	345.1	2.3	PFP +	4.91E+05		
UMP	$C_9H_{13}N_2O_9P$	325.0	2.5	PFP +	2.89E+06	1.61E+06	4.21E+06
cAMP	$C_{10}H_{12}N_5O_6P$	330.1	8.5	Scherzo +	1.02E+05	7.78E+04	
AMP	$C_{10}H_{14}N_5O_7P$	348.1	5.3	Scherzo +		4.50E+07	4.41E+07
AMP	$C_{10}H_{14}N_5O_7P$	348.1	7.8	Scherzo +	3.44E+05	3.61E+05	6.61E+05
AICAR	$C_9H_{15}N_4O_8P$	339.1	7.2	Scherzo +			5.83E+04
Citicoline	$C_{14}H_{26}N_4O_{11}P_2$	489.1	3.1	Scherzo +	8.23E+05	3.23E+04	4.27E+05
CMP	$C_9H_{14}N_3O_8P$	324.1	3.0	Scherzo +		1.98E+06	3.20E+06
dAMP	$C_{10}H_{14}N_5O_6P$	332.1	6.8	Scherzo +	2.94E+05	2.84E+05	3.37E+05
dGMP	$C_{10}H_{14}N_5O_7P$	348.1	11.7	Scherzo +		3.13E+05	6.35E+05
Glucose phosphate	$C_6H_{13}O_9P$	260.9	8.5	Scherzo +			4.58E+06
Glycerol 3-phosphate	$C_3H_9O_6P$	173.0	9.7	Scherzo +	4.50E+06	1.75E+06	7.38E+06
Glycerophosphocholine	$C_8H_{20}NO_6P$	258.1	2.8	Scherzo +	7.28E+06		
GMP	$C_{10}H_{14}N_5O_8P$	363.7	11.0	Scherzo +		2.42E+07	4.30E+07
Inosinic acid	$C_{10}H_{13}N_4O_8P$	349.3	5.1	Scherzo +			2.29E+06
NAD	$C_{21}H_{27}N_7O_{14}P_2$	664.1	5.9	Scherzo +		1.00E+05	
Nicotinamide mononucleotide	$C_{11}H_{15}N_2O_8P$	335.1	2.9	Scherzo +	4.00E+05		3.97E+05
Phosphorylcholine	$C_5H_{14}NO_4P$	184.1	2.8	Scherzo +		1.46E+05	7.47E+06
Phosphorylethanolamine	$C_2H_8NO_4P$	142.0	2.6	Scherzo +	3.56E+05		5.41E+05
Phosphoserine	$C_3H_8NO_6P$	186.0	7.0	Scherzo +	1.13E+05	1.09E+05	
Phosphotyrosine	$C_9H_{12}NO_6P$	262.0	12.9	Scherzo +			1.10E+05
Pyridoxal phosphate	$C_8H_{10}NO_6P$	247.9	7.0	Scherzo +			2.25E+05
Thiamine Monophosphate	$C_{12}H_{17}N_4O_4PS$	345.1	2.3	Scherzo +	3.41E+05		4.34E+05

From the heatmap and table of the identified phosphometabolites of the putative metabolites, the three methods were able to detect a number of overlapping phosphometabolites. As such, to better understand if the TiO_2 method is able to better detect phosphometabolites, XICs of the phosphometabolites were examined (Figure 3.12). From these results, all three methods were able to identify and detect inosinic acid, phosphoryl-ethanolamine, CMP, and pyridoxal-5-phosphate. However, when the intensity of the peaks were compared, the TiO_2 enrichment method produced higher intensity peaks compared to the other methods. This shows that, while the TiO_2 enrichment method does not significantly increase the number of phosphometabolites identified from these *C. elegans* samples, this enrichment method improves the quality of the detection of phosphometabolites in general.

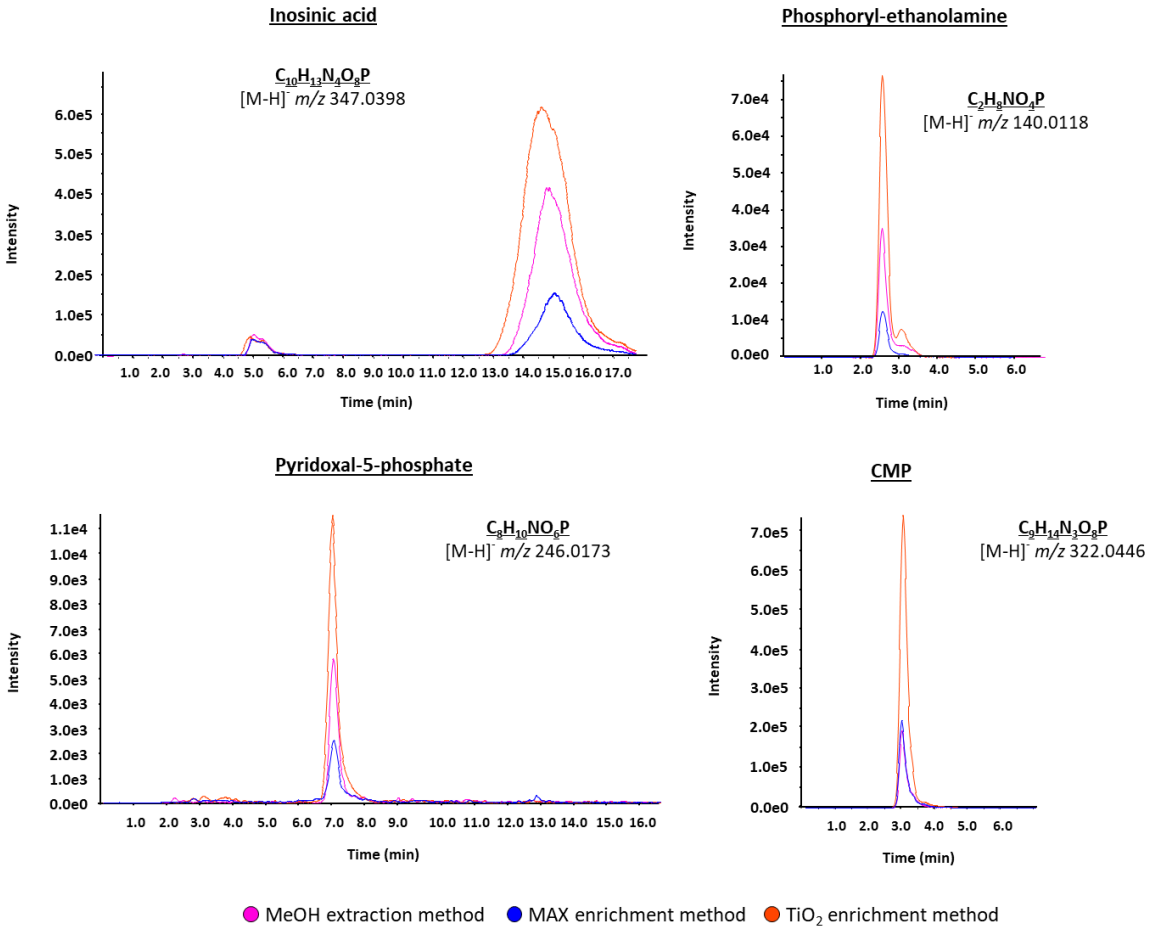

Figure 3.12 Extracted ion chromatograms to compare sensitivity of detection of four phosphometabolites detected in the three extraction methods using the Scherzo column in negative mode

CHAPITRE 4

Strategies to optimize the detection and quantitation of thiol and disulfide metabolites

Reactive oxygen species (ROS) increase in tissues and cells when exposed to high levels of oxygen and toxins, including some xenobiotics or environmental pollutants. These reactive species can cause an imbalance and disrupt normal cell function, leading to oxidative stress. This phenomenon is often linked to cancer and cardiovascular diseases, as well as tissue damage associated with aging. As such, a well-regulated redox state of an organism is essential for normal physiological function and cellular metabolism. This state is largely controlled by the cell's antioxidant defense system, where many thiols are used to maintain homeostasis of the system (Baba & Bhatnagar, 2018). In biological systems, thiols and disulfides are involved in a disulfide exchange reactions, where thiols can be oxidized to form disulfides. These disulfides can then be reduced back to free thiols by the reduction of the disulfide bond (Winther & Thorpe, 2014). While important for the maintenance of the redox state of an organism, this reaction can make it difficult to quantify free thiol metabolites as the oxidation of free thiols can take place even during storage. This can lead to the incorrect identification of endogenous free thiols as the disulfide exchange reaction makes it difficult to differentiate between a free thiol that is freely present and a free thiol present as a result of the reduction of disulfides.

An important step in studying thiol- and disulfide-containing compounds in biological samples is the ability to assess thiol-disulfide status. As free thiols are reactive and unstable, they could oxidize to form disulfides (including mixed-disulfides), as well as other oxidized species (for example, sulfoxides), during sample storage or preparation steps, making it difficult to accurately quantify the levels of a particular free thiol or disulfide. The common approaches taken to preserve free thiols involve using an acid to reduce the potential for oxidation or the use of a trapping agent that can alkylate the free thiol and thus stabilize it. In this work, the potential for using thiol alkylation as a strategy for stabilization and better detection of biological thiols by LC-MS/MS was examined (Hansen & Winther, 2009). By using alkylating agents such as iodoacetamine (IAM), the sulfhydryl (-SH) group of a thiol forms a thioether (R-S-R', also known as a sulfide) which effectively blocks and "traps" the free thiol from oxidation, as well as making it more suitable for LC-MS analysis. Depending on the agent, the addition modifies the target compound in various ways such as decreased volatility, modified chromatographic properties, and greater ionization efficiency (Ghafari & Sleno, 2024). Disulfides are also often difficult to detect by LC-MS as they can be very polar. These compounds can be reduced in order to study them by using reducing agents such as dithiothreitol (DTT).

With a reducing agent, the disulfide bond (R-S-S-R') is reduced to form their corresponding thiols. Through the derivatization of the newly formed free thiols, one can assess the amount of thiols present, as well as their disulfide forms, including mixed disulfides, in a given sample (Erel & Erdoğan, 2020; Hansen & Winther, 2009).

Therefore, to determine if free thiols are endogenous or from a disulfide, the workflow proposed in this project involves using light and heavy labeled derivatization agents to create pairs for the detection of derivatized thiols, from their free or disulfide forms, respectively (Figure 4.1). The light labeled derivatization agent would first alkylkate and stabilize free thiols present in biological samples. DTT can then be added to reduce the disulfide bonds present in the sample, creating new free thiols, which could then be alkylyzed by the heavy labeled derivatization agent. This would allow for the differentiation between true free thiols and free thiols that are a product of the reduction of disulfide compounds, and thus better establish the thiol-disulfide status of a given metabolite.

By modifying the target compounds, derivatization leads to an improved ionization efficiency and reduced matrix effect as derivatization would increase the molecular weight of the LMW thiols. By using a light and heavy labeled derivatization agents, it would also improve identification of a compound as the RT of both derivatives would be similar. Additionally, the use of a light and heavy labeled derivatization agent can provide Q1/Q3 transitions that can then be used for quantitative MRM analysis (Ghafari & Sleno, 2024; Phipps et al., 2019).

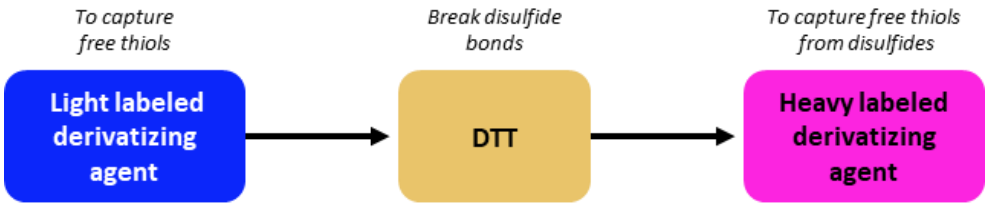

Figure 4.1 Experimental workflow hypothesis using light and heavy labeled derivatization agents

4.1 Derivatization testing

To test the efficiency of two derivatization agents with similar chemistries (iodoacetamide (IAM) and N-(4-hydroxyphenyl-2-iodoacetamide (IPAP)), two standard mixes, where one contained free thiols and the other contained disulfides (Chapter 2, Table 2.2) was used. DTT was added to reduce the disulfide bond to

create a free thiol. For both mixes, DTT was added prior to the derivatization to ensure no disulfides are present at the time of alkylation with IAM or IPAP (Figures 4.3 and 4.4). As IAM is commonly used for the alkylation in proteomics workflows, it was tested alongside the in-house IPAP compound which follows the same chemistry of reaction, but with a larger side chain added which would increase the hydrophobicity of the resulting products.

To study the free thiols, 495 µL of a mix of 11 free thiols at 20 µg/mL in H_2O each was combined with 5 µL of 100 mM DTT and incubated for 15 min at 37^oC. After incubation, 150 µL of the mix was separated into two different tubes to test the two derivatization agents. To each tube, 50 µL of 100 mM ABC buffer pH 8.0 and 5 µL of either 100 mM IAM or 100 mM IPAP was added to the mix and incubated for 30 min at 37^oC under light sensitive conditions (in the dark). To study the efficiency of the derivatization, four states of each compound were monitored: as the free thiol, the disulfide, as well as its IAM and IPAP alkylated products (derivatives). As such, the free thiol mix before and after the addition of DTT injected (3 µL of 20 µg/mL of free thiol), along with the mixes containing IAM and IPAP (4 µL of 15 µg/mL of the free thiol), with 4 samples for each of the 11 free thiols. These reactions (the monitored high-resolution XIC of the protonated precursors of interest in Table 4.1) were monitored by LC-HRMS using a short gradient of a Mercury column (Table 2.3 for dimensions and Table 2.4 for parameters). By the addition of derivatization agents, the free thiols derivatives should produce XICs of higher intensities compared to their non-derivatized counterparts. In Figure 4.2, the example of 4-chlorobenzene methanethiol (CBMT) as a model thiol is shown, with no detection of the non-alkylated species. When looking at the free thiol and disulfide states, no peaks of interest were seen in the XICs. Nicely defined peaks were seen for the forms of derivatized CBMT. When comparing the two derivatization agents, the IPAP derivative had a higher intensity and increased retention time.

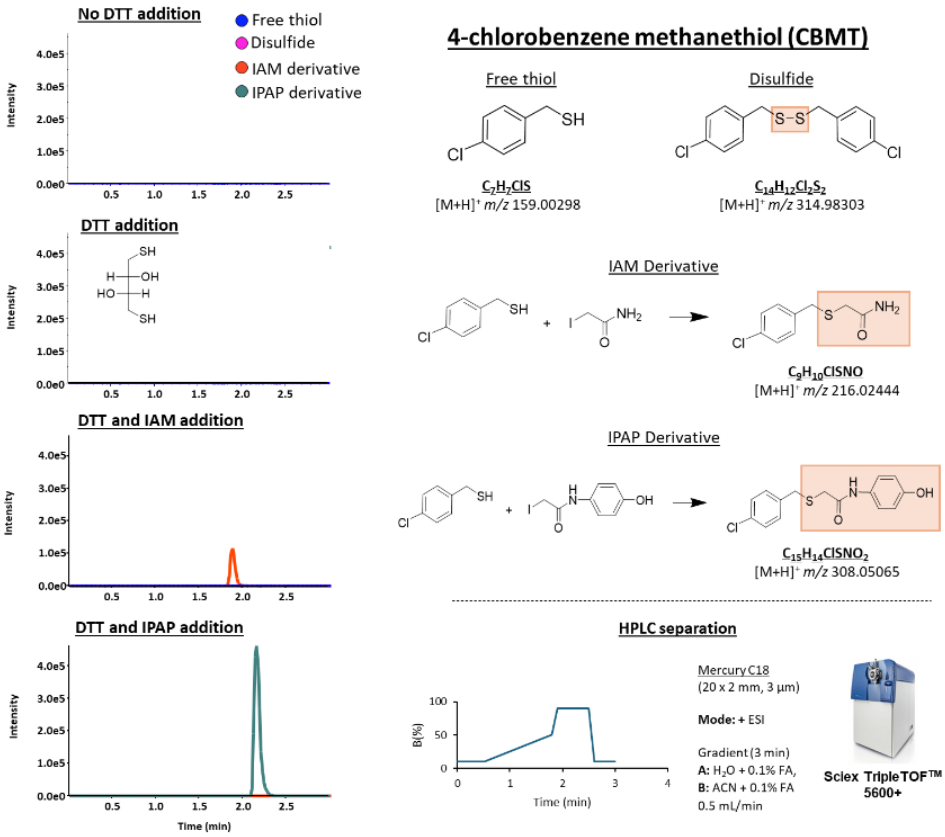

Figure 4.2 CBMT, a model thiol where four species (free thiol, disulfide, IAM, and IPAP derivatives) were monitored. The HPLC separation parameters used are also indicated.

Table 4.1 XIC list of the monitored states of free thiol compounds tested showing their $[M+H]^+$ *m/z* values and related formulas

Compound	State	Formula	MW	$[M+H]^+$ *m/z*
N-acetyl cysteine (NAC)	Free thiol	$C_5H_9NO_3S$	163.03032	164.03759
	Disulfide	$C_{10}H_{16}N_2O_6S_2$	324.04498	325.05226
	IAM derivative	$C_7H_{12}N_2O_4S$	220.05178	221.05906
	IPAP derivative	$C_{13}H_{16}N_2O_5S$	312.07799	313.08527
4-Aminothiophenol	Free thiol	C_6H_7NS	125.02992	126.0372
	Disulfide	$C_{12}H_{12}N_2S_2$	248.04419	249.05147
	IAM derivative	$C_8H_{10}N_2OS$	182.05138	183.05866
	IPAP derivative	$C_{14}H_{14}N_2O_2S$	274.0776	275.08488
4-chlorobenzene methanethiol (CBMT)	Free thiol	C_7H_7ClS	157.9957	159.00298
	Disulfide	$C_{14}H_{12}Cl_2S_2$	313.97575	314.98303
	IAM derivative	$C_9H_{10}ClSNO$	215.01716	216.02444
	IPAP derivative	$C_{15}H_{14}ClSNO_2$	307.04338	308.05065
L-Cysteine ethyl ester	Free thiol	$C_5H_{11}NO_2S$	149.05105	150.05833
	Disulfide	$C_{10}H_{20}N_2O_4S_2$	296.08645	296.0859
	IAM derivative	$C_7H_{14}N_2O_3S$	206.07251	207.07979
	IPAP derivative	$C_{13}H_{18}N_2O_4S$	298.09873	299.10601
Cysteine (Cys)	Free thiol	$C_3H_7NO_2S$	121.01975	122.02703
	Disulfide	$C_6H_{12}N_2O_4S_2$	240.02385	241.03113
	IAM derivative	$C_5H_{10}N_2O_3S$	178.04121	179.04849
	IPAP derivative	$C_{11}H_{14}N_2O_4S$	270.06743	271.07471
2,6-dimethylbenzenethiol	Free thiol	$C_8H_{10}S$	138.05032	139.0576
	Disulfide	$C_{16}H_{18}S_2$	274.08499	275.09227
	IAM derivative	$C_{10}H_{13}SNO$	195.07179	196.07906
	IPAP derivative	$C_{16}H_{17}SNO_2$	287.098	288.10528
GSH	Free thiol	$C_{10}H_{17}N_3O_6S$	307.08381	308.09108
	Disulfide	$C_{20}H_{32}N_6O_{12}S_2$	612.15196	613.15924
	IAM derivative	$C_{12}H_{20}N_4O_7S$	364.10527	365.11255
	IPAP derivative	$C_{18}H_{24}N_4O_8S$	456.13149	457.13876
Methyl propanethiol	Free thiol	$C_4H_{10}S$	90.05032	91.0576
	Disulfide	$C_8H_{18}S_2$	178.08499	179.09227
	IAM derivative	$C_6H_{13}NOS$	147.07179	148.07906
	IPAP derivative	$C_{12}H_{17}SNO_2$	239.098	240.10528
Propanethiol	Free thiol	C_3H_8S	76.03467	77.04195
	Disulfide	$C_6H_{14}S_2$	150.05369	151.06097
	IAM derivative	$C_5H_{11}SNO$	133.05614	134.06341
	IPAP derivative	$C_{11}H_{15}SNO_2$	225.08235	226.08963
Thioglycolic acid	Free thiol	$C_2H_4O_2S$	91.9932	93.00048
	Disulfide	$C_4H_6O_4S_2$	181.97075	182.97803
	IAM derivative	$C_4H_7O_3NS$	149.01467	150.02194
	IPAP derivative	$C_{10}H_{11}O_4NS$	241.04088	242.04816
Thiophenol	Free thiol	C_6H_6S	110.01902	111.0263
	Disulfide	$C_{12}H_{10}S_2$	218.02239	219.02967
	IAM derivative	C_8H_9SNO	167.04049	168.04776
	IPAP derivative	$C_{14}H_{13}SNO_2$	259.0667	260.07398

The compiled results from the free thiols are shown in Figure 4.3, where all thiols tested were detected in their IPAP derivatized states. While a few of the thiols were still detectable in their free thiol forms, these peaks are at much lower intensities compared to their derivatized counterparts, as well as being much less retained on the HPLC column (lower RT). When comparing the IPAP derivatives to IAM derivatives, only three thiols were well detected as IAM derivatives. Five more IAM derivatives were detected but at much lower intensities and with very early retention times compared to their IPAP derivatives. In general, IPAP always resulted in better detectability and higher retention of the resulting species, due to its increased hydrophobicity.

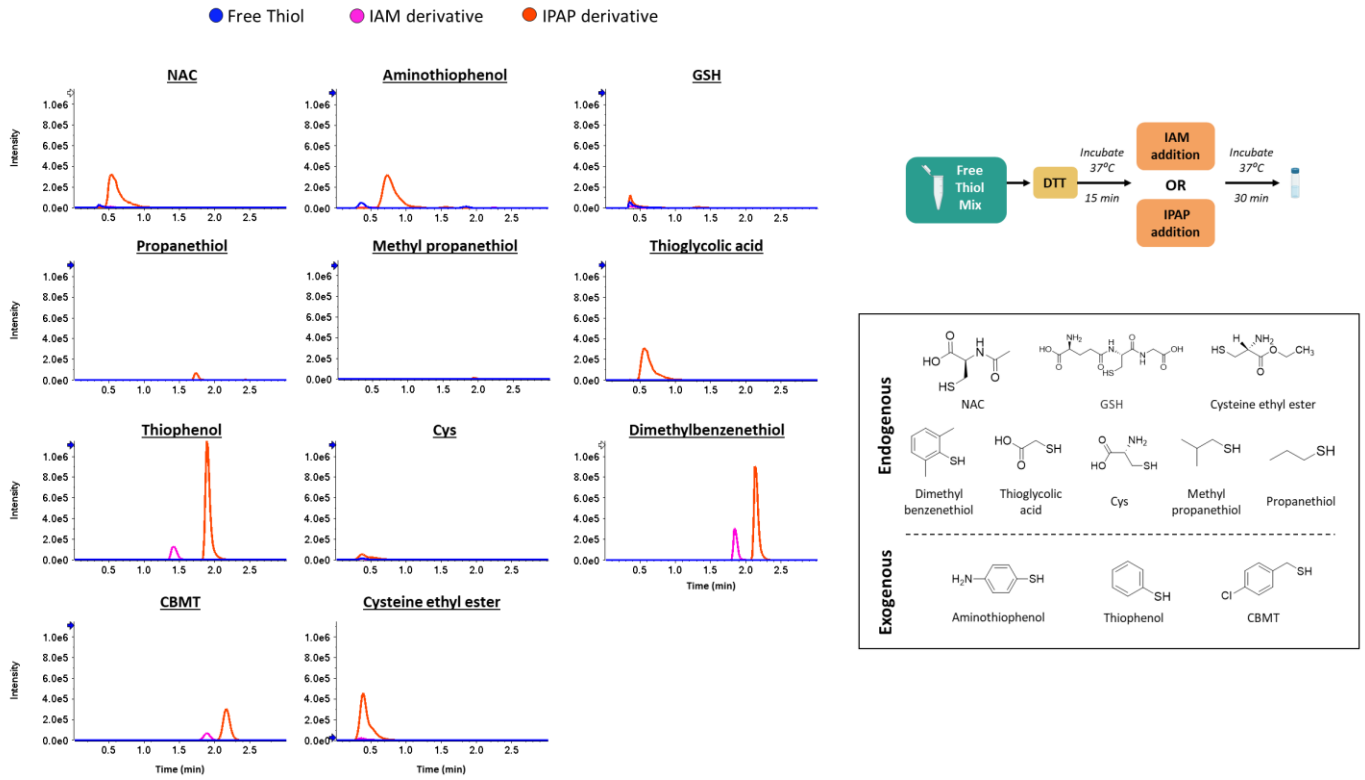

Figure 4.3 XIC of the free thiols tested using IAM and IPAP as derivatization agents

To study the disulfides, a similar test to the free thiol mix was performed. As the test with the free thiols mix demonstrated that IPAP is able to produce well detected derivatives, only IPAP was used for this test. For this study, 495 µL of a mix of 8 disulfides at 20 µg/mL each in H_2O was combined with 5 µL of 100 mM DTT and incubated for 15 min at 37°C. After incubation, 150 µL of the mix was placed into a separate tube. To this tube, 90 µL of 100 mM ABC buffer pH 8.0 and 60 mL of 10 mM IPAP was added to

the mix and incubated for 30 min at 37°C in the dark. Similar to the free thiols, two states of each compound were monitored (the disulfide and its IPAP derivative) by LC-HRMS (Table 4.2). For these samples, 3 µL of the 20 µg/mL disulfide mix and 6 µL of the 15 µg/mL disulfide mix containing IPAP was injected on the Mercury C18 column.

Table 4.2 XIC list of the monitored states of disulfide compounds tested showing their $[M+H]^+$ *m/z* values and related formulas

Compound	State	Formula	MW	$[M+H]^+$ *m/z*
S-Methyl methanethiosulfonate	Disulfide	$C_2H_6O_2S_2$	125.98092	126.9882
	IPAP derivative	$C_9H_{11}O_2S$	197.05105	198.05833
Dithiodiglycolic acid	Disulfide	$C_4H_6O_4S_2$	181.97075	182.97803
	IPAP derivative	$C_{10}H_{14}N_2O_2S$	226.0776	227.08488
Thioctic acid	Disulfide	$C_8H_{14}O_2S_2$	206.04352	207.0508
	IPAP derivative (One site)	$C_{16}H_{23}NO_4S_2$	357.10685	358.11413
	IPAP derivative (Two sites)	$C_{24}H_{30}O_6N_2S_2$	506.15453	507.16181
Cystamine	Disulfide	$C_4H_{12}N_2S_2$	152.04419	153.05147
	IPAP derivative	$C_{10}H_{14}N_2O_2S$	226.0776	227.08488
Cystine	Disulfide	$C_6H_{12}N_2O_4S_2$	240.02385	241.03113
	IPAP derivative	$C_{11}H_{14}N_2O_4S$	270.06743	271.07471
Tetraethylthiuram disulfide	Disulfide	$C_{10}H_{20}N_2S_4$	296.05094	297.05821
	IPAP derivative	$C_{13}H_{18}N_2O_2S_2$	298.08097	299.08825
5,5-dithiobis(2-nitrobenzoic acid)	Disulfide	$C_{14}H_8N_2O_8S_2$	395.97221	396.97949
	IPAP derivative	$C_{15}H_{12}N_2O_6S$	348.04161	349.04888
Glutathione oxidized (GSSG)	Disulfide	$C_{20}H_{32}N_6O_{12}S_2$	612.15196	613.15924
	IPAP derivative	$C_{18}H_{24}N_4O_8S$	456.13149	457.13876

From the disulfide mix (Figure 4.4), improved detection of the disulfides of interest as derivatives wasalso seen, similar to the free thiols. With these results, it was confirmed that all disulfides were better detected as IPAP derivatives than in their disulfide forms. These results further demonstrated the need to derivatize free thiols and disulfides for their increased detection, especially in the context of complex biological samples when matrix effects will impede their detection even further without derivatization.

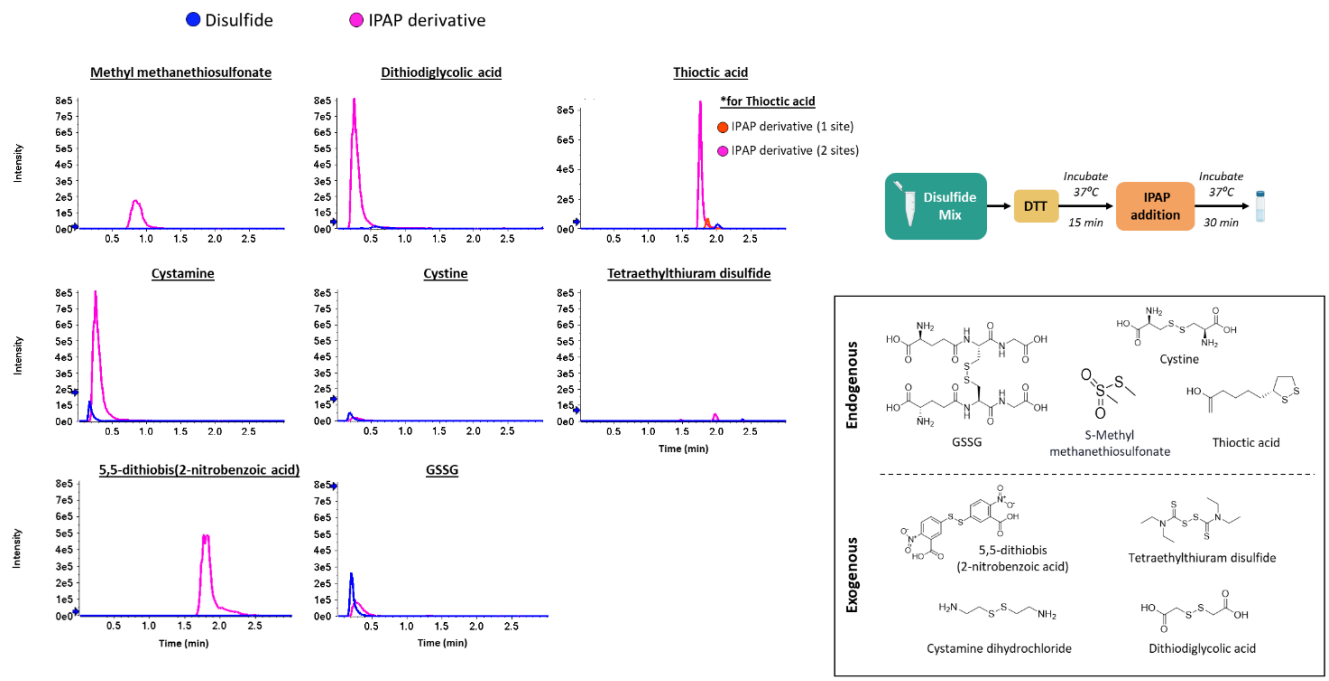

Figure 4.4 High resolution extraction ion chromatograms of disulfides tested and their IPAP derivatives formed

Similar to IAM, IPAP is sensitive to light and was prepared fresh before use for these initial tests. However, as IPAP is dissolved in ACN, while IAM is usually dissolved in H_2O, the stability of the storage of IPAP in solution was tested. To study this stability, a fresh 10 mM IPAP in ACN solution was prepared and a previously prepared and stored 10 mM IPAP in ACN solution was used for the derivatization of a mix of free thiols and disulfides. In a tube containing 100 µL of a mix of free thiols and disulfides at 10 µg/mL each in H_2O, 150 µL of 100 mM ABC buffer pH 8.0 and 20 µL of the fresh 10 mM IPAP solution or stored 10 mM IPAP solution was added and incubated for 30 min at 37°C in the dark. If IPAP is indeed stable as a stored solution, there would be little to no difference between the responses seen from the samples using fresh IPAP solution and the stored IPAP solution, as seen in the example of dimethylbenzenthiol in Figure 4.5. By calculating the difference in peaks areas of IPAP derivatives from the fresh and stored IPAP (Table 4.1), it was determined that IPAP solution was stable for at least 3 months. With the increased stability of this solution, there is a reduction in waste of the reagent as a fresh solution does not need to be weighed out and prepared fresh for each experiment.

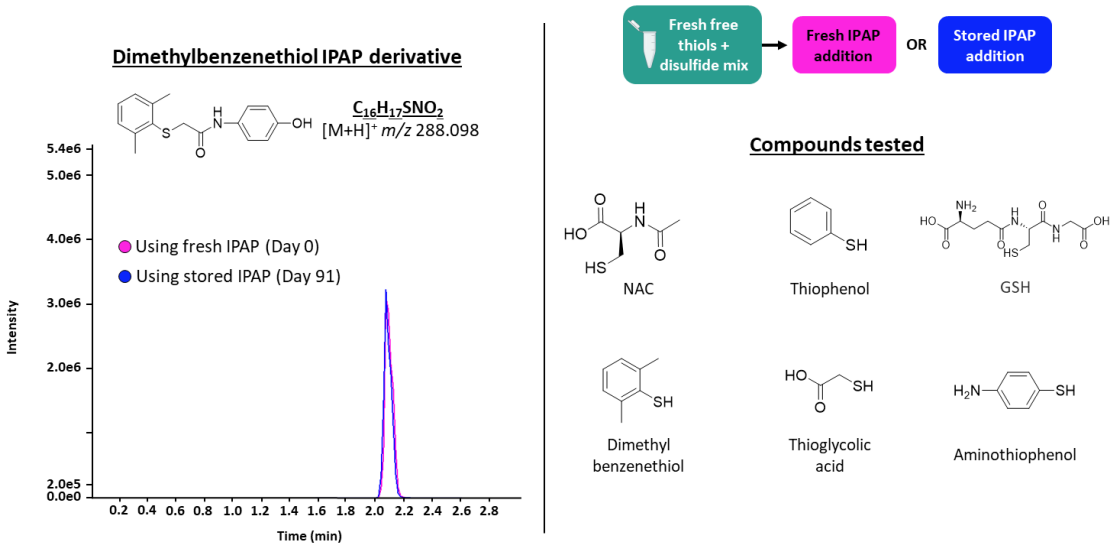

Figure 4.5 Overlaid extracted ion chromatograms of dimethylbenzenethiol IPAP derivatives formed when using fresh and stored IPAP reagent shown as an example

Table 4.3 Results for the comparison of using fresh IPAP and stored IPAP for selected thiols

Name	[M+H⁺] *m/z* (Da)		Error (ppm)	Area	% Area Difference (Fresh IPAP/Stored IPAP)
NAC $C_{13}H_{16}SN_2O_5$	313.08527	Fresh IPAP	0.9	47192	1%
		Stored IPAP	0.7	47484	
Aminothiophenol $C_{14}H_{14}SN_2O_2$	275.08488	Fresh IPAP	0.6	188353	2%
		Stored IPAP	1	192710	
GSH $C_{18}H_{24}SN_4O_8$	457.13876	Fresh IPAP	2.5	416512	-1%
		Stored IPAP	3	414328	
Thioglycolic acid $C_{10}H_{11}O_4SN$	242.04816	Fresh IPAP	0.5	29001	-1%
		Stored IPAP	0.6	28747	
Thiophenol $C_{14}H_{13}SNO_2$	260.07398	Fresh IPAP	0.9	187318	1%
		Stored IPAP	0.9	190069	
Dimethylbenzenethiol $C_{16}H_{17}SNO_2$	288.10528	Fresh IPAP	0.6	202978	-3%
		Stored IPAP	2.1	197826	

Once IPAP was chosen as the derivatization agent, both light and heavy labeled IPAP (IPAP and D_4-IPAP, respectively) with a mix of free thiols and disulfides was tested. Based on the proposed hypothesis workflow (Figure 4.1), the free thiols would be derivatized with the light reagent, followed by the reduction of disulfide bonds with DTT, and subsequent labeling of the thiols produced from disulfide cleavage with the heavy D_4-IPAP reagent. In this reaction, 100 µL of a mix of free thiols and disulfides at

10 µg/mL each was used. To this mix, 150 µL of 100 mM ABC buffer pH 8.0 and 20 µL of 10 mM IPAP solution was added and incubated for 30 min at 37°C in the dark. After this incubation, 90 µL of 10 mM DTT was added and subsequently incubated for 15 min at 37°C. Following the second incubation, 50 µL of 100 mM D_4-IPAP solution was then added and incubated for 30 min at 37°C in the dark. An additional 50 µL of 10 mM DTT was added at the end to quench the alkylation reaction. In particular, DTT was added in excess to the amount of IPAP added to break disulfide bonds and to quench the first reaction, since DTT would theoretically capture residual IPAP (Figure 4.6).

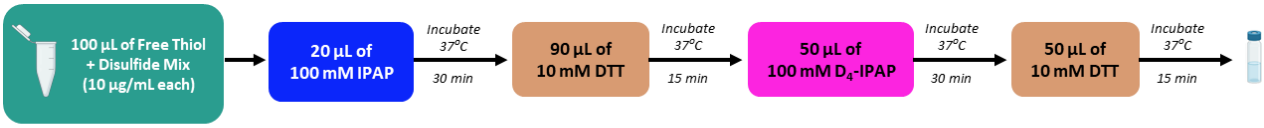

Free Thiols	Disulfides
Dimethylbenzenethiol	Thioctic acid
Thiophenol	Dithiodiglycolic acid
NAC	GSSG
Aminothiophenol	Methyl methanethiosulfonate
Cysteine ethyl ester	

Figure 4.6 Workflow to test the ability of light and heavy labeled IPAP (IPAP and D_4-IPAP) to form derivative pairs that can be used to differentiate between free thiols and disulfides

Based on the hypothesis of this reaction, the free thiols in the mix would only form IPAP derivatives and no D_4-IPAP derivatives would form as all free thiols present would be alkylated with IPAP. On the other hand, the disulfide compounds in the mix would not produce any IPAP derivatives as there would be no derivatization sites for the alkylation reaction of IPAP to take place as there are no -SH groups present. Therefore, only D_4-IPAP derivatives of the disulfide would form once DTT is added which would reduce the disulfides to their free thiol form. However, this test produced some unexpected results (Figures 4.7 and 4.8). The free thiols dimethylbenzenethiol, aminothiophenol and thiophenol, all aromatic thiols, follow the proposed hypothesis, where only the IPAP derivatives of these compounds were detected. For NAC (*N*-acetyl cysteine) and cysteine ethyl ester, peaks for both IPAP and D_4-IPAP derivatives were seen in a close 1:1 ratio, suggesting the presence of NAC and cysteine ethyl ester as both a free thiol and a disulfide with itself or other free thiols. These results seem to demonstrate that stored stocks of these free thiols were able to form disulfides more readily than the aromatic thiols tested.

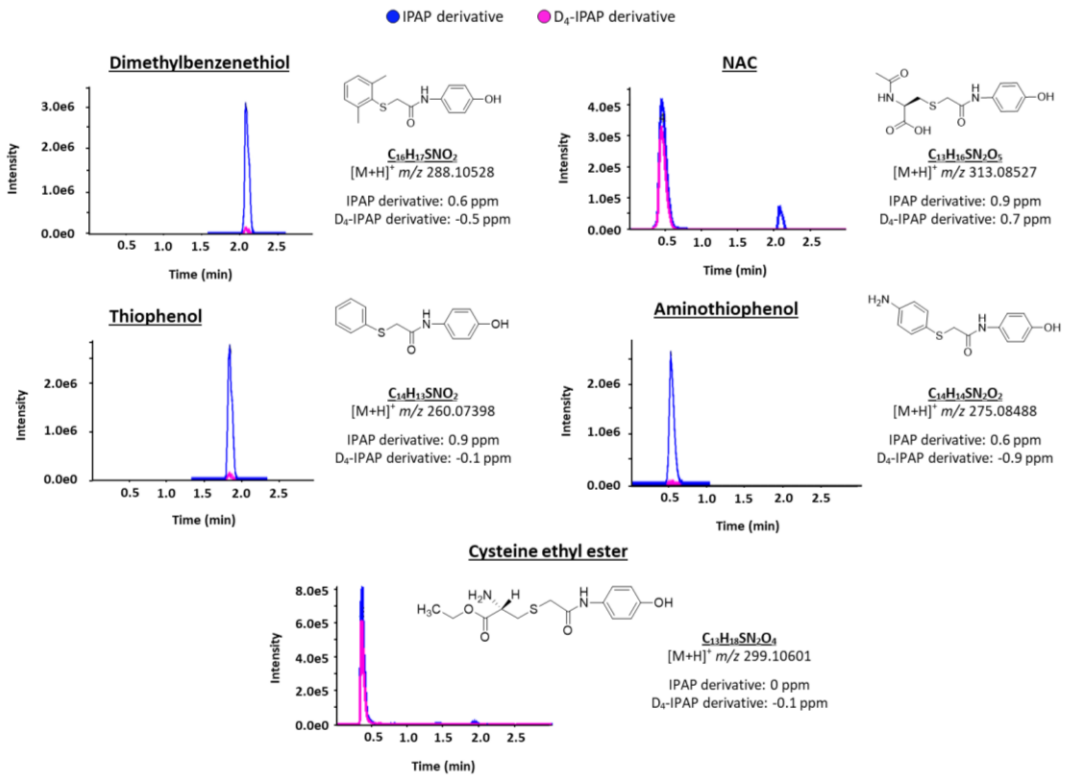

Figure 4.7 Overlaid XIC of the IPAP and D_4-IPAP derivatives of free thiols, with the ppm of each derivative detected

For the disulfides tested, it was theorized that only the D_4-IPAP derivatives would be detected, however in each case their IPAP derivative was also detected. Methyl methanethiosulfonate is not a traditional disulfide compound, however the S-S bond does get cleaved by DTT. The resulting free thiol, methanethiol, formed mainly the D_4-IPAP derivative but a significant proportion of the IPAP derivative was still present (Figure 4.8). Thioctic acid is a molecule that has an intramolecular disulfide bond and therefore has two -SH groups as possible alkylation sites. As such, the reduced thioctic acid can be singly or doubly derivatized, which resulted in the detection of the doubly derivatized version by both IPAP and D_4-IPAP. For dithiodiglycolic acid and GSSG, although it was expected that only the D_4-IPAP derivative would be detected given the experimental set-up, there was essentially an equal amount of the IPAP and D_4-IPAP derivatives formed. Therefore, it was concluded that, although DTT was added in excess to IPAP, it does not completely quench it's ability to continue to alkylate once disulfides are reduced. Therefore, once the free thiols are formed, both IPAP and D_4-IPAP are present to create their corresponding derivatives.

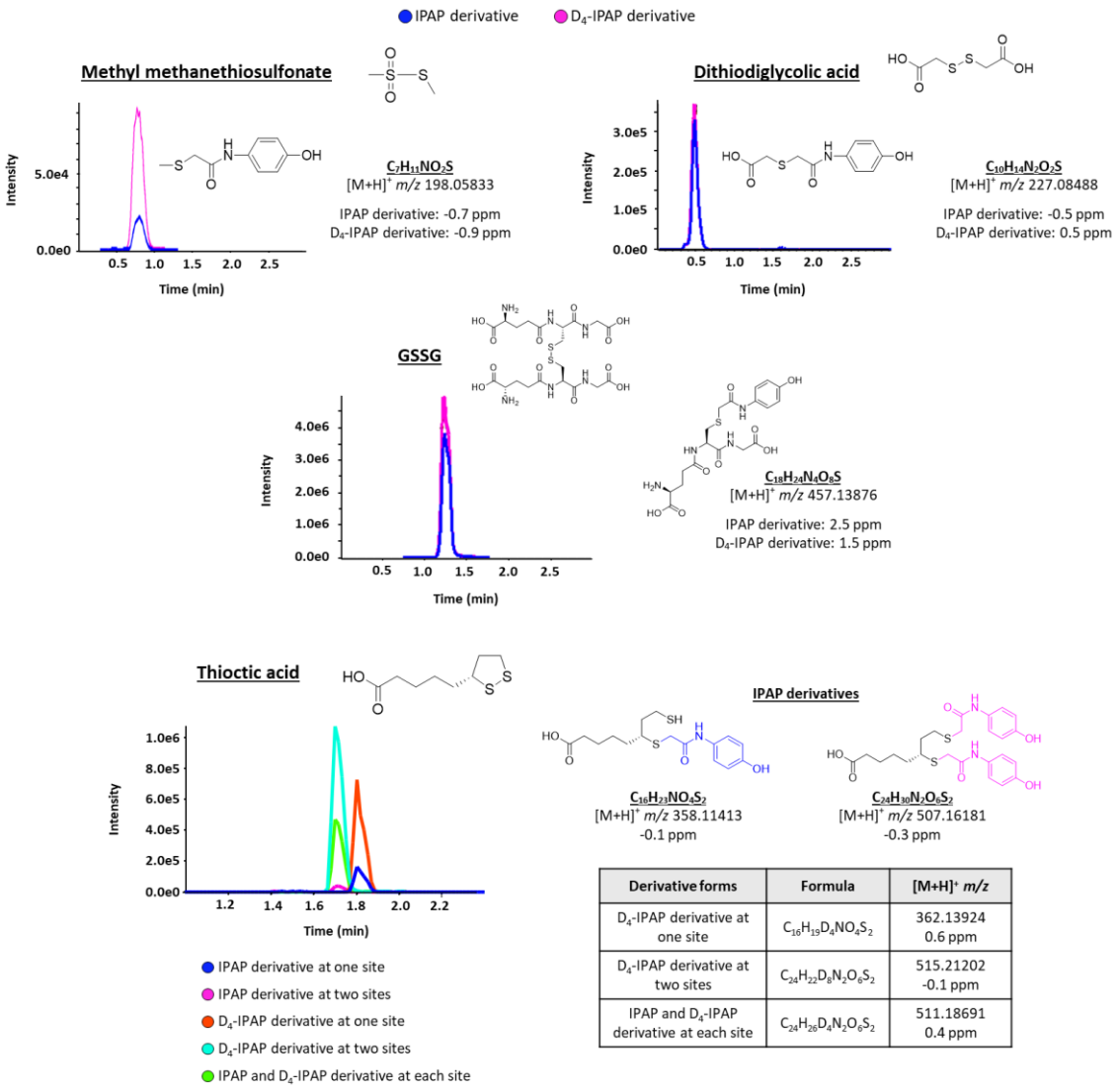

Derivative forms	Formula	[M+H]+ m/z
D_4-IPAP derivative at one site	$C_{16}H_{19}D_4NO_4S_2$	362.13924 0.6 ppm
D_4-IPAP derivative at two sites	$C_{24}H_{22}D_8N_2O_6S_2$	515.21202 -0.1 ppm
IPAP and D_4-IPAP derivative at each site	$C_{24}H_{26}D_4N_2O_6S_2$	511.18691 0.4 ppm

Figure 4.8 Overlaid XIC of IPAP and D_4-IPAP derivatives of disulfides with ppm of each derivative detected

4.2 Testing with biological samples

Using fresh biological mouse tissue samples available (liver, brain, serum, and feces), the derivatization reactions for endogenous thiols in complex metabolite extracts using IPAP and D_4-IPAP was investigated. The samples were prepared as described in Chapter 2, Section 2.2.2.3. These samples were then subjected to the derivatization reaction as described below (Table 4.4) and the resulting samples were analysed using the untargeted metabolomics workflows using the Scherzo column on the QqTOF instrument in positive mode, with an injection volume of 15 µL. When studying the results of this test, cysteine (Cys), GSH, and

NAC were specifically focused on. In this experiment, if free thiols are present in the samples, they would produce a 1:1 ratio of IPAP and D_4-IPAP derivatives as both derivatization agents were added at the same time.

Table 4.4 For the derivatization reaction of mouse tissue samples, the procedures followed are described below. The liver and brain samples were processed in the same way, while the feces and serum samples were processed slightly differently.

Sample	PPE		Derivatization reaction	Quenching reaction
100 µL of feces homogenate	NA		+ 100 µL 100 mM ABC buffer pH 8.0 + 50 µL 10 mM IPAP + 50 µL 10 mM D_4-IPAP Incubation for 30 min at 37°C in the dark	+ 100 µL 10 mM DTT Incubation for 15 min at 37°C
100 µL of liver homogenate	+ 200 µL MeOH	200 µL supernatent used for extraction	+ 200 µL 100 mM ABC buffer pH 8.0 + 50 µL 10 mM IPAP + 50 µL 10 mM D_4-IPAP Incubation for 30 min at 37°C in the dark	+ 100 µL 10 mM DTT Incubation for 15 min at 37°C
100 µL of brain homogenate				
15 µL of serum	+ 60 µL MeOH	200 µL supernatent used for extraction	+ 100 µL 100 mM ABC buffer pH 8.0 + 50 µL 10 mM IPAP + 50 µL 10 mM D_4-IPAP Incubation for 30 min at 37°C in the dark	+ 100 µL 10 mM DTT Incubation for 15 min at 37°C

From the results of this study, differing levels of GSH, Cys, and NAC were detected. When looking at the exact mass for the GSH IPAP derivative (Figure 4.9), a large peak eluting at 10.5 min was seen in all samples. A second smaller peak at around 8 min was also observed in the brain, liver, and serum samples with varying intensities, with the highest intensity seen in the liver sample and the lowest intensity seen in the serum sample. However, this peak was not observed in the feces samples. When looking more closely at the mass spectra for each of these peaks (Figure 4.10), the peak at 10.5 min exhibited a triplet isotopic pattern, whereas the peak at 7.8 min contained the expected double isotopic pattern. The doublet had peaks at *m/z* 457.1345 and *m/z* 461.1596. The triplet had peaks at *m/z* 453.1113, *m/z* 457.1364 and *m/z*

461.1614, where the middle peak was higher than the others. When a heavy labeled compound is used with its corresponding light labeled version, it produces a doublet with a mass difference that corresponds to the difference between the heavy labeled compound and the light labeled compound, which was 4.02511 Da (where four H atoms are replaced with deuterium atoms (^{2}H) from the D_4-IPAP compound) in this case. Therefore, the differences between the peaks of the doublet (at 7.8 min) and the triplet (at 10.5 min) were calculated, and were confirmed to have a mass shift of 4.02511 Da between the peaks in their respective spectra.

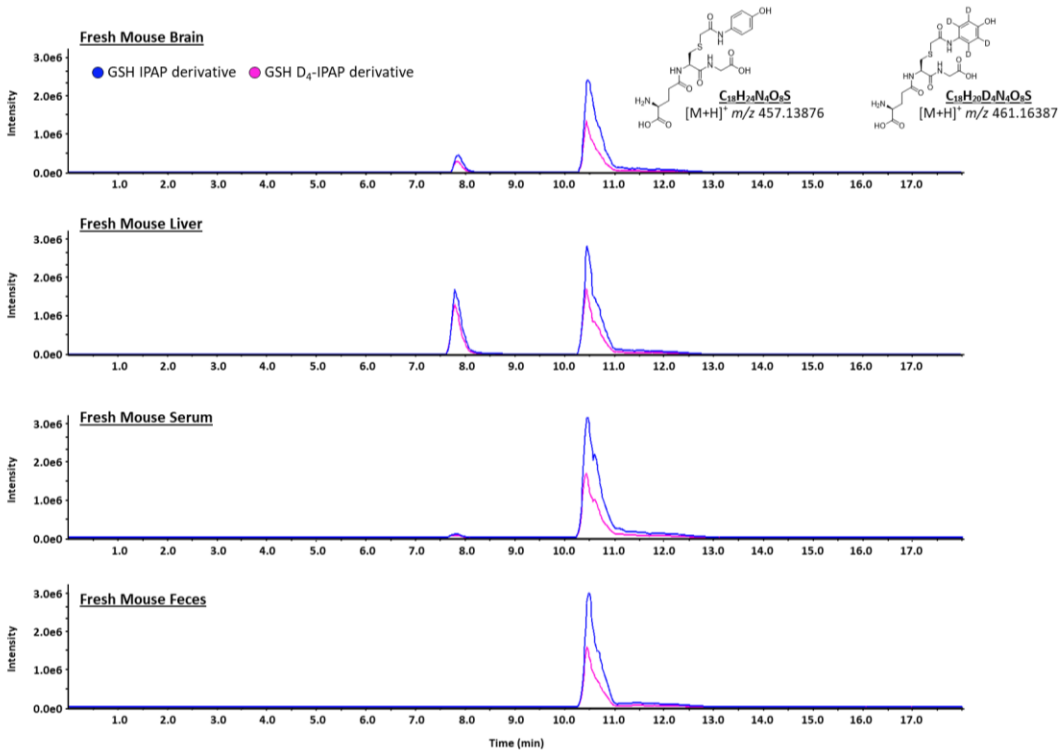

Figure 4.9 XIC for exact masses of GSH IPAP and D_4-IPAP derivatives in fresh mouse brain, liver, serum, and feces samples

Between each monoisotopic peak in both the doublet and the triplet, there was a difference of 4.02511 Da. This difference is the exact difference between the IPAP and the D_4-IPAP, showing the presence of a light and heavy labeled derivative pair. However, the triplet shows that the compound is double deuterated while the doublet shows the compound is deuterated once. While DTT is used to reduce disulfide bonds, it is also a thiol that can be derivatized. In particular, DTT is a thiol with two alkylation sites, and can therefore be derivatized with IPAP at two sites or with D_4-IPAP at two sites. As IPAP and D_4-IPAP is present

in the same mix, it is possible that both IPAP and D_4-IPAP derivatizes the DTT at the same time, producing a compound alkylated by IPAP at one site and by D_4-IPAP on the other site. This scenario was seen with the triplet at 10.5 min. The peak at *m/z* 453.1113 represents DTT that has been derivatized by IPAP at two sites. The peak at *m/z* 457.1364 represents DTT that has been derivatized by IPAP at one site and D_4-IPAP at another site. The peak at *m/z* 461.1614 represents DTT that has been derivatized by D_4-IPAP at two sites. For the peak at 7.8 min, the peak at *m/z* 461.1596 represents the GSH IPAP derivative and *m/z* 457.1345 represents the GSH D_4-IPAP derivative, with a mass difference of 4.02511 Da. These results confirmed that the GSH peak seen in the sample at 7.8 min was that of the GSH IPAP derivative. The triplet peak would have to then come from a doubly derivatized compound based on the unique isotopic pattern. When considering all the samples, it was proposed that this peak would be the result of derivatized DTT (as shown in Figure 4.10 below), with exact mass measurements confirming this hypothesis. It is therefore very important to closely examine high-resolution MS traces and consider any side reactions that can occur in a complex sample.

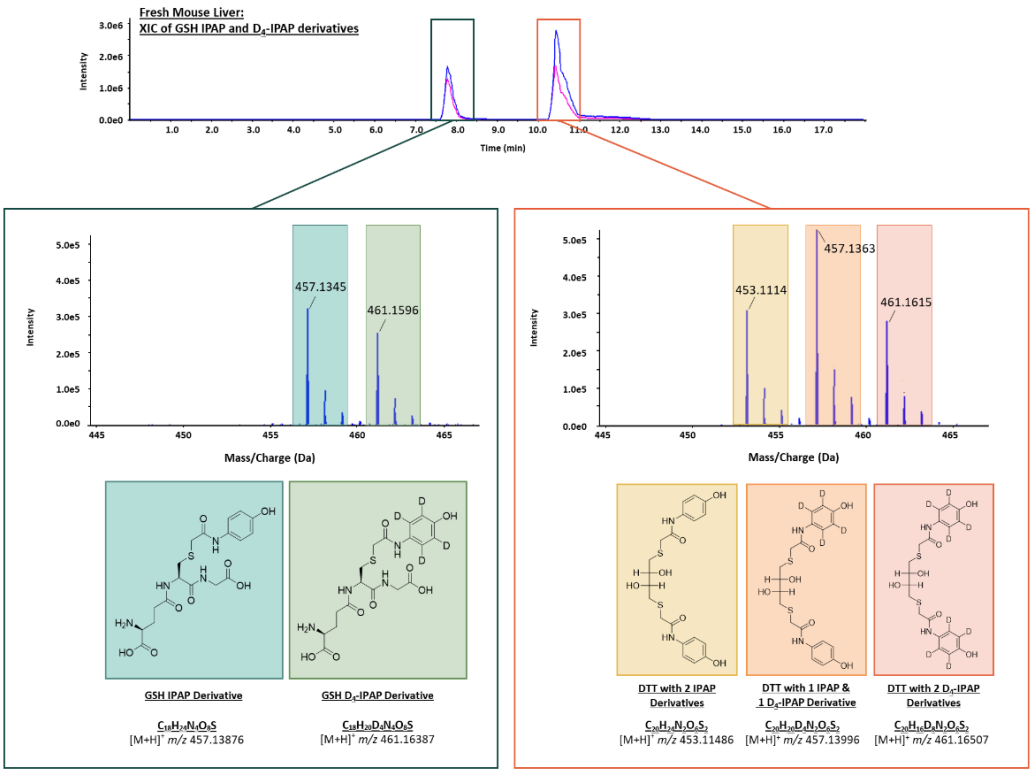

Figure 4.10 TOF-MS of the two peaks seen in the mouse liver samples in the extracted ion chromatogram of GSH IPAP and GSH D_4-IPAP derivatives

For the detection of Cys, a wide peak corresponding to the Cys IPAP derivative eluted at around 6 min, with the liver sample having the highest intensity compared to the other three biological samples (Figure 4.11). When looking at the MS spectrum, a doublet was seen with a mass difference of 4.0248 Da. The peak at *m/z* 271.0730 represents the Cys IPAP derivative and the peak at *m/z* 275.0980 represents the Cys D_4-IPAP derivative. While the peak at 6.4 min was not as well defined as the GSH IPAP peak at 7.8 min, it can be determined that the peak is in fact that of the Cys IPAP derivative by using the MS spectrum (Figure 4.12), even if the chromatographic method used with the Scherzo column is not ideal for this specific compound. The NAC IPAP derivative was not detected in these samples using this untargeted method.

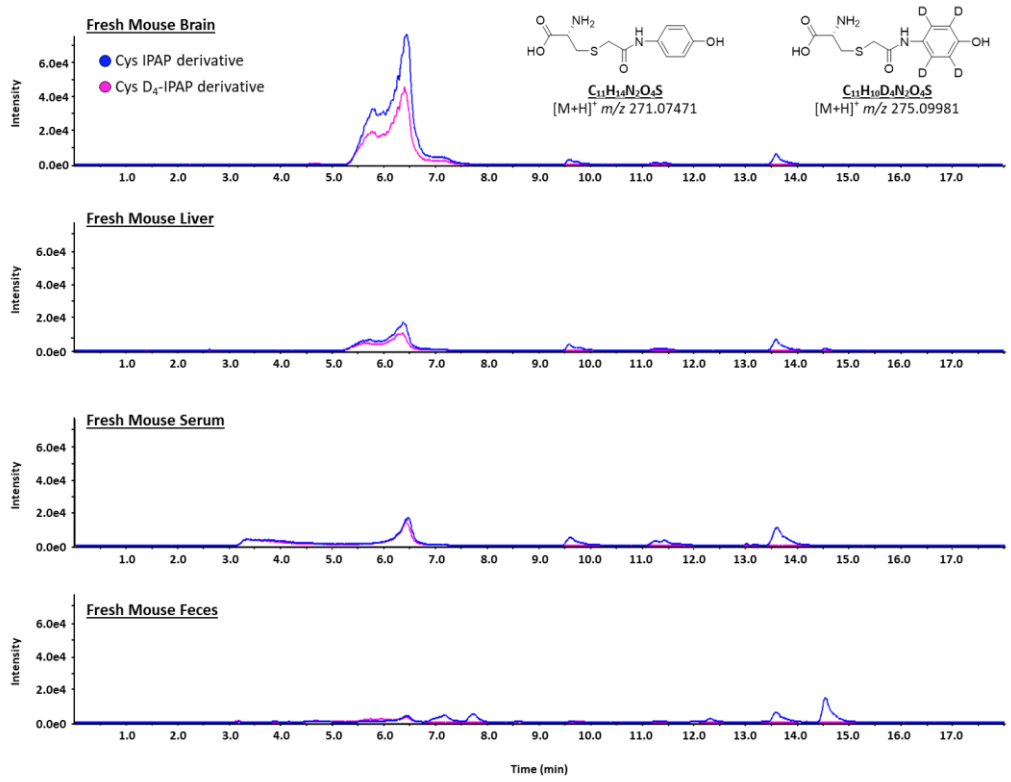

Figure 4.11 Extracted ion chromatograms for exact masses of Cys IPAP and D_4-IPAP derivatives in fresh mouse brain, liver, serum, and feces samples

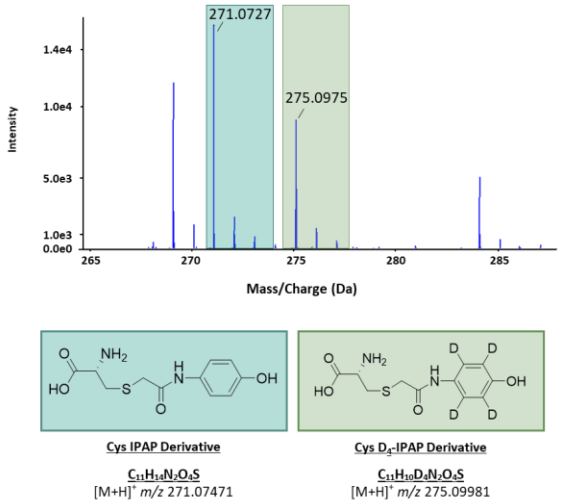

Figure 4.12 TOF-MS spectra of Cys IPAP and Cys D_4-IPAP derivatives

As a complementary method to the untargeted approach using the Scherzo column, and to improve the peak shapes seen, a targeted method on the triple quadrupole (QqQ) platform in MRM mode was developed for the specific detection of the IPAP and D_4-IPAP derivatives of GSH, Cys, and NAC in these samples. This method was developed using a ZORBAX column (as described in Chapter 2, Section 2.3), resulting in a 9 min method including re-equilibration time. GSH, Cys, and NAC standard stocks were derivatized with IPAP to form their corresponding derivatives using the LC-MRM targeted method. The transitions for each IPAP derivative were chosen based on fragmentation seen on the MS/MS spectra obtained using the QqTOF high-resolution analysis. From the fragmentation of the GSH IPAP derivative, the product ion at *m/z* 382 corresponds to the loss of the glycine neutral (loss of 75 Da, with ion formula $C_{16}H_{20}N_3O_6S^+$), the product ion at *m/z* 328 corresponds to loss of gamma-Glu portion of the molecule (loss of 129 Da, with ion formula $C_{13}H_{18}N_3O_5S^+$). Other fragment ions chosen in the targeted method (*m/z* 208, 182, 144) are analogous to those previously described for the fragmentation spectrum of the adduct between acetaminophen and cysteine (a positional isomer of Cys IPAP) (Sleno et al., 2007). Using this relatively high throughput method, excellent separation between the three compounds was seen. The GSH IPAP derivative eluted at 3.1 min, the Cys IPAP derivative at 2.2 min, and the NAC IPAP derivative at 4.0 min (Figure 4.13). Based on these results, the chosen transitions for the IPAP and D_4-IPAP derivatives

were optimized for collision energies (CE) yielding the best sensitivity of detection. Table 2.5 (Chapter 2) outlines the final list of MRM transitions (based on nominal masses), dwell times, and CE used.

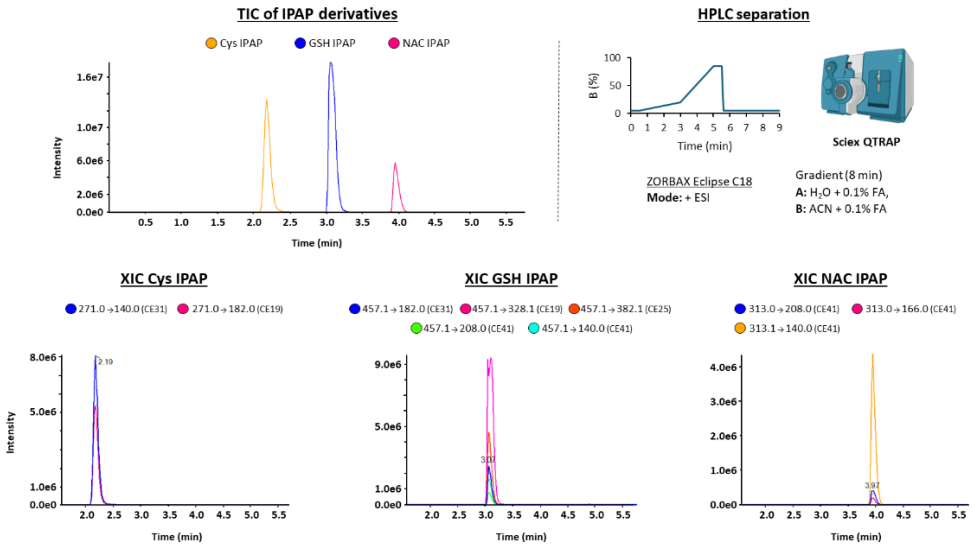

Figure 4.13 LC-MRM traces for the detection of GSH IPAP, Cys IPAP, and NAC IPAP of derivatized stock solutions, 15 pg of each injected on ZORBAX column

Once the LC-MRM method was optimized, the biological samples previously analysed on the QqTOF were re-injected (at 5 µL, which is half the injection volume previously used for untargeted method) on the QqQ using the optimized targeted method. An important step for the optimization of a MRM method is the use of standards whenever possible, since transition ratios (signal intensity ratios between different transitions for the same analyte) can be determined along with the correct RT of each compound of interest, which can be used to confirm the presence of compound without interferences in complex samples. This is important as interference peaks can elute at the same RT as the compound of interest. Therefore, to study the results of these biological samples, all the transitions of GSH IPAP, Cys IPAP, and NAC IPAP derivatives were analyzed in detail. From the results shown in Figure 4.14, the MRM method confirmed the results from the QqTOF, where GSH IPAP and Cys IPAP derivatives were well detected, while the NAC IPAP derivative could not be confirmed with confidence due to very low signal. While a small peak was seen at the relevant RT, based on the transition ratio of the NAC IPAP standard, it was determined that this peak is most probably the result of interference. This confirmed that for this sample set, NAC IPAP was not detected, similar to the results seen when injected on the QqTOF. The peak at 4.9 min (Figure 4.15), which showed a large signal in a number of transitions for the GSH IPAP derivative, did not correspond to any of

the three compounds of interest. This peak was present in all biological samples and they all had the same intensity, pointing towards it coming from an interference in the derivatization reaction, and not from the actual biological sample. In these samples, IPAP and D_4-IPAP was used in a 1:1 ratio and therefore a 1:1 ratio for the signal intensity of the IPAP and D_4-IPAP derivatives was expected when looking at the MS spectrum of this peak at 4.9 min. As the peak of interest for the GSH IPAP derivative was confirmed with the standard at 3.1 min, it was clear that this other rather large peak was the same derivatized DTT peak that had been characterized previously using the high-resolution untargeted LC-QqTOF method (Figure 4.10).

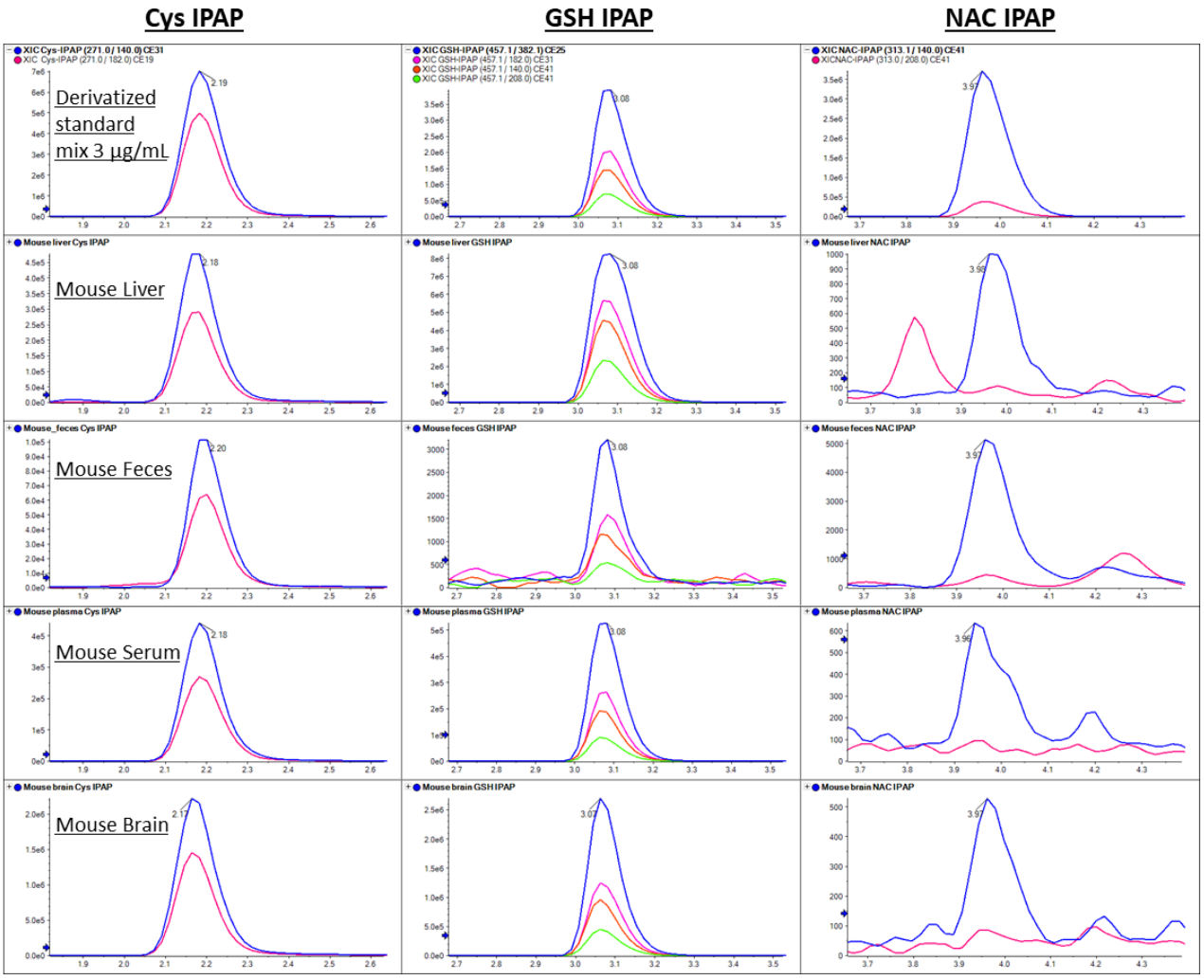

Figure 4.14 Overlaid XIC of MRM transitions of Cys IPAP, GSH IPAP, and NAC IPAP in derivatized standard mix (at 3 µg/mL), as well as mouse liver, feces, brain and serum samples. The GSH IPAP derivative transition *m/z* 457 → 328 was omitted in these traces due to signal saturation in liver sample

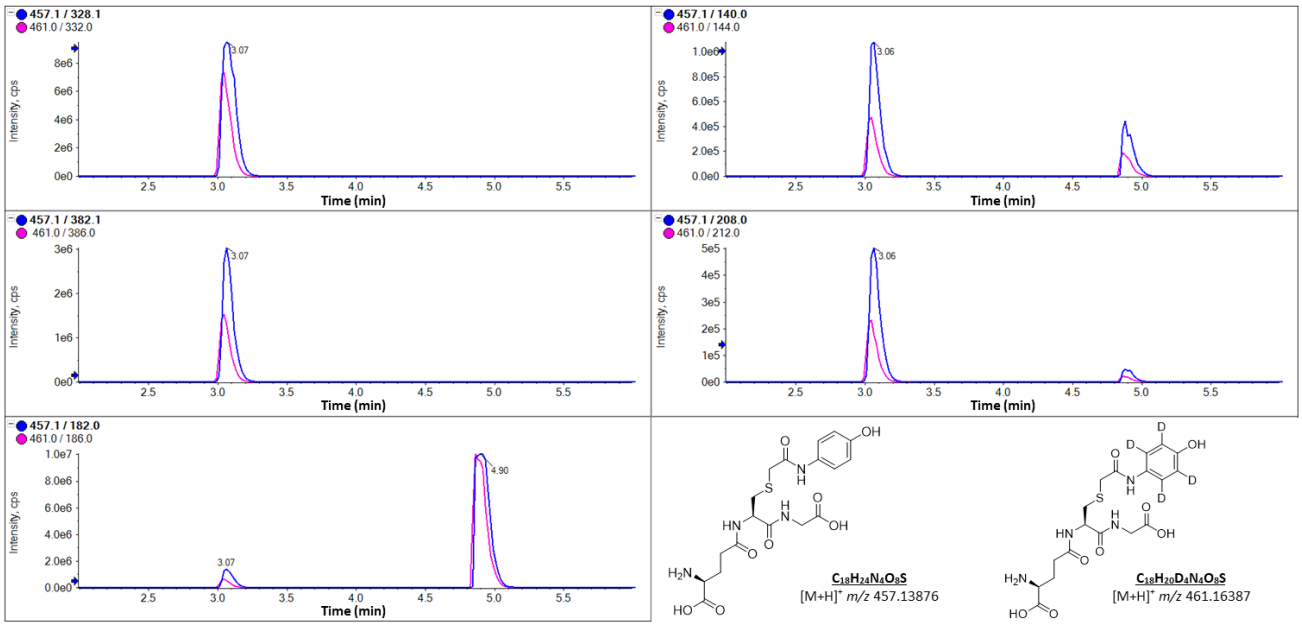

Figure 4.15 Overlaid extracted ion chromatograms of GSH IPAP and GSH D_4-IPAP transitions shown from a mouse brain sample

4.3 Quantitative analysis of GSH-GSSG mixtures

Previous testing performed resulted in some unexpected results in terms of the ratios seen between the IPAP and D_4-IPAP derivatives, as seen in Figure 4.15. Therefore, to further study these results, GSH-GSSG mixtures of varying ratios were tested. By using known concentrations of the free thiol and disulfide, the hypothesized workflow (Figure 4.1) was tested for its ability to accurately quantify the thiol-disulfide ratio in real samples. For this test, GSH-GSSG mixtures with various ratios of GSH and GSSG (50:0, 40:10, 25:25, 10:40, 0:50 (GSH:GSSG)) were prepared and tested using fresh solutions of GSH and GSSG prepared in H_2O at a starting concentration of 10 µg/mL. In individual tubes, different volumes of the 10 µg/mL GSH and GSSG solutions were combined (50 µL GSH: 0 µL GSSG, 40 µL GSH: 10 µL GSSG, 25 µL GSH: 25 µL GSSG, 10 µL GSH: 40 µL GSSG, and 0 µL GSH: 50 µL GSSG). In each tube, 90 µL of 100 mM ABC buffer pH 8.0 and 20 µL of 10 mM IPAP solution was added to alkylate the free thiols in the mix. The addition of IPAP was performed in the dark and incubated for 30 min at 37°C. To quench the reaction and cleave disulfide bonds, 20 µL of 10 mM of DTT was then added and incubated for 15 min at 37°C. A volume of 40 µL of 10 mM D_4-IPAP was then added to the mix and incubated for another 30 min at 37°C in the dark. This step of the derivatization reaction would then alkylate the newly formed GSH from the reduction of GSSG. The

optimized LC-MRM method was used to monitor the GSH IPAP and D_4-IPAP derivatives formed (with 1 µL injections).

Based on the initial hypothesis, a decreasing amount of GSH would result in the reduced formation of GSH IPAP derivatives. As the amount of GSSG increases, there would be an increased formation of GSH D_4-IPAP derivatives as there is more GSSG available to be reduced into GSH following the addition of DTT. Therefore, as the ratio of GSH decreases and the GSSG ratio increases, the ratio between the IPAP and D_4-IPAP peaks would also change. At 50:0, the GSH IPAP peak should be the only peak present. As the GSSG amount increases, the intensity of the GSH D_4-IPAP derivative peak would increase, while the intensity of the GSH IPAP derivative peak would decrease. As a ratio of 25:25, the peak height of the two derivatives would be equal. At the ratio of 0:50, the GSH D_4-IPAP derivative would be the only peak present as there would be no GSH present as a free thiol for the alkylation of IPAP to take place. However, when examining the results (Figure 4.16), they did not reflect this theoretical hypothesis. From the results, even at a ratio of 50:0, a substantial proportion of the GSH D_4-IPAP derivative was detected. At 25:25, the IPAP and D_4-IPAP derivative peaks were not present in a 1:1 ratio as predicted. Instead, the GSH D_4-IPAP derivative peak had a lower intensity compared to the GSH IPAP derivative. At a ratio of 0:50, both IPAP and D_4-IPAP derivatives were formed. This test suggests that IPAP was still present when the DTT cleaves the disulfide bond. Therefore, when the disulfide bonds are reduced to form the free thiols, IPAP was still available to form GSH IPAP derivatives. By performing this test, it also seems to suggest that DTT is not able to quench the IPAP reaction as previously hypothesized. This was quite surprising since this procedure is used routinely in proteomics workflows to reduce potential overalkylation of peptides by using IAM (having the same reactive groups). But since it was demonstrated that IPAP was much more stable in solution compared to IAM, there are some definite differences between the two molecules, with the ability for DTT to quench its reaction being one of them.

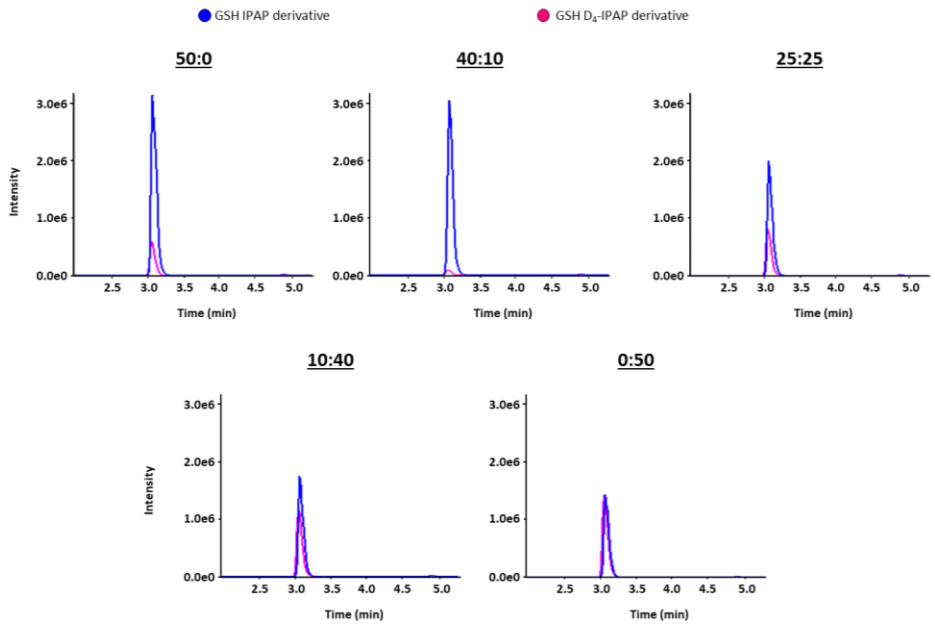

Figure 4.16 Overlaid extracted ion chromatograms of GSH IPAP (*m/z* 457.1 → 328.0) and GSH D_4-IPAP (*m/z* 461.0 → 332.0) derivatives formed in a GSH-GSSG mixture with varying ratios of GSH and GSSG to study the derivatization reaction using IPAP and D_4-IPAP

4.4 Quenching Test

To precisely quantify the free thiols present in a biological sample by using light and heavy labeled reagents, it is important to be able to quench the reaction of the light labeled reagent. This is particularly important as a reducing agent such as DTT is needed to reduce disulfides to allow for the derivatization of their free thiol products with the heavy labeled reagent. If the light labeled reagent reaction is not properly quenched, it would still be present along with the heavy labeled reagent. This would then lead to both reagents reacting with the newly formed free thiols, and therefore, leading to potential light labeled derivatives being misidentified as free thiols rather than reduced disulfides.

From the results described above in Section 4.3, it suggests that DTT does not quench the alkylating reaction of IPAP very well. Therefore, acidifying the solution with FA was tested as an alternate quenching solution in a time course reaction with GSSG and IPAP solution. In this reaction, 10 mM DTT and 2.5% FA were used as the two quenching solutions. To perform this experiment, 10 mM of IPAP was added to a solution of 10 µg/mL of GSSG dissolved in 100 mM ABC buffer pH 8.0 in the dark. This mix was then incubated at 37^{o}C for 0 min, 5 min, 10 min, 15 min, and 30 min. At the end of each timepoint, either the

DTT or FA solution was added, with the exception of the 0 min timepoint, where the quenching solution was added before the addition of IPAP (Figure 4.17), to be used as a control. As FA would not reduce GSSG, no GSH IPAP derivatives would form at 0 min. At the other timepoints, if the reaction is quenched by the quenching solutions added in excess compared to free thiol or the acidified environment, no IPAP derivatives would be able to form as the alkylation reaction would be halted even if free thiols are present.

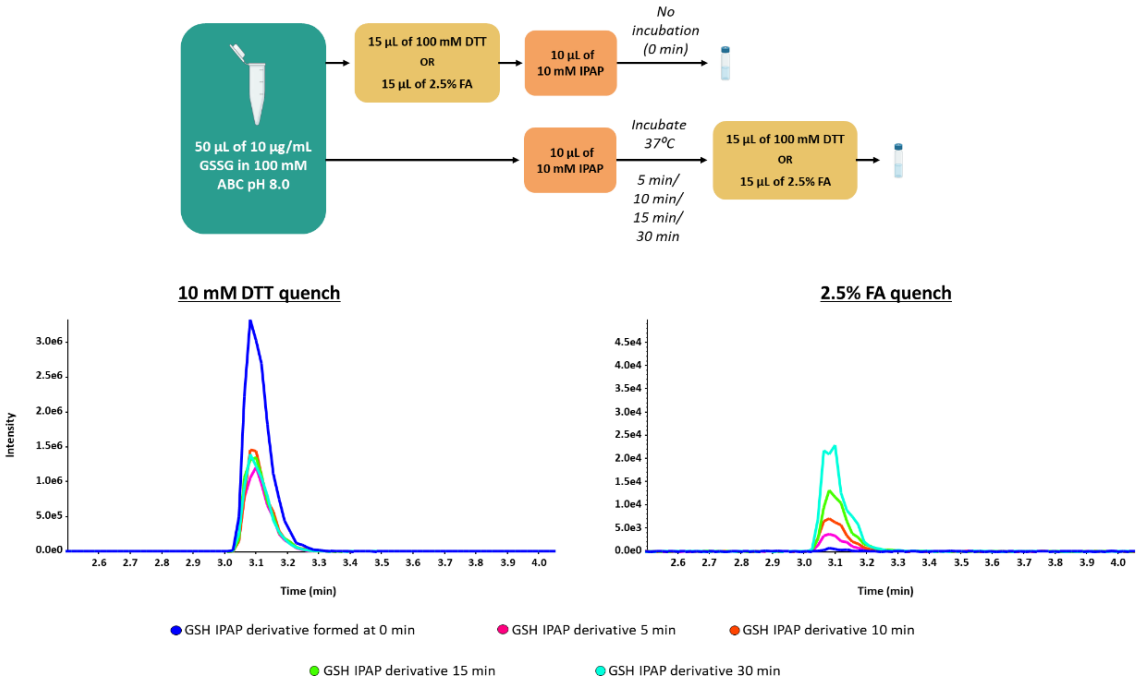

Figure 4.17 Overlaid extracted ion chromatograms of GSH IPAP transition *m/z* 457 → 328 from a time course experiment comparing the ability of DTT and FA to quench the IPAP derivatization reaction. A simplified workflow illustrates the sample preparation steps.

With a final concentration of 6.6 µg/mL of GSSG, 2 µL of each sample was injected onto the ZORBAX column using the LC-MRM method. To study the difference between the two quenching solutions, the *m/z* 457.1 → 328.1 GSH IPAP derivative transition was studied (Figure 4.17). When looking at the DTT quench, a large GSH IPAP derivative peak with an intensity of 3.2e6 was seen at the 0 min timepoint. As DTT was added before the addition of IPAP, GSSG was reduced to form GSH which would then react with the IPAP to form GSH IPAP derivatives. When adding DTT at each timepoint, the intensity of the GSH IPAP derivative peak did not change. When studying the FA quench, the GSH IPAP derivative peak with the highest intensity was seen after the 30 min timepoint with an intensity of 2.2e4, which is almost 100 times smaller than the lowest intensity GSH IPAP derivative peak formed when using the DTT quench (1.5e6

intensity formed at 10 min). The difference in the intensity of the GSH IPAP derivative peaks confirmed the hypothesis that DTT is not able to quench the IPAP reaction. As the alkylation reaction is not stopped, the remaining IPAP will react with the newly formed free thiols to form IPAP derivatives. The acidification strategy is therefore quite promising for quenching the reaction prior to reducing the disulfides and completing the heavy labeling reaction (with pH adjustment for the second alkylation reaction, of course). This formation also helped demonstrate that an incubation time as low as 5 min is sufficient for the IPAP alkylation reaction to take place. This is advantageous as it could significantly reduce the time needed for sample preparation using this derivatization strategy in real biological samples.

4.5 Depletion Test using thiol-containing solid phase resins

Another method to quench the IPAP reaction was explored involving the use of a solid phase resin with thiol groups which could react with the IPAP solution. Based on this reaction, the resin can be used to remove any excess light labeled IPAP that is present before the addition of DTT for the reduction of disulfides in the sample. This would then theoretically allow the newly formed thiols to react with only the D_4-IPAP and not IPAP, which would, in turn, allow for the improved identification of thiols and reduced disulfides. For this method, two thiol resins that were available in the lab were tested: a polystyrene-based thiophenol resin (PS-thiophenol) and a silica based alkyl thiol resin (Si-Thiol). Acting as scavenger resins for alkylating compounds, residual IPAP present in the reaction would react with the free thiols in the resin.

Each resin was tested by adding IPAP and DTT to a 10 µg/mL GSSG solution in 100 mM ABC buffer pH 8.0. To prepare the resins for use, they were washed with 500 µL of 100 mM ABC buffer pH 8.0 twice, spinning down the mix and removing the supernatant. Once washed, 1 mg of resin (as a slurry in 20 µL of ABC buffer) was transferred into a new tube containing 200 µL of ABC buffer along with 10 µL of 10 mM IPAP solution with its subsequent incubation period of 15 min at 37^{o}C in the dark. The resin was then removed by transferring 200 µL of the supernatant, taking care to not transfer any resin, followed by the addition of 50 µL of 10 µg/mL GSSG solution and 15 µL of 10 mM DTT and incubated for 15 min at 37^{o}C in the dark. To prepare control samples for this reaction, 2 samples were prepared using no resin. In one sample, 50 µL of the 10 µg/mL GSSG solution in ABC and 15 µL of 10 mM DTT was combined together in a tube and incubated for 15 min at 37^{o}C and was used as a positive control for the presence of GSH IPAP derivatives. In the other sample, 50 µL of the 10 µg/mL GSSG solution in ABC was added into a tube and was used as a negative control for the presence of GSH IPAP derivatives. Samples were then analysed using the LC-MRM method with 2 µL injections. As a control, the sample with GSSG and DTT with no resin would form GSH

IPAP derivatives while the sample with GSSG and no resin would not form GSH IPAP derivatives as the GSSG would remain as a disulfide. To test if the resins need to be reduced prior to use, the resins were also reduced using DTT before being washed with 100 mM ABC buffer, similar to the previously described test. As the results of DTT treated resins and the non-DTT treated resins were the same, it seems to suggest that the resins do not need to be reduced prior to use.

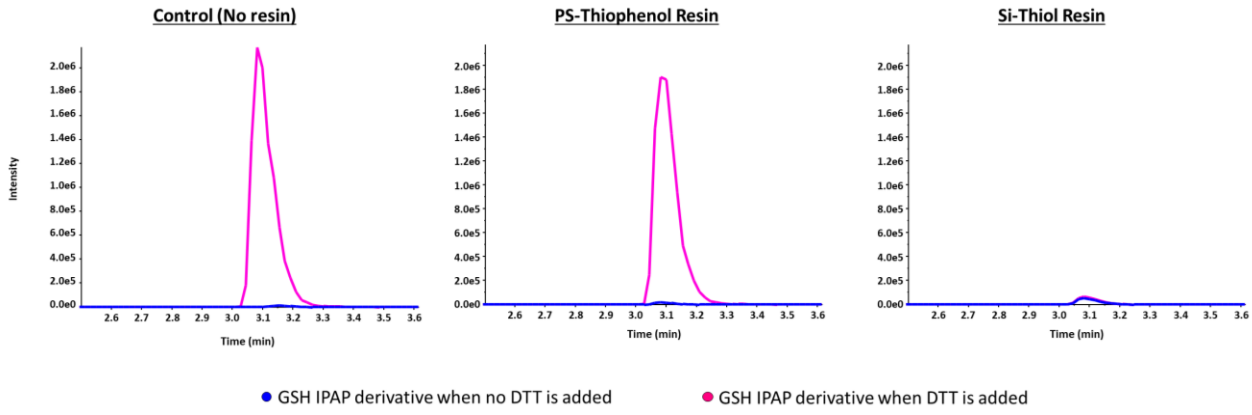

Figure 4.18 Extracted ion chromatograms of GSH IPAP derivative (transition *m/z* 457.1 → 328.1) formed when using two different resins for IPAP depletion

From the results of the GSH IPAP derivative peak (using *m/z* 457.1 → 328.1 transition) (Figure 4.18), a high intensity peak at 2.0e6 was seen in the positive control, with no GSH IPAP derivative peak was detected in the negative control as expected. By using the results of the positive control, the ability of the resins to deplete IPAP can be studied where if the resins are able to deplete the IPAP, the intensity of the GSH IPAP derivative peak formed when using the resins would be significantly lower than that of the control peak. A large GSH IPAP derivative peak similar to the positive control was seen when using the PS-Thiophenol resin. A GSH IPAP derivative peak was also seen when using the Si-Thiol resin, however the intensity of this peak was at 1.0e5, which was more than 20 times lower than the peak height seen when using the PS-Thiophenol resin. This shows that PS-Thiophenol resin was not able to deplete IPAP, while Si-Thiol resin was able to deplete it. Therefore, for the depletion of the alkylation reagent IPAP, Si-Thiol resin is a promising candidate. This would then allow the alkylation of free thiols from reduced disulfides by the heavy labeled D_4-IPAP to take place more accurately in real samples, although this still needs to be verified with further testing.

4.6 Detection of oxidative species from oxidative stress

When exposed to oxidative environments, thiols can form oxidized species such as R-SOH, R-S(O)OH and R-S(O_2)OH (Figure 4.19). Among these species, sulfenic acid is known as a reaction intermediate due to its instability and high reactivity, making it difficult to detect and study, while the other species are more stable. However, the presence of these species help better understand the redox signaling of a system (Bindoli et al., 2008). A simple oxidation stress test was performed to study the formation of oxidative species from GSH and GSSG using the derivatization procedure with IPAP. This test was performed with GSSG and GSH with increasing amounts of hydrogen peroxide (H_2O_2), at varying concentrations, representing approximately 15X, 30X, 75X, and 300X the concentration of thiol tested.

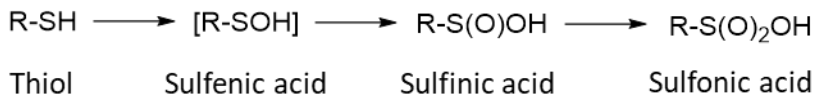

Figure 4.19 Oxidized species formed from the oxidation of thiols

For this experiment, separate GSH and GSSG solutions of 1 mg/mL each were freshly prepared. In separate tubes, increasing levels of 0.5 mM H_2O_2 was added to 100 µL of each solution (GSH or GSSG) for a final concentration of 0.2 mg/mL of GSH and/or GSSG in each tube, followed by the addition of DTT and IPAP. These samples were then analyzed using the LC-MRM method, targeting GSH IPAP derivatives. From these results (Figure 4.20), it was observed that GSH IPAP derivatives still formed in both the GSSG and GSH solutions until 30X H_2O_2. At 75X, a drop in the intensity of the GSH IPAP derivative peak formed was observed, with a complete disappearance of the GSH IPAP derivative at 300X. The GSSG solution was not affected at 75X as expected since GSSG is protected against oxidative stress in their disulfide forms. However, GSSG yielded similar results at 300X as GSH where no GSH IPAP derivative peak was detected. The samples were then analyzed on the QqTOF to determine if oxidized species formed by 75X and 300X with GSH could be detected, using the same 9 min chromatographic method with the ZORBAX column as the method used for the LC-MRM data.

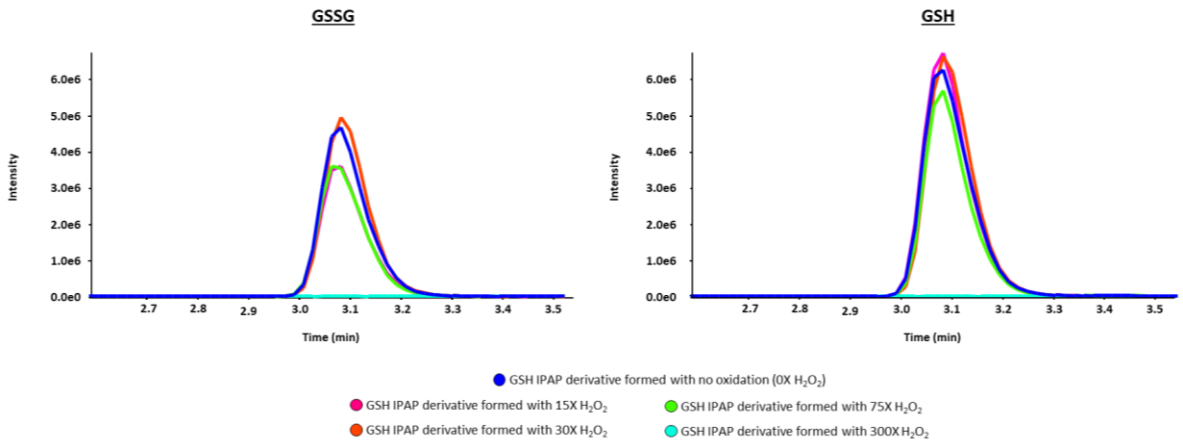

Figure 4.20 XICs of GSH IPAP derivatives formed under increasing levels of oxidation when analyzed using the MRM method

From the results from the QqTOF, the TIC showed the presence of some species in the oxidative sate of 300X that is not seen at a lower oxidative state, with a peak seen at 4.9 min that was seen in both the GSH and GSSG solutions. From the TOF-MS spectra, it was determined that this peak is actually intact IPAP (Figure 4.21). This seems to suggest that high levels of H_2O_2 actually prevents the derivatization reaction as IPAP is still present in the mix only under these conditions.

To determine if oxidative species can be derivatized for identification, the sulfenic and sulfoxide versions of the GSH IPAP derivative formations were monitored. From the results, the only oxidative species that was observed was a singly oxidized (+1O, GSH+O) species when GSH was tested at 75X H_2O_2. As the other oxygen derivatives were not detected, it could suggest that they cannot be derivatized in this manner. As this is rather preliminary data, more experiments should be planned to continue to study the usefulness of using the derivatization method developed to study oxidized versions of thiols in biological samples.

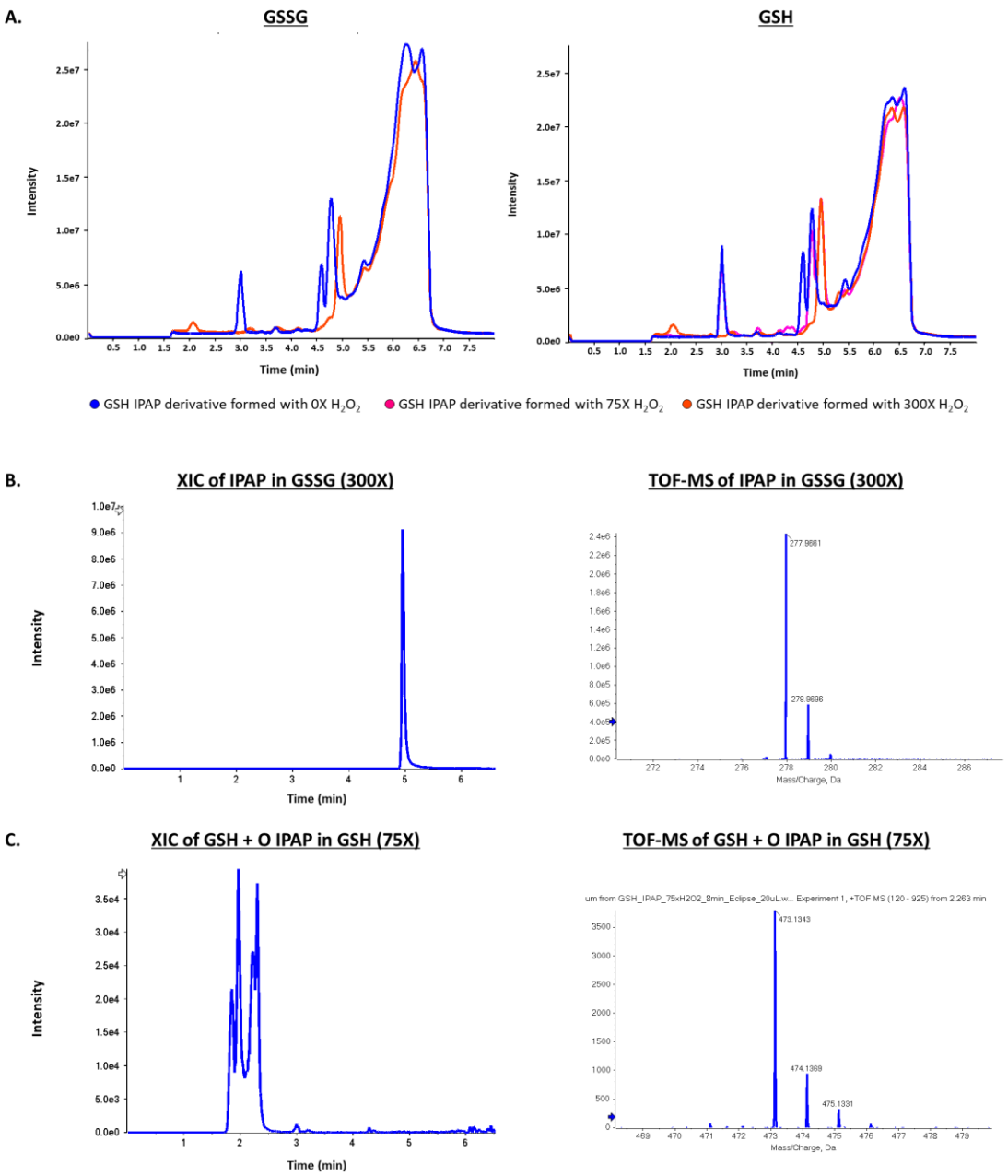

Figure 4.21 A) TIC of GSSG and GSH IPAP derivatives formed when performing an oxidative stress test. B) To confirm the peak at 4.9 min, the extracted ion chromatogram of the GSH IPAP derivative was verified, along with its TOF-MS spectra. C) The singly oxidised GSH + O IPAP derivative was seen in the 75X sample, with the TOF-MS spectra for confirmation.

CONCLUSION

The detection of phosphorylated and thiol-containing metabolites continues to be a challenge largely due to their range of polarities, low abundance, and matrix effects affecting their detection in complex biological samples. A particular challenge seen when studying thiol and disulfide metabolites is their unstable exchange reactions and instability to oxidation. These two metabolic subclasses play cruicial biological roles in several metabolic pathways, many of which involve the body's antioxidant defence mechanisms. Thus, pertubations in their concentrations can be useful indications of imbalances occurring in cancers, energy disorders, and oxidative stress, for example. As such, it is important to be able to detect and quantify these compounds to better understand certain biological events. With this in mind, tailored workflows have been developed in this research project to improve the detection of these compounds by LC-MS/MS.

While there is a breadth of literature available for the detection and quantitation of phosphoproteins, the same cannot be said for phosphometabilites. As such, to optimize the detection of phosphometabolites, the development of an enrichment method that would allow these low abundant compounds to be better detected was the focus. In particular, MAX and TiO_2 enrichment methods were studied using LC-HRMS/MS analysis on a QqTOF platform in untargeted analyses. From the results of both mouse liver and *C. elegans* extracts, the TiO_2 enrichment method often yielded less metabolites, but with a higher proportion of phosphometabolites. While not as specific for the phosphorylated compounds of interest, the MAX SPE method remains an interesting alternative for these compounds with its broader selectivity for acidic analytes. In the context of studying disease models, using the two enrichment methods allowed for more complementary data to be gained compared to a more general sample preparation method. This allows for a broader understanding of a disease, as was the case when applied to a MPS mouse model to investigate changes in metabolite levels in the liver. Additionally, these methods were compared in the analysis of *C. elegans* samples.

A key result of this project was the ability to demonstrate the exploitation of the interaction between TiO_2 and the phosphate groups to improve the detection of phosphometabolites. Although the methods tested in this project showed promise, there is still much work to be done to further optimize this approach. The take away message is that both MAX and TiO_2 are interesting but do not necessarily yield increased phosphometabolites that are significantly changing in the MPS model compared to the more generic EtOH

extraction. Therefore, more work needs to be performed to optimize protocols to have the best selectivity for phosphometabolites, such as exploring different enrichment methods that use TiO_2.

Future work for improved phosphometabolite detection could involve testing a workflow that has a TiO_2 capture step (using a spin cartridge column that contains a TiO_2 sorbent) and analysing both captured and non-captured metabolites for increased coverage. As the spin column is already filled with TiO_2 resin, it would remove the need to prepare an in-house cartridge or performing bulk extractions in tube format. Additionally, it would be interesting to investigate combining 2 to 3 subsequent SPE steps with complementary interaction mechanisms (for instance MAX and MCX) to yield even higher coverage in untargeted metabolomics workflows.

Another potentially interesting avenue involves using a TiO_2 HPLC column to reduce the need to perform pre-extraction enrichment methods. By employing a system that would involve two columns, such as a TiO_2 trapping column and another analytical LC column, they can be used in conjunction with one another. Complementary data could potentially be obtained by first analysing compounds not trapped on the pre-column, followed by their elution and subsequent analysis of phosphometabolites in a subsequent injection (with a tailored LC gradient possible for increased throughput). This would also reduce the quantity of biological samples required as only one sample would need to be prepared for two analyses.

To improve the detection of thiol- and disulfide-containing compounds, thiol-specific derivatization reactions were investigated, where the main objective was to use light and heavy labeled derivatizing agents to distinguish between true free thiols and disulfides in complex biological matrices. However, testing the initial planned hypothesis revealed contradictory information, where the IPAP seemed to derivatize both true free thiols and free thiols formed from the disulfide reduction. This led to the exploration of methods that would halt the light reagent reaction such as using free thiol resins to deplete IPAP, or changing the pH level of the sample. By using free thiol resin, it was demonstrated that the resin tested was able to remove any excess unreacted IPAP still present after the alkylation reaction, thus quenching the IPAP reaction before the reduction reaction. Additionally, a preliminary oxidative stress test revealed that certain oxidized species of GSH was derivatized and detected, while confirming that disulfides are not susceptible oxidation as free thiols under *in vitro* oxidative conditions.

The main goal in the investigation of thiol metabolites was to gain a better understanding of the chemistry of these metabolites, some of which have low stability in samples stored prior to analysis, as well as to

improve their detection. Free thiols benefit greatly by derivatization to stabilize their oxidizable sites as well as increase their hydrophobicity and thus their detectability. Preliminary work with a free thiol silica resin showed promise for halting the alkylation reaction of free thiols in a sample, prior to cleavage of disulfides and their subsequent alkylation with a heavy labeled reagent.

Future work for improved thiol detection involve incorporating the use of a thiol-containing resin in a biological context and further testing the ability for accurate quantitation of free thiol–disulfide ratios. This would allow for further exploration of the detection of oxidized species, and other free thiol compounds, as it was noted that there are differences in their propensity to form disulfides from free thiols in simple solutions based on their structures, with aromatic thiols being much more stable and even NAC having increased stability compared to Cys in solution. By developing targeted methods for thiol- and disulfide-containing metabolites, their pertubations can be studied in the context of diseases linked to oxidative stress in a facile way with increased sensitivity compared to untargeted workflows.

BIBLIOGRAPHIE

Acclaim Columns Overview. (n.d.).

Agilent ZORBAX Eclipse Plus C18. (n.d.). Retrieved April 2, 2025, from https://www.agilent.com/cs/library/specifications/public/820114-002.pdf

Alberts, B., Johnson, A., Lewis, J., Raff, M., Roberts, K., & Walter, P. (2002). From DNA to RNA. In *Molecular Biology of the Cell. 4th edition*. Garland Science. https://www.ncbi.nlm.nih.gov/books/NBK26887/

Aryal, U. K., & Ross, A. R. S. (2010). Enrichment and analysis of phosphopeptides under different experimental conditions using titanium dioxide affinity chromatography and mass spectrometry. *Rapid Communications in Mass Spectrometry*, *24*(2), 219–231. https://doi.org/10.1002/rcm.4377

Baba, S. P., & Bhatnagar, A. (2018). Role of thiols in oxidative stress. *Current Opinion in Toxicology*, *7*, 133–139. https://doi.org/10.1016/j.cotox.2018.03.005

Badawy, M. E. I., El-Nouby, M. A. M., Kimani, P. K., Lim, L. W., & Rabea, E. I. (2022). A review of the modern principles and applications of solid-phase extraction techniques in chromatographic analysis. *Analytical Sciences*, *38*(12), 1457–1487. https://doi.org/10.1007/s44211-022-00190-8

Batalha, I. L., Lowe, C. R., & Roque, A. C. A. (2012). Platforms for enrichment of phosphorylated proteins and peptides in proteomics. *Trends in Biotechnology*, *30*(2), 100–110. https://doi.org/10.1016/j.tibtech.2011.07.004

Becker, S., Kortz, L., Helmschrodt, C., Thiery, J., & Ceglarek, U. (2012). LC–MS-based metabolomics in the clinical laboratory. *Journal of Chromatography B*, *883–884*, 68–75. https://doi.org/10.1016/j.jchromb.2011.10.018

Berthou, M., Clarot, I., Gouyon, J., Steyer, D., Monat, M. A., Boudier, A., & Pallotta, A. (2022). Thiol sensing: From current methods to nanoscale contribution. *Microchemical Journal*, *183*, 107994. https://doi.org/10.1016/j.microc.2022.107994

Bessman, S. P. (1974). An automated apparatus for quantitative aliquot measurement of phosphorylated intermediates. *Analytical Biochemistry*, *59*(2), 524–532. https://doi.org/10.1016/0003-2697(74)90306-6

Bindoli, A., Fukuto, J. M., & Forman, H. J. (2008). Thiol Chemistry in Peroxidase Catalysis and Redox Signaling. *Antioxidants & Redox Signaling*, *10*(9), 1549–1564. https://doi.org/10.1089/ars.2008.2063

Camera, E., Rinaldi, M., Briganti, S., Picardo, M., & Fanali, S. (2001). Simultaneous determination of reduced and oxidized glutathione in peripheral blood mononuclear cells by liquid chromatography–electrospray mass spectrometry. *Journal of Chromatography B: Biomedical Sciences and Applications*, *757*(1), 69–78. https://doi.org/10.1016/S0378-4347(01)00081-0

Collins, S. L., Koo, I., Peters, J. M., Smith, P. B., & Patterson, A. D. (2021). Current Challenges and Recent Developments in Mass Spectrometry–Based Metabolomics. *Annual Review of Analytical Chemistry*, *14*(1), 467–487. https://doi.org/10.1146/annurev-anchem-091620-015205

Coskun, O. (2016). Separation Tecniques: CHROMATOGRAPHY. *Northern Clinics of Istanbul*. https://doi.org/10.14744/nci.2016.32757

Cui, L., Lu, H., & Lee, Y. H. (2018). Challenges and emergent solutions for LC-MS/MS based untargeted metabolomics in diseases. *Mass Spectrometry Reviews*, *37*(6), 772–792. https://doi.org/10.1002/mas.21562

Dwivedi, P., Schultz, A. J., & Hill, H. H. (2010). Metabolic Profiling of Human Blood by High Resolution Ion Mobility Mass Spectrometry (IM-MS). *International Journal of Mass Spectrometry*, *298*(1–3), Article 1–3. https://doi.org/10.1016/j.ijms.2010.02.007

Emwas, A.-H. M. (2015). The Strengths and Weaknesses of NMR Spectroscopy and Mass Spectrometry with Particular Focus on Metabolomics Research. In J. T. Bjerrum (Ed.), *Metabonomics* (Vol. 1277, pp. 161–193). Springer New York. https://doi.org/10.1007/978-1-4939-2377-9_13

Erel, Ö., & Erdoğan, S. (2020). Thiol-disulfide homeostasis: An integrated approach with biochemical and clinical aspects. *Turkish Journal of Medical Sciences*, *50*(7), 1728–1738. https://doi.org/10.3906/sag-2003-64

Fiehn, O. (2016). Metabolomics by Gas Chromatography–Mass Spectrometry: Combined Targeted and Untargeted Profiling. *Current Protocols in Molecular Biology*, *114*(1). https://doi.org/10.1002/0471142727.mb3004s114

Gafken, P. R., & Lampe, P. D. (2006). Methodologies for Characterizing Phosphoproteins by Mass Spectrometry. *Cell Communication & Adhesion*, *13*(5–6), 249–262. https://doi.org/10.1080/15419060601077917

Garg, E., & Zubair, M. (2025). Mass Spectrometer. In *StatPearls*. StatPearls Publishing. http://www.ncbi.nlm.nih.gov/books/NBK589702/

Ghafari, N., & Sleno, L. (2024). Challenges and recent advances in quantitative mass spectrometry-based metabolomics. *Analytical Science Advances*, *5*(5–6), e2400007. https://doi.org/10.1002/ansa.202400007

Gross, J. (2004). *Mass Spectrometry: A Textbook*. Springer.

Haag, A. M. (2016). Mass Analyzers and Mass Spectrometers. In H. Mirzaei & M. Carrasco (Eds.), *Modern Proteomics – Sample Preparation, Analysis and Practical Applications* (Vol. 919, pp. 157–169). Springer International Publishing. https://doi.org/10.1007/978-3-319-41448-5_7

Haggarty, J., & Burgess, K. E. (2017). Recent advances in liquid and gas chromatography methodology for extending coverage of the metabolome. *Current Opinion in Biotechnology*, *43*, 77–85. https://doi.org/10.1016/j.copbio.2016.09.006

Häkkinen, H. (2012). The gold–sulfur interface at the nanoscale. *Nature Chemistry*, *4*(6), 443–455. https://doi.org/10.1038/nchem.1352

Hanai, T. T. (with Smith, R. M.). (2007). *HPLC: A Practical Guide* (1st ed). Royal Society of Chemistry.

Hansen, R. E., & Winther, J. R. (2009). An introduction to methods for analyzing thiols and disulfides: Reactions, reagents, and practical considerations. *Analytical Biochemistry*, *394*(2), 147–158. https://doi.org/10.1016/j.ab.2009.07.051

Ho, C., Lam, C., Chan, M., Cheung, R., Law, L., Lit, L., Ng, K., Suen, M., & Tai, H. (2003). Electrospray Ionisation Mass Spectrometry: Principles and Clinical Applications. *The Clinical Biochemist Reviews*, *24*(1), 3–12.

Horgan, R. P., & Kenny, L. C. (2011). 'Omic' technologies: Genomics, transcriptomics, proteomics and metabolomics. *The Obstetrician & Gynaecologist*, *13*(3), 189–195. https://doi.org/10.1576/toag.13.3.189.27672

Imtakt Scherzo Metal Free Column. (n.d.). Retrieved March 6, 2025, from https://uvison.com/download/Imtakt/Imtakt_Metal-Free_Columns_Brochure.pdf

Johnson, C. H., Ivanisevic, J., & Siuzdak, G. (2016). Metabolomics: Beyond biomarkers and towards mechanisms. *Nature Reviews. Molecular Cell Biology*, *17*(7), 451–459. https://doi.org/10.1038/nrm.2016.25

Kauffman, F. C., Brown, J. G., Passonneau, J. V., & Lowry, O. H. (1969). Effects of Changes in Brain Metabolism on Levels of Pentose Phosphate Pathway Intermediates. *Journal of Biological Chemistry*, *244*(13), 3647–3653. https://doi.org/10.1016/S0021-9258(18)83418-4

Koley, S., Chu, K. L., Gill, S. S., & Allen, D. K. (2022). An efficient LC-MS method for isomer separation and detection of sugars, phosphorylated sugars, and organic acids. *Journal of Experimental Botany*, *73*(9), 2938–2952. https://doi.org/10.1093/jxb/erac062

Kuehnbaum, N. L., & Britz-McKibbin, P. (2013). New Advances in Separation Science for Metabolomics: Resolving Chemical Diversity in a Post-Genomic Era. *Chemical Reviews*, *113*(4), 2437−2468. https://doi.org/dx.doi.org/10.1021/cr300484s

Kumar, D., Gautam, N., & Alnouti, Y. (2022). Analyte Recovery in LC-MS/MS Bioanalysis: An Old Issue Revisited. *Analytica Chimica Acta*, *1198*, 339512. https://doi.org/10.1016/j.aca.2022.339512

Kweon, H. K., & Håkansson, K. (2006). Selective Zirconium Dioxide-Based Enrichment of Phosphorylated Peptides for Mass Spectrometric Analysis. *Analytical Chemistry*, *78*(6), 1743–1749. https://doi.org/10.1021/ac0522355

LeBlanc, A., Shiao, T. C., Roy, R., & Sleno, L. (2014). Absolute Quantitation of NAPQI-Modified Rat Serum Albumin by LC–MS/MS: Monitoring Acetaminophen Covalent Binding in Vivo. *Chemical Research in Toxicology*, *27*(9), 1632–1639. https://doi.org/10.1021/tx500284g

Lepoittevin, M., Blancart-Remaury, Q., Kerforne, T., Pellerin, L., Hauet, T., & Thuillier, R. (2023). Comparison between 5 extractions methods in either plasma or serum to determine the optimal extraction and matrix combination for human metabolomics. *Cellular & Molecular Biology Letters*, *28*(1), Article 1. https://doi.org/10.1186/s11658-023-00452-x

Li, Y., Wang, Y., Li, P., Zhou, Q., Zheng, X., & Gu, Q. (2023). Caenorhabditis elegans: A nature present for advanced food science. *Current Opinion in Food Science*, *49*, 100971. https://doi.org/10.1016/j.cofs.2022.100971

Madeira, P. J. A., & Florêncio, M. H. (2012). Applications of Tandem Mass Spectrometry: From Structural Analysis to Fundamental Studies. In J. Prasain (Ed.), *Tandem Mass Spectrometry—Applications and Principles*. InTech. https://doi.org/10.5772/31736

Matuszewski, B. K., Constanzer, M. L., & Chavez-Eng, C. M. (1998). Matrix Effect in Quantitative LC/MS/MS Analyses of Biological Fluids: A Method for Determination of Finasteride in Human

Plasma at Picogram Per Milliliter Concentrations. *Analytical Chemistry*, *70*(5), 882–889. https://doi.org/10.1021/ac971078+

Menkovic, I., Lavoie, P., Boutin, M., & Auray-Blais, C. (2019). Distribution of Heparan Sulfate and Dermatan Sulfate in Mucopolysaccharidosis Type Ii Mouse Tissues Pre- and Post-Enzyme-Replacement Therapy Determined By Uplc–Ms/Ms. *Bioanalysis*, *11*(8), 727–740. https://doi.org/10.4155/bio-2018-0306

Nguyen, H. P., Yang, S. H., Wigginton, J. G., Simpkins, J. W., & Schug, K. A. (2010). Retention behavior of estrogen metabolites on hydrophilic interaction chromatography stationary phases. *Journal of Separation Science*, *33*(6–7), 793–802. https://doi.org/10.1002/jssc.200900680

Pang, Z., Chong, J., Zhou, G., de Lima Morais, D. A., Chang, L., Barrette, M., Gauthier, C., Jacques, P.-É., Li, S., & Xia, J. (2021). MetaboAnalyst 5.0: Narrowing the gap between raw spectra and functional insights. *Nucleic Acids Research*, *49*(W1), W388–W396. https://doi.org/10.1093/nar/gkab382

Panuwet, P., Hunter, R. E., D'Souza, P. E., Chen, X., Radford, S. A., Cohen, J. R., Marder, M. E., Kartavenka, K., Ryan, P. B., & Barr, D. B. (2016). Biological Matrix Effects in Quantitative Tandem Mass Spectrometry-Based Analytical Methods: Advancing Biomonitoring. *Critical Reviews in Analytical Chemistry / CRC*, *46*(2), Article 2. https://doi.org/10.1080/10408347.2014.980775

Phenomenex LC Product Guide. (n.d.).

Phipps, W. S., Jones, P. M., & Patel, K. (2019). Amino and organic acid analysis: Essential tools in the diagnosis of inborn errors of metabolism. In *Advances in Clinical Chemistry* (Vol. 92, pp. 59–103). Elsevier. https://doi.org/10.1016/bs.acc.2019.04.001

Pinkse, M. W. H., Uitto, P. M., Hilhorst, M. J., Ooms, B., & Heck, A. J. R. (2004). Selective Isolation at the Femtomole Level of Phosphopeptides from Proteolytic Digests Using 2D-NanoLC-ESI-MS/MS and Titanium Oxide Precolumns. *Analytical Chemistry*, *76*(14), 3935–3943. https://doi.org/10.1021/ac0498617

Poole, C. F., & Poole, S. K. (2012). Principles and Practice of Solid-Phase Extraction. In *Comprehensive Sampling and Sample Preparation: Analytical Techniques for Scientists* (pp. 273–297). Elsevier.

Product Guide MagReSyn Zr-IMAC HP. (2022). https://resynbio.com/wp-content/uploads/2022/09/IFU_ZrIMAC_HP.pdf

Qiu, D., Wilson, M. S., Eisenbeis, V. B., Harmel, R. K., Riemer, E., Haas, T. M., Wittwer, C., Jork, N., Gu, C., Shears, S. B., Schaaf, G., Kammerer, B., Fiedler, D., Saiardi, A., & Jessen, H. J. (2020). Analysis of inositol phosphate metabolism by capillary electrophoresis electrospray ionization mass spectrometry. *Nature Communications*, *11*, 6035. https://doi.org/10.1038/s41467-020-19928-x

Resins and Reagents. (n.d.). Retrieved May 5, 2025, from https://www.artisantg.com/info/Argonaut_Resins_and_Reagents.pdf?srsltid=AfmBOoqi3CfwsRBMwDKGFKVxlki0Oqh6D_8Z9l4H0NkrEYwepL1CaJVp

Ryan, M. C., Stucky, M., Wakefield, C., Melott, J. M., Akbani, R., Weinstein, J. N., & Broom, B. M. (2020). *Interactive Clustered Heat Map Builder: An easy web-based tool for creating sophisticated clustered heat maps* (No. 8:1750). F1000Research. https://doi.org/10.12688/f1000research.20590.2

Salim, M., Fowler, G. J. S., Wright, P. C., & Vaidyanathan, S. (2012). A selective metabolite array for the detection of phosphometabolites. *Analytica Chimica Acta*, *724*, 119–126. https://doi.org/10.1016/j.aca.2012.02.024

Salovska, B., Tichy, A., Fabrik, I., Rezacova, M., & Vavrova, J. (2013). Comparison of Resins for Metal Oxide Affinity Chromatography with Mass Spectrometry Detection for the Determination of Phosphopeptides. *Analytical Letters*, *46*(10), 1505–1524. https://doi.org/10.1080/00032719.2013.773437

Salovska, B., Tichy, A., Rezacova, M., Vavrova, J., & Novotna, E. (2012). Enrichment strategies for phosphoproteomics: State-of-the-art. *Reviews in Analytical Chemistry*, *31*(1). https://doi.org/10.1515/revac-2011-0025

Sass, J. O., & Endres, W. (1997). Quantitation of total homocysteine in human plasma by derivatization to its N(O,S)-propoxycarbonyl propyl ester and gas chromatography–mass spectrometry analysis. *Journal of Chromatography A*, *776*(2), 342–347. https://doi.org/10.1016/S0378-4347(97)00080-7

Scherzo C18 Family. (n.d.).

Si-Hung, L., Troyer, C., Causon, T., & Hann, S. (2019). Sensitive quantitative analysis of phosphorylated primary metabolites using selective metal oxide enrichment and GC- and IC- MS/MS. *Talanta*, *205*, 120147. https://doi.org/10.1016/j.talanta.2019.120147

SiliaMetS Specification Sheet. (n.d.). Retrieved May 5, 2025, from https://www.silicycle.com/ca/media/specsheets/spec-R51030B.pdf

Sleno, L., Varesio, E., & Hopfgartner, G. (2007). Determining protein adducts of fipexide: Mass spectrometry based assay for confirming the involvement of its reactive metabolite in covalent binding. *Rapid Communications in Mass Spectrometry*, *21*(24), 4149–4157. https://doi.org/10.1002/rcm.3329

Sleno, L., & Volmer, D. A. (2004). Ion activation methods for tandem mass spectrometry. *Journal of Mass Spectrometry*, *39*(10), 1091–1112. https://doi.org/10.1002/jms.703

Snyder, L. R. ., Kirkland, J. J., & Dolan, J. W. (2011). Introduction to Modern Liquid Chromatography, Third Edition. *Journal of the American Society for Mass Spectrometry*, *22*(1), 196–196. https://doi.org/10.1007/s13361-010-0021-8

Stapleton, M., Kubaski, F., Mason, R. W., Yabe, H., Suzuki, Y., Orii, K. E., Orii, T., & Tomatsu, S. (2017). Presentation and Treatments for Mucopolysaccharidosis Type II (MPS II; Hunter Syndrome).

Expert Opinion on Orphan Drugs, *5*(4), 295–307. https://doi.org/10.1080/21678707.2017.1296761

Steen, H., Kuster, B., Fernandez, M., Pandey, A., & Mann, M. (2002). Tyrosine Phosphorylation Mapping of the Epidermal Growth Factor Receptor Signaling Pathway. *Journal of Biological Chemistry*, *277*(2), 1031–1039. https://doi.org/10.1074/jbc.M109992200

Tan, S. Z., Begley, P., Mullard, G., Hollywood, K. A., & Bishop, P. N. (2016). Introduction to metabolomics and its applications in ophthalmology. *Eye*, *30*(6), 773–783. https://doi.org/10.1038/eye.2016.37

TenBroek, E. M., Lampe, P. D., Solan, J. L., Reynhout, J. K., & Johnson, R. G. (2001). Ser364 of connexin43 and the upregulation of gap junction assembly by cAMP. *The Journal of Cell Biology*, *155*(7), 1307–1318. https://doi.org/10.1083/jcb.200102017

Thingholm, T. E., Jensen, O. N., & Larsen, M. R. (2009). Analytical strategies for phosphoproteomics. *PROTEOMICS*, *9*(6), 1451–1468. https://doi.org/10.1002/pmic.200800454

Tominaga, T. (1996). Identification de l'acetate de 3-mercaptohexanol, compose aforte odeur de buis, intervenant dans l'arome des vins de Sauvignon. *Vitis*, *35*(4), 207–210.

Trufelli, H., Palma, P., Famiglini, G., & Cappiello, A. (2011). An overview of matrix effects in liquid chromatography–mass spectrometry. *Mass Spectrometry Reviews*, *30*(3), 491–509. https://doi.org/10.1002/mas.20298

Wang, L., Jin, F., Jiang, X., Chen, J., Wang, M. C., & Wang, J. (2022). Fluorescent Probes and Mass Spectrometry-Based Methods to Quantify Thiols in Biological Systems. *Antioxidants & Redox Signaling*, *36*(4–6), 354–365. https://doi.org/10.1089/ars.2021.0204

Wang, L., Yao, Z. P., Li, P., Chen, S., So, P., Shi, Z., Hu, B., Liu, L., & Xin, G. (2016). Global detection and semi-quantification of *Fritillaria* alkaloids in Fritillariae Ussuriensis Bulbus by a non-targeted multiple reaction monitoring approach. *Journal of Separation Science*, *39*(2), 287–295. https://doi.org/10.1002/jssc.201500880

Wang, Z., Zhu, H., & Xiong, W. (2023). Advances in mass spectrometry-based multi-scale metabolomic methodologies and their applications in biological and clinical investigations. *Science Bulletin*, *68*(19), 2268–2284. https://doi.org/10.1016/j.scib.2023.08.047

Waters. (2007). *MassPREP Phosphopeptide Enrichment Kit Care and Use Manual*. https://help.waters.com/help/en/support/library-details.html?documentid=715001457

Waters. (2010). *Oasis Sample Extraction Products: Chemistry & Formats*.

Winther, J. R., & Thorpe, C. (2014). Quantification of thiols and disulfides. *Biochimica et Biophysica Acta (BBA) - General Subjects*, *1840*(2), 838–846. https://doi.org/10.1016/j.bbagen.2013.03.031

Wishart, D. S. (2008). Applications of Metabolomics in Drug Discovery and Development. *Drugs in R&D*, *9*(5), 307. https://doi.org/10.2165/00126839-200809050-00002

Wohlgemuth, R. (2023). Advances in the Synthesis and Analysis of Biologically Active Phosphometabolites. *International Journal of Molecular Sciences*, *24*(4), 3150. https://doi.org/10.3390/ijms24043150

Wu, Q., Xu, Y., Ji, H., Wang, Y., Zhang, Z., & Lu, H. (2019). Enhancing coverage in LC-MS-based untargeted metabolomics by a new sample preparation procedure using mixed-mode solid-phase extraction and two derivatizations. *Analytical and Bioanalytical Chemistry*, *411*(23), Article 23. https://doi.org/10.1007/s00216-019-02010-x

Yang, S., Sadilek, M., & Lidstrom, M. E. (2010). Streamlined pentafluorophenylpropyl column liquid chromatography-tandem quadrupole mass spectrometry and global (13)C-labeled internal standards improve performance for quantitative metabolomics in bacteria. *Journal of Chromatography. A*, *1217*(47), 7401–7410. https://doi.org/10.1016/j.chroma.2010.09.055

Yu, Y. Q., Ahn, J., Dubey, A., & Gilar, M. (2007). Phosphopeptide Enrichment Method Using High Affinity Solid-Phase Extraction µ Elution Plate. *Waters Publication*.

Zhang, Y., Chen, R., Zhang, D., Qi, S., & Liu, Y. (2023). Metabolite interactions between host and microbiota during health and disease: Which feeds the other? *Biomedicine & Pharmacotherapy*, *160*, 114295. https://doi.org/10.1016/j.biopha.2023.114295